THE SEDIMENTOLOGY AND DEPOSITIONAL HISTORY OF THE ST. ROCH FORMATION NEAR ST. JEAN-PORT-JOLI, QUEBEC

By

Percy George Strong, B.Sc. (Hons.)

A Thesis
Submitted to the School of Graduate Studies
in Partial Fulfulment of the Requirements
for the Degree
Master of Science

McMaster University
August 1978

THE SEDIMENTOLOGY AND DEPOSITIONAL HISTORY OF THE ST. ROCH FORMATION NEAR ST. JEAN-PORT-JOLI, QUEBEC

Master of Science (1978)
(Geology)

McMaster University
Hamilton, Ontario

Title: The Sedimentology and Depositional History of the St. Roch Formation near St. Jean-Port-Joli, Quebec

Author: Percy George Strong, B.Sc. (Hons.) (Memorial University of Newfoundland)

Supervisor: Dr. Roger G. Walker

Number of Pages: i-xi; 1-128

ABSTRACT

The St. Roch Formation (Cambrian), near St. Jean-Port-Joli, Quebec is composed of northeast striking, steep, southerly dipping strata. The stratigraphic sequence (minimum thickness 534 m) is disrupted by several northeast trending, high angle reverse faults which divide the area into a series of imbricated fault blocks.

Eight sedimentary facies were recognized in the stratigraphic section: (1) Red mudstone (2) Massive sandstone (3) Pebbly sandstone (4) Classical turbidite - siliceous or calcareous (5) Slurry (6) Pebbly mudstone (7) Pillar greywacke (8) Slump - there are two types: calcisiltite and red mudstone - fine grained turbidite.

These facies occur in associations which make up four types of lithologic units:

1. The Red Mudstone Units - They are 10-90 m thick and are mainly composed of the red mudstone facies. The red mudstone-fine grained turbidite slump is found in one of these units.

2. The Massive Sandstone Units - They are 30-95 m thick and are composed of two facies divisions: a slurry division composed of interbedded slurry beds and classical

turbidites forms the lower part of these units and a massive sandstone division composed of the massive sandstone, the classical turbidite plus/minus the pillar greywacke facies forms the upper part.

3. The Siliceous Classical Turbidite Units - They are 10-20 m thick and are composed of siliceous classical turbidites and slurry beds.

4. The Calcareous Classical Turbidite Units - They are 30-100 m thick and are dominated by the classical turbidite facies. The only occurrences of the calcisiltite slump and the pebbly mudstone facies are found in these units.

The stratigraphic section is characterized by the alternation of sandstone and mudstone units. The sandstone units in the lower part of the sequence show a coarsening and thickening upward sequence. No vertical trend in bed thickness or grain size is evident in individual units.

The red mudstone, massive sandstone and siliceous classical turbidite units contain paleoflow indicators which have a vector mean of 140°. The calcareous classical turbidites interbedded with the red mudstones and forming the classical turbidite unit at the top of the section have a paleoflow vector mean of 90°. The petrology of the calcareous and noncalcareous sandstones indicates that they were derived from two different sources.

The red mudstone, massive sandstone and siliceous classical turbidite units are interpreted as being formed as part of a submarine fan complex. The red mudstone units represent interlobe mud blankets that envelope upper and lower suprafan deposits. The calcareous classical turbidites represent encroachment on the fan system of sediments transported longitudinally along the basin from another source.

ACKNOWLEDGEMENTS

I would sincerely like to thank my supervisor, Dr. R.G. Walker, who provided impetus for this study and aided the progress with many constructive criticisms. Special thanks are extended to my wife, Jean, and my brother, Jim, who provided field assistance and encouragement during the writing of this thesis, and my father, who constructed the grain size estimator and scale.

While in Quebec my work was aided by the friendliness of Mme. Frances Deschènes, M. and Mme. André Robitaille and their children, as well as the people of St. Jean-Port-Joli.

Thanks are also extended to Jack Whorwood, for his photographic advice and expertise, Len Zwicker, for thin section preparation, Helen Elliott, for typing the manuscript and those graduate students who provided helpful discussion which generated the ideas presented.

This work was carried out under a grant from the National Research Council of Canada to Dr. Walker.

TABLE OF CONTENTS

LIST OF FIGURES

LIST OF TABLES

CHAPTER 1

INTRODUCTION

Raison d'Etre

Submarine fans are fan shaped geomorphic features composed of terrigenous sediments (Reineck and Singh, 1975). They develop at the debouching mouths of submarine valleys where the coarse grained terrigenous sediments are deposited due to a sudden change in slope (Mutti, 1974). The growth of a deep sea fan is controlled by sediment supply, the grain size distribution of the sediments and tectonic activity in the source area (Normark, 1974).

Modern deep sea fans have three morphological divisions: the upper fan, characterized by the deposition of coarse sediment in a leveed fan valley; a mid fan (or suprafan) composed of massive and pebbly sandstones located in braided channels which feed suprafan lobes composed of classical turbidites; and the lower fan composed of thin bedded turbidites and hemipelagic mudstones (Normark, 1970a; Walker, 1978) (Figure 1-1).

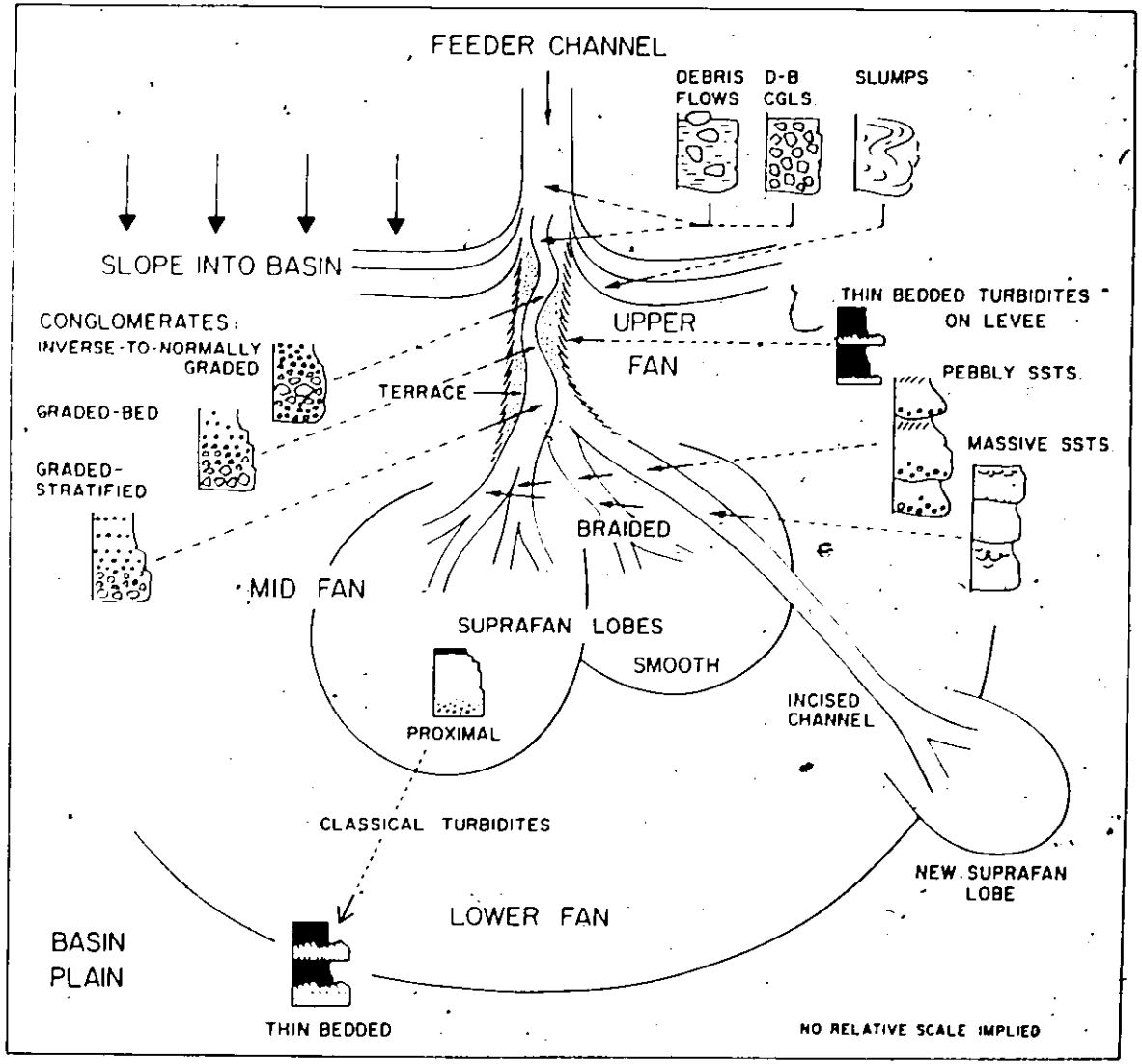

Figure 1-1 Submarine fan model proposed by Walker (1978, Figure 13) showing the depositional setting of the various facies.

The two main processes which control the development of vertical trends in bed thickness and grain size are channel switching and fan progradation. As the sediment supply decreases, channel abandonment occurs and a thinning and fining upward sequence develops. Progradation of a suprafan lobe or of the whole fan will develop a thickening and coarsening upward sequence as the progressively coarser facies of the mid, and inner fan are stacked on top of those of the outer fan (Figure 1-2).

The St. Roch Formation near St. Jean-Port-Joli, Quebec is composed of alternating sandstone units (10-100 m thick) and mudstone units (10-90 m thick). The sandstone units were either composed of slurry beds (Wood and Smith, 1959), massive sandstones, pebbly sandstones and classical turbidites, or simply classical turbidites and slurry beds. The mudstone units were composed of thick mudstone beds and thin bedded turbidites. The contacts between the units were sharp and not marked by a thickening and coarsening upwards sequence. However, a thickening and coarsening upwards sequence can be seen in the lower three sandstone units.

Comparison of these features with the submarine fan model (Fig. 1-1) shows that the presence of the massive and pebbly sandstones indicates deposition on the upper suprafan. But

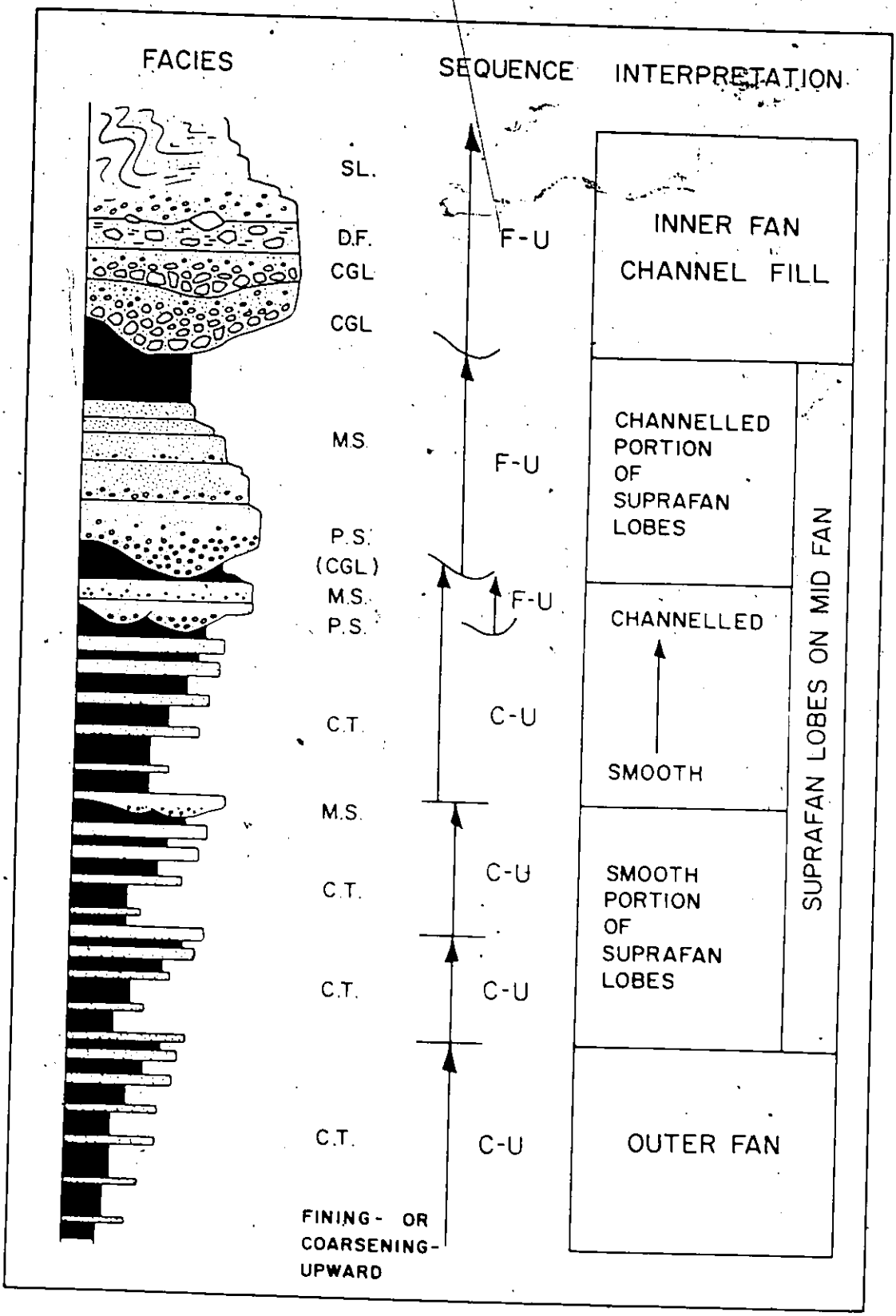

Figure 1-2 Thickening and coarsening upward sequence formed by a prograding submarine fan (Walker, 1978, Fig. 14).

the tremendous thickness of the mudstone units and the dearth of classical turbidites is not predicted for that environment by the model. Thus the main problem of this thesis is to determine whether or not these sediments were deposited on a submarine fan.

The St. Roch Formation sediments formed part of a continental rise prism which developed on an Atlantic type (Dewey and Bird, 1970) continental margin (St. Julien and Hubert, 1975). However, petrological and paleocurrent studies of the St. Roch Formation (Hubert, 1965, 1973) were interpreted as suggesting that two sources, one to the northwest and one to the southeast, contributed sediments to the depositional basin. The paleocurrent and petrological studies of the study area were undertaken to clarify this apparent contradiction.

The St. Roch Formation in the St. Jean-Port-Joli area was chosen because the stratigraphy could be tied in with that of the Plage Victor area reported by Hubert (1969). The St. Roch Formation is poorly exposed in inland areas, but coastal exposure is excellent due to the macrotidal range which provides a wide wave cut bench. The beds strike at an oblique angle to the shoreline and therefore both a vertical section and their lateral continuity can easily be studied.

Regional Geology

The Quebec Complex refers to the strata which underlie 50-100 per cent of the area between the St. Lawrence River and the United States' border and between Cap-des-Rosiers in the northeast and the Chaudière River in the southwest (Figure 1-3). It ranges in age from Lower Cambrian to Middle Ordovician and is composed of four formations and one group (Table 1-1).

Structurally, the Quebec Complex is present in both the internal and external domains of the Quebec Appalachians (St. Julien and Hubert, 1975). The external domain is composed of an outer belt of thrust imbricated slices and an inner belt of nappes. The folding trends northeast and is overturned to the northwest. Deformation occurred during the Taconic Orogeny.

The L'Islet-Kamouraska area is part of the outer belt of the external domain and consists of four litho-structural slices: the St. Roch, the La Pocatiere I and II, and the Armagh (Figure 1-4). The study area is part of the St. Roch slice.

The St. Roch Formation is defined as "an assemblage of mudstone with intercalated bands of shales and siltstones sandstones and conglomerates distributed in a northeast-

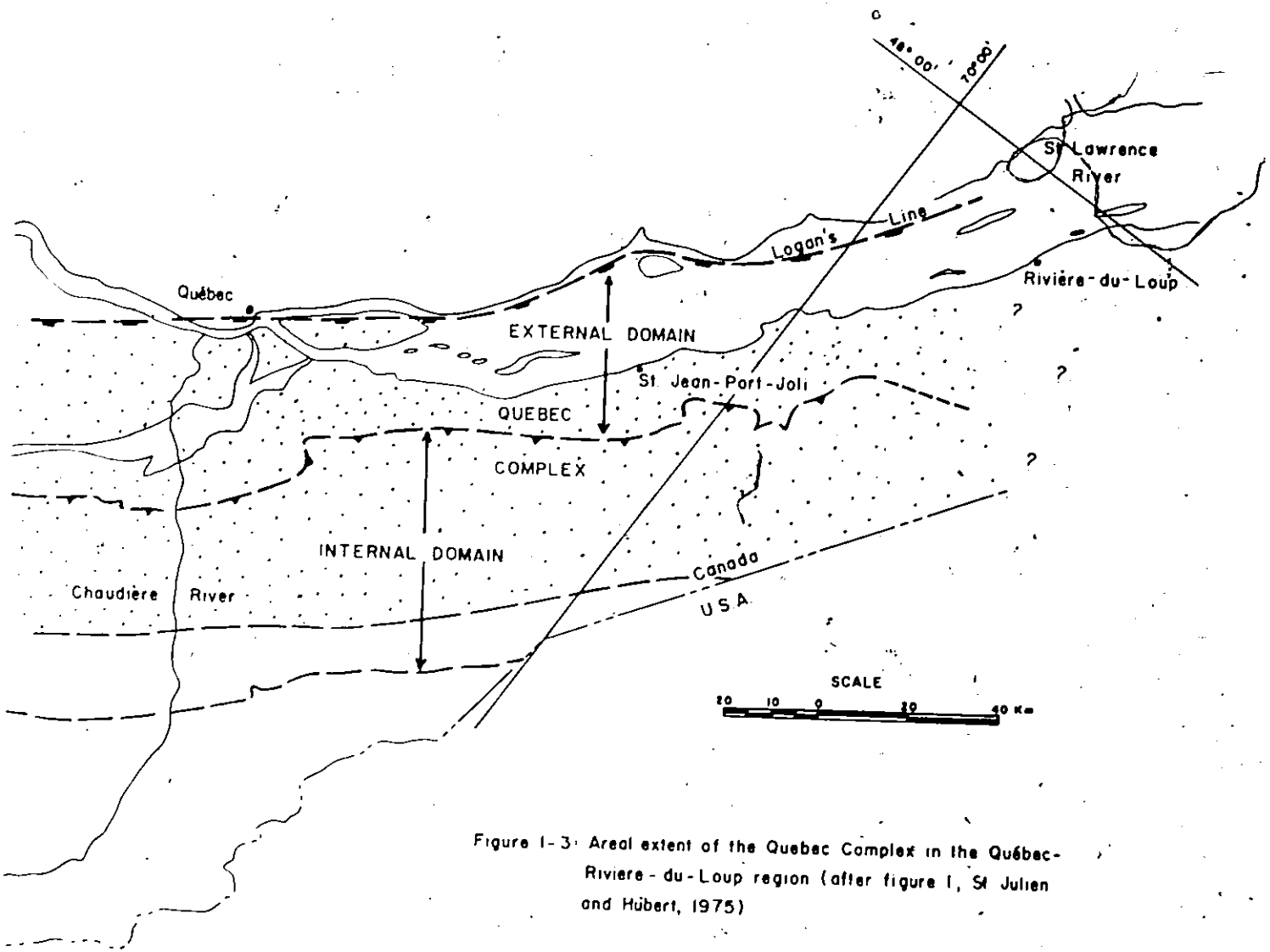

Figure I-3: Areal extent of the Quebec Complex in the Québec-Riviere-du-Loup region (after figure 1, St Julien and Hubert, 1975)

Table 1-1 Table of Formations of the Quebec Complex (from Table 1, Hubert, 1973)

Period	Group/Formation	Thickness (m)
	Rivière Ouelle Formation	600+
Ordovician	Kamouraska Formation	up to 740
	St. Damase Formation	
	Ste. Anne Member	330
	La Pocatière Member	up to 210
Cambrian	Des Aulnaies Member	210+
	St. Roch Formation	1210+
Cambrian?	Armagh Group	up to 3030?
unknown	Rosaire Group	unknown

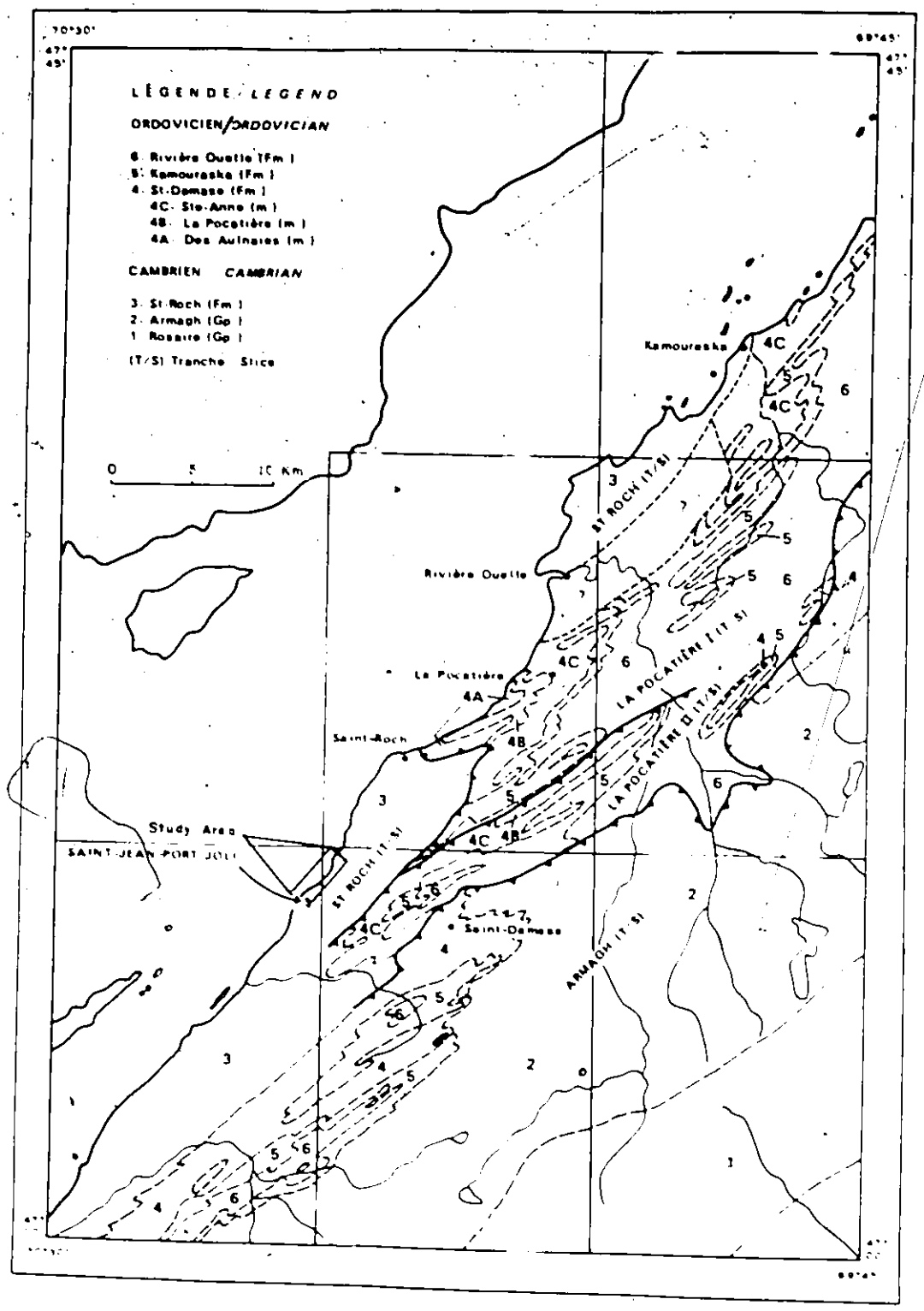

Figure I-4: Structure of the l'Islet-Kamouraska area (from figure 3, p 18, Hubert, 1973)

southwest trending belt across the electoral districts of Montmagny, L'Islet and Kamouraska" (Hubert, 1973, p.38). The formation is Lower to Upper Cambrian in age. Its lower contact is covered by the St. Lawrence River, but it has a conformable upper contact with the Lower Ordovician St. Damase Formation. The thickness of the formation ranges from 330 m to over 1210 m.

The St. Roch Formation makes up all of the St. Roch slice of the external domain's outer belt. It is bounded by the St. Lawrence River to the northwest, and the La Pocatiere I and Armagh thrust faults to the southeast. Folding in the St. Roch Formation is tight and accompanied by much parasitic folding. The trends of the fold axes concur with those of the regional structure.

In the L'Islet-Kamouraska area the St. Roch Formation is a lateral equivalent of the Armagh Group (Hubert, 1965, 1973). Regionally, the St. Roch Formation is correlated with the Charny Group of the Quebec area and the Cap Enragé Formation in the St. Fabien area.

The St. Roch Formation is composed of: mudstone - 40%, arkosic conglomerate and arkose (after Folk, 1954) - 35%, siltstone - 10%, shale - 10%, limestone bearing arkosic conglomerate, shale conglomerate and breccia, oligomictic limestone conglomerate, subarkose, calcarenite

and calcisiltite - 5%. The formation is interpreted as the deep water lithosome of the Quebec Complex because of the great amount of very fine grained sediments it contains (Hubert, 1965, 1973).

Mapping and Section Measuring

Three months (June-September, 1977) were spent mapping the shore between Plage Victor and just west of the wharf at St. Jean-Port-Joli (approximately 3 km). Air photos, taken at low tide (scale 1:9600) of the south shore of the St. Lawrence River were enlarged to a scale of 1 cm = 10 m and the geology plotted directly on them.

The first month of the study was taken up with structural reconnaissance. This was followed by detailed stratigraphic measurement and finally detailed surveys of facies of interest. In the sandstone units, several sections were measured at intervals up to 100 m to study lateral facies variations and also to clarify structural complexities. By convention, bed thickness included a sandstone-shale couplet and a sandstone-shale ratio was denoted in the description. For very thick beds only the sandstone thickness was recorded. Cumulative thicknesses of beds which showed one

or more amalgamations were recorded and the height of each amalgamation above the base noted. The thicknesses of the mudstone units were estimated by tape and compass and trigonometric methods. The thickness of the maximum, minimum and mode of the thin bedded sandstones interbedded with the mudstones was recorded, as well as the sedimentary structures found in them.

The bed description included color, grain size, grading, base type, amalgamation, sedimentary structures and fossils. Grain size was estimated by comparison with a grain size scale composed of six compartments, each containing sand from a 1 ϕ division from the range -2 to 4 ϕ (after Hiscott, 1977; see scale in Figure 3-6).

For paleocurrent measurements, the clinometer on the Brunton compass was used to measure the angle between the axis of the feature and the horizontal. This angle was then either added to or subtracted from the strike of the bed. Since the stratigraphy in the area forms the south limb of an anticline, all minor fold axes in the area were plotted on a stereonet to estimate the plunge. The comparison of this plunge and the dip of bed on which the paleocurrent indicator was found were then compared with Figure 5 of Ramsay (1961), and the error due to neglecting the plunge was estimated. This error was then subtracted from the

orientation obtained in the field.

Preview of Facies and Paleocurrents

Eight facies were recognized in the field: classical turbidite, massive sandstone, pebbly sandstone, slurry and slurry-breccia, red mudstone, pillar greywacke, slump, and pebbly mudstone. The red mudstone facies dominates the section forming units which alternate with sandstone units composed of massive sandstones, pebbly sandstones, slurry beds and classical turbidites, or simply classical turbidites and slurry beds. There are two types of classical turbidites: calcareous and noncalcareous. The calcareous turbidites only occur at the top of the section.

The paleocurrent measurements have a grand vector mean of 128°. The calcareous classical turbidites indicate transport to the east; whereas the noncalcareous sandstones indicate transport to the southeast.

CHAPTER 2

STRUCTURE AND STRATIGRAPHY

Introduction

Cursory examination of the study area suggests that the structure is relatively simple, with most of the stratigraphic sequence being located on the south limb of a large anticline that has only minor parasitic folding associated. However, several reverse faults occur which have substantially repeated parts of the stratigraphy and greatly complicated others. This chapter deals with the structural features observed in the area and their effects on the measured stratigraphic section.

The reader is referred to the map in the pocket for the subsequent description and stratigraphic interpretation.

Structure

Folding - The folds in the area have northeast trending

axes and are characterized by axial planes which dip from 68°S to 64°N but most commonly dip south. The folds generally plunge northeast but southwest plunges are evident. The maximum northeast plunge recorded was 77°, while the maximum southwest plunge recorded was 50°. However, these are exceptional and plunges of 10-20° were most common. The fold axis data, when plotted and contoured on an equal area stereographic projection (Figure 2-1), suggests that the folds are parasitic on a structure which is doubly plunging but has a more dominant plunge, 17°NE.

Sinistral (S-shaped), parasitic folds are very common in the section and have amplitudes as great as 50 m, for example, unit 18 at Pointe Caronette. Faulting and subsequent erosion of these folds often gives the appearance that there are several sandstone units rather than one, for example, unit 25 between Anse aux Sauvages and St. Jean-Port-Joli wharf.

Faulting - Steep, south dipping, northeast striking reverse faults dominate the structure of the area. There are five main reverse faults which divide the area into a series of imbricated blocks. These are the Demi Lieu, Au P'tit Fribourg, "Anse à Confusion", Anse aux Sauvages and St. Jean-Port-Joli faults (Figure 2-2).

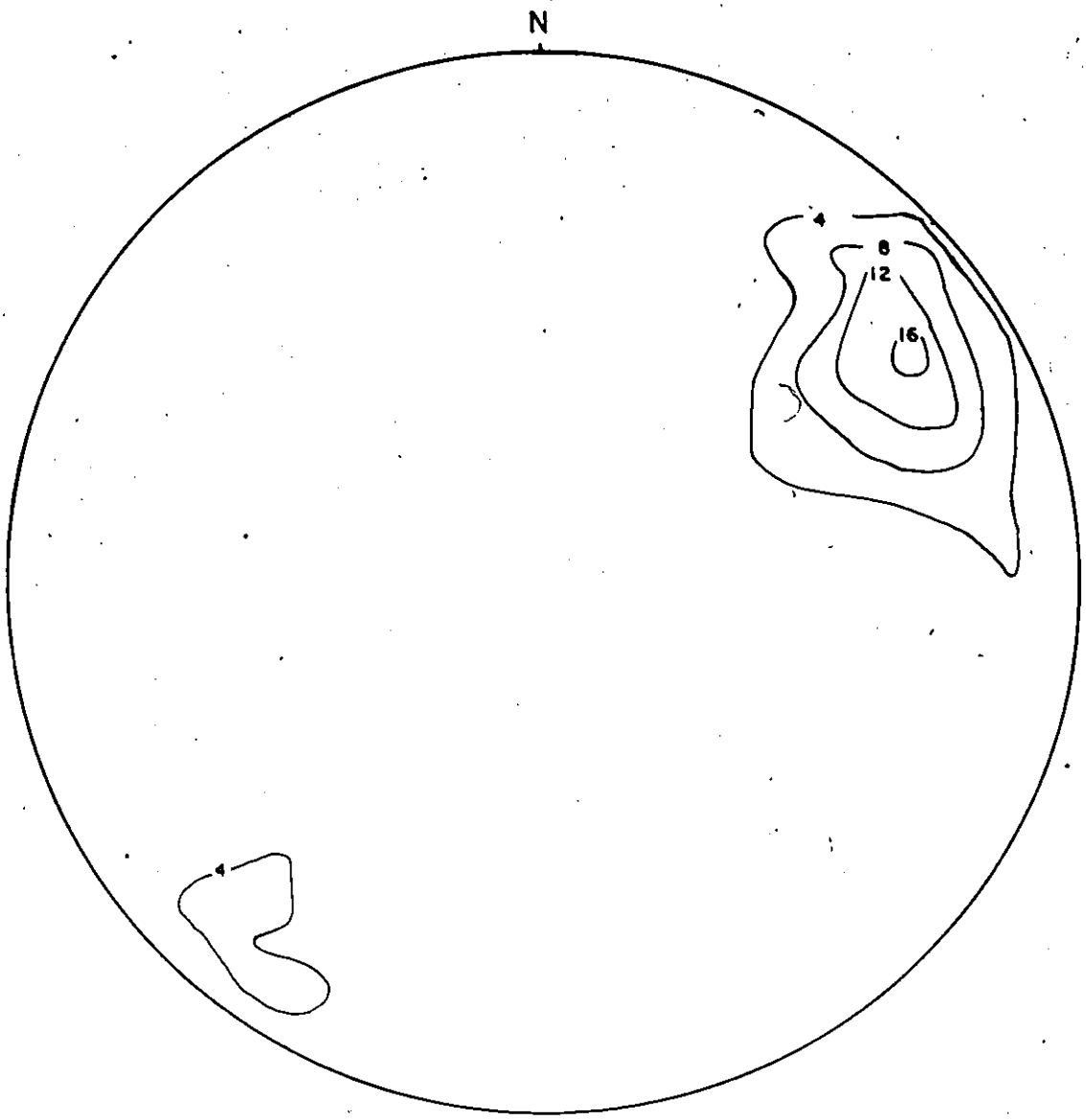

Figure 2-1 Contoured stereoplot of 119 tectonic fold axes
Contour interval: 4 %. Major plunge 17°/058°

The amount of movement along these faults is difficult to estimate because detailed correlation is impeded by the lack of fossils. Nevertheless, reasonable correlation is possible between the sandstone units on either side of the faults. The maximum amount of movement is estimated in the order of 100's of meters.

Re-examination, by the author, of units 14 and 15 at Plage Victor (originally mapped by Hubert, 1969) indicates that faulting has been responsible for the lenticular shape of the classical turbidites in unit 15. But this is not thought to be substantial as comparison of the stratigraphy of units 1-15 and 16-30 shows no repetition has occurred (Figure 2-5).

The truncation of several fold axes, for example unit 23 at Anse à Caronette, suggests that reverse faulting was post-folding (map in pocket).

Strike-slip faults in the area trend from southeast to southwest and show movement up to 15 m. They commonly occur as conjugate sets as exemplified by unit 16 at Plage Victor. They formed after folding but their relationship to reverse faulting is unknown.

The southeast trending faults between Anse aux Sauvages and "Anse à Confusion"[1] may show vertical or

[1]Name given to the cove half way between Anse à Caronette and Anse aux Sauvages which aptly describes its structure.

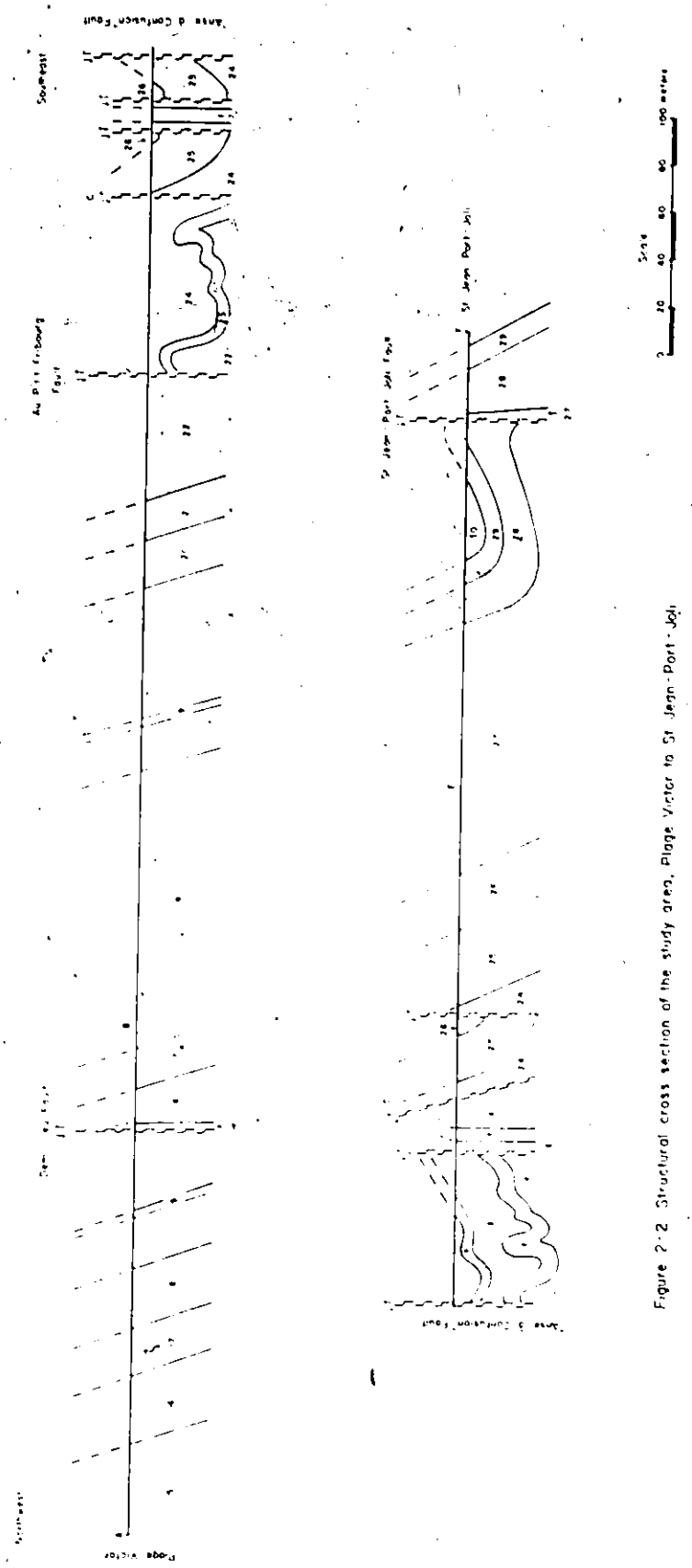

Figure 2-2 Structural cross section of the study area, Plage Victor to St Jean-Port-Joli

lateral movement. They are truncated by the reverse faults in the area and therefore precede them, but are post folding as they truncate the fold axes. The exact stratigraphic relationship between the blocks is unknown, therefore it is impossible to suggest the movement along them.

Stratigraphy

Introduction

The area can be divided into three structural zones: east, central and west. The eastern and western blocks are structurally simple consisting of steep, southerly dipping strata with some internal repetition due to faulting. Faulting has provided a stratigraphic overlap which enables correlation between the two zones.

The central zone is structurally complex as it is transected by several faults. Some of its strata can be correlated with that of the western zone, and thus linked with the eastern zone, but the rest of the sequence in the zone seems to be unique.

Eastern Zone

The eastern zone consists of units 16-26. It is bounded by a conformable contact between units 15 and 16 at

its base, and the "Anse à Confusion" Fault at its top. The zone is disrupted by two major reverse faults: the Demi Lieu Fault and the Au P'tit Fribourg Fault.

The Demi Lieu Fault repeats units 16-19. Stratigraphic comparison of units 16-18 north and south of the fault (Figure 2-3) shows excellent agreement between the types of facies divisions, their thicknesses and their sequence. However, comparison of the thickness of unit 18 north and south of the fault shows that there is a major discrepancy between the two; unit 18 is approximately three times thicker at Pointe Caronette than at Plage Victor.

The excellent agreement (Figure 2-3) between the eight facies of units 16-18 north and south of the fault is too coincidental to be ignored. There is no basis to expect the exact order of depositional processes to be repeated so closely. It is easier to explain the thickness change in unit 18 than it is the repetition of the depositional processes in the same order and proportion.

The Au P'tit Fribourg Fault is marked by considerable discordance between units 22 and 23 in Anse à Caronette. No great amount of movement has occurred along it since fold axes 8-11 north of the fault can be correlated with fold axes 12-15 south of it, and unit 23 is found on both sides of the fault.

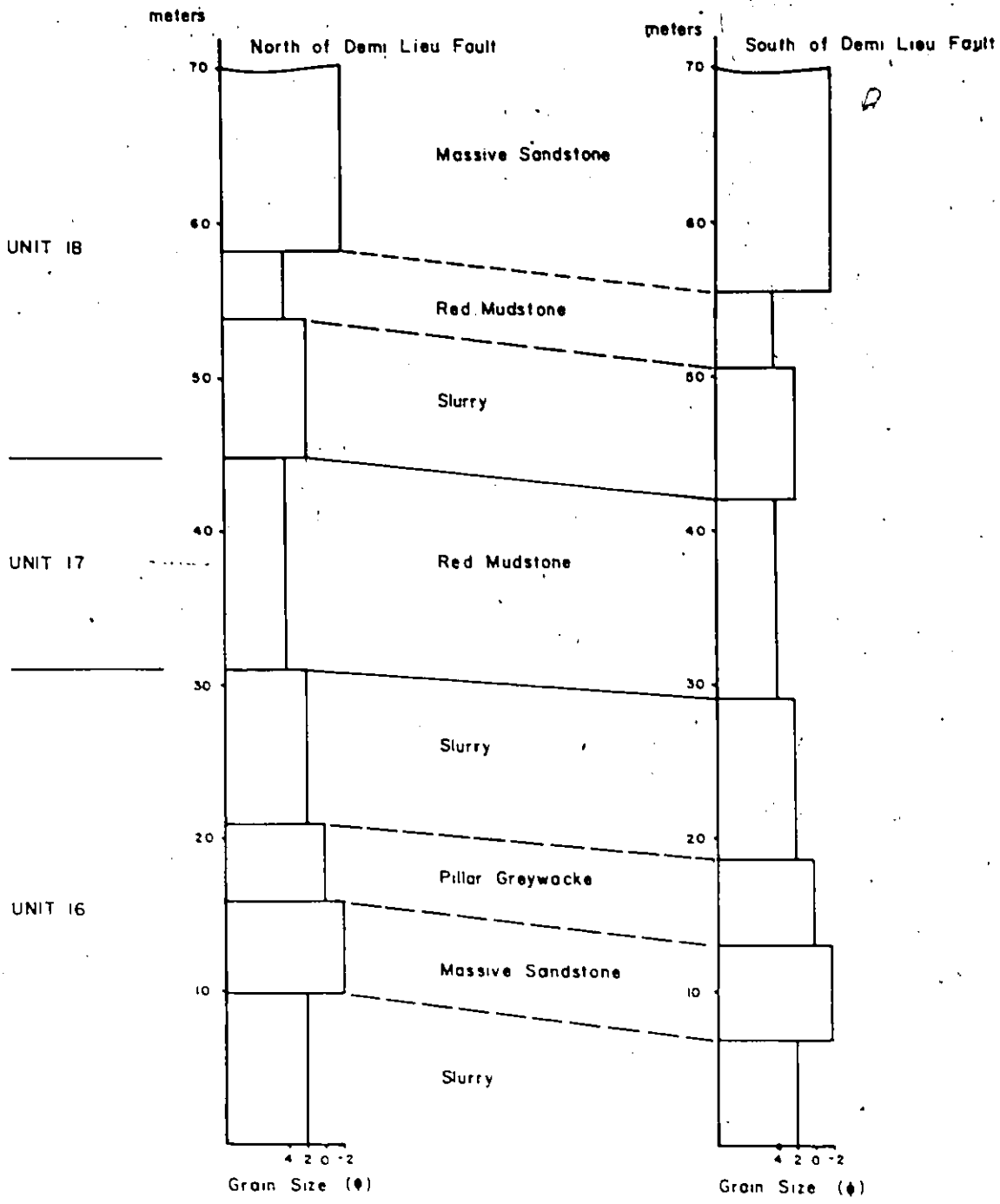

Figure 2-3 Comparison of facies sequence in Units 16-18, north and south of the Demi Lieu Fault

Western Zone

This zone is composed of the stratigraphic sequence from Anse aux Sauvages to the St. Jean-Port-Joli Fault. Most of the strata dip steeply south, but the centre is characterized by very tight folding and faulting which is responsible for the repetition of unit 23_w[1]. Unit 25_w is also repeated by several faulted sinistral folds (verified by measured sections).

The stratigraphic base of the zone is covered by the St. Lawrence River. The lower part of the zone consists of massive sandstone, siliceous classical turbidite and red mudstone units, whereas the top is dominated by thin to thick bedded, calcareous, classical turbidites and black shale.

The best correlation between the eastern and western zones is between units 25_e and 25_w. The units below these also compare reasonably well (Figure 2-4).

Central Zone

This zone is the smallest of the three, but is the most structurally complex. The northern boundary is the "Anse à Confusion" Fault, whereas the southern boundary is covered. It is composed of five fault bounded blocks. The faulting between the blocks obscures the stratigraphic

[1]A unit number which has a letter subscript refers to the zone it is found in, e.g. 23_w - unit 23, western zone.

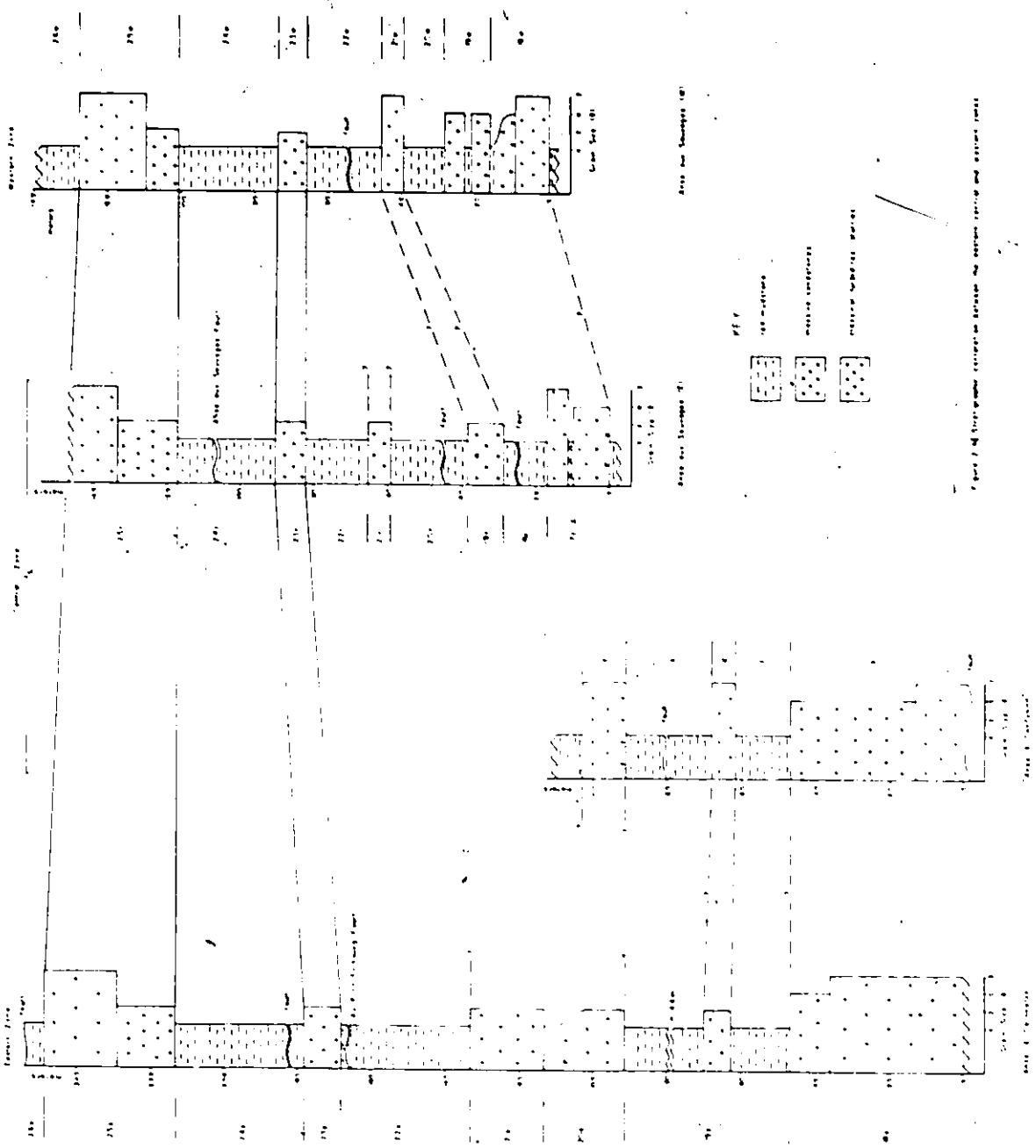

relationships between them so that a stratigraphic section can be obtained by either measuring along the fold axis linking units $A(17_c)$ through e or units $A(17_c)$ to 25_c.

The zone is composed of massive sandstone, siliceous classical turbidite, and red mudstone units.

The correlation between the central zone and the other two zones is not very good. Only unit 25 can be correlated between the eastern and central zones. However, unit 25 and the stratigraphic sequence below it can be correlated across Anse aux Sauvages between the central and western zones.

Correlation

The "best fit" correlation between these three zones is presented in Figure 2-4. The thickness of the stratigraphic column thus obtained is 534 m (Figure 2-5). This is a minimum thickness and is based on the assumptions that the Demi Lieu and Au P'tit Fribourg Faults can be correlated across, that the correlation between units 25_e, 25_c and 25_w is correct, and that the stratigraphic sequence in the western zone is conformable.

Units b through f, of the Central Zone, are

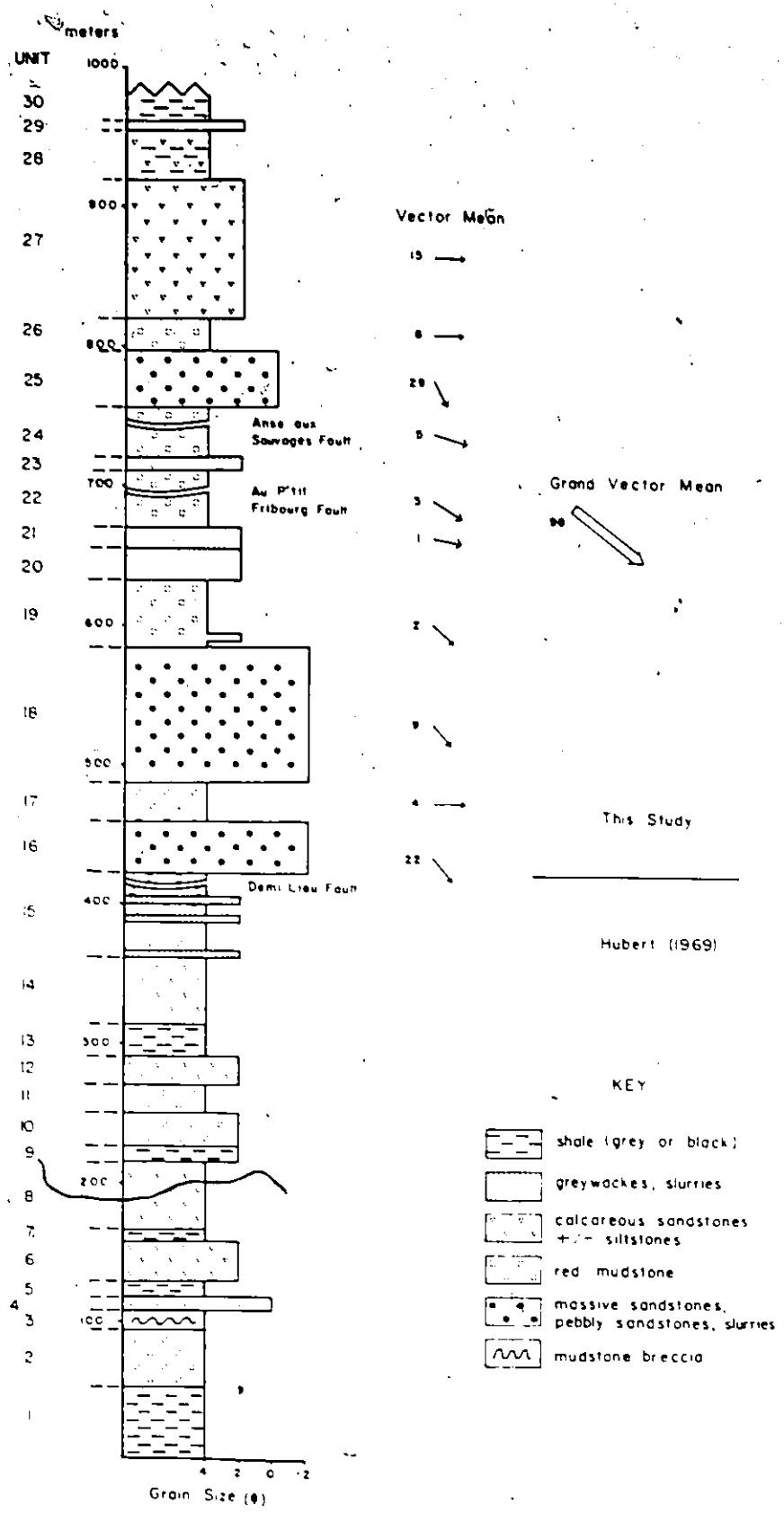

Figure 2-5 Stratigraphic column of the study area including the strata of Plage Victor

tentatively correlated with units 18_e and 19_e. However, if this is incorrect then an extra 65 m must be added to the thickness of the stratigraphic section.

Paleoflow Directions

Measurement of flutes (36), grooves (22), rib and furrow structures (15), current lineations (13) and scours (12) were taken from all units except 20, 23, 28, 29, and 30. The grand vector mean of these ninety-eight paleoflow indicators is 128.4° (standard deviation = 37°).

Comparison of the vector means of the units (Figure 2-5, Table 2-1) shows that the massive sandstone units (16, 18 and 25) have a stronger southerly component than the red mudstone and the siliceous classical turbidite units (17, 19, 21, 22 and 24). However, the greatest divergences are in units 17, 26 and 27. In units 26 and 27 this abrupt change is associated with a petrographic change (siliceous to calcareous), but this is not the case in unit 17. The difference in the vector means of units 16-25 (140°) and units 26 and 27 (90°) is statistically significant (Appendix 1).

The flutes are the most important paleoflow indicators, occurring in all but one of the units in which measurements

were taken. The paleoflow difference between units 16-25 and units 26-27 are best shown by these structures. The vector mean of the flutes has a greater easterly component than any of the other structures, but this is due to the large number of them measured in units 26 and 27, compared to the other units. In units where both flutes and grooves were measured, the flutes show a consistently greater easterly component. The vector means of the flutes do not show a consistent relationship with those of any of the other structures in any of the units.

For any one unit, the vector mean of the grooves has a greater southerly component than that of any of the other structures. However, this is not the case when the vector means of all the structures is compared (Table 2-1). The grooves and current lineations show the same vector means.

Table 2-1 Paleoflow Vector Means for Units 16,17,18,19,21, 22,24,25,26,27

Unit	Flutes	#	Grooves	#	Rib & Furrow	#	Current Lineations	#	Scours	#	Vector Mean	#
16	157.0	5	-	-	139.6	9	-	-	132.8	8	141.1	22
17	84.5	2	-	-	93.5	2	-	-	-	-	89.1	4
18	139.0	3	167.0	1	129.0	3	110.0	1	147.0	1	140.0	9
19	157.0	1	-	-	-	-	109.0	1	-	-	133.0	2
21	-	-	-	-	-	-	-	-	101.0	1	101.0	1
22	122.9	3	-	-	-	-	-	-	-	-	122.9	3
24	115.0	2	120.5	2	-	-	116.0	1	-	-	116.1	5
25	142.6	5	160.4	13	131.0	1	155.0	9	165.0	1	154.7	29
26	88.8	5	92.0	2	-	-	-	-	88.0	1	89.5	8
27	92.2	10	91.7	4	-	-	70.0	1	-	-	90.6	15
	116.4	36	138.9	22	130.7	15	138.7	13	130.4	12	128.4	98
Standard Deviation	32		39		26		36		25		37	

CHAPTER 3

FACIES DESCRIPTIONS

Introduction

Before an interpretation of the depositional environment is attempted, it is very important to provide a full description of the facies studied (Blatt, Middleton and Murray, 1972). Such a description does four things:

(1) It enables a systematic comparison with various facies models;

(2) It provides input into existing facies models;

(3) It provides a basis for continued work within the study area;

(4) It allows scrutiny of the interpretation.

There were eight facies recognized in the study area: red mudstone, massive sandstone, pebbly sandstone, slurry, classical turbidite, pillar greywacke, slump and pebbly mudstone. The first five are the most common and most diagnostic of the mode and locus of deposition of the St. Roch Formation sediments.

This chapter provides a comprehensive description of these facies, which form a basis for interpretation later in the thesis.

The Red Mudstone Facies

The red mudstone facies (Figure 3-1) forms approximately one third of the measured section. It occurs as units 10-40 m thick which alternate with the sandstone units. The facies is dominated by red mudstone which has intercalated thin bedded turbidites and pink and grey limestone conglomerates (Figure 3-2). It has a turbidite-mudstone ratio of 1:10.

The red mudstones also occur as thin interbeds with the slurry and classical turbidite facies. But regardless of where it occurs, it is always devoid of primary sedimentary structures. A bedding plane cleavage is well developed in all examples. The red color of the mudstones is prevalent throughout the section, but locally there are isolated grey horizons. The grey horizons are also common along the contacts with sandstone beds.

In thin section the red mudstones may show thin disrupted laminae (Lajoie and Chagnon, 1973) and they are composed of poorly sorted, coarse silt size quartz, feldspar

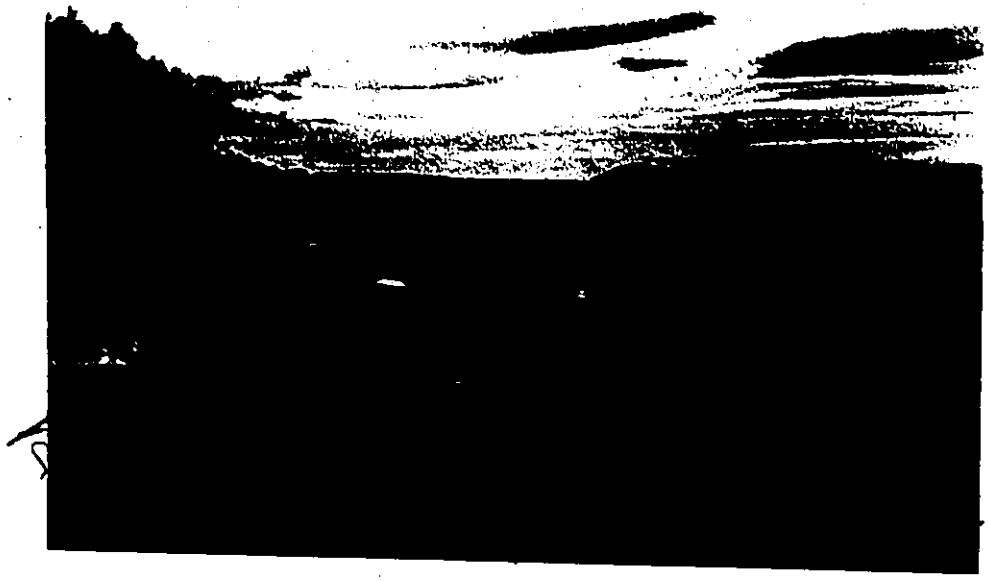

Figure 3-1 Interbedded red mudstone and thin bedded turbidites of unit 24, Anse à Caronette. View west. Stratigraphic top to the left. Discontinuity of turbidites due to structural deformation.

Figure 3-2 Pink limestone conglomerate lens interbedded with red mudstone of unit 26, east of St. Jean-Port-Joli wharf. Scale is 18 cm long.

and mica in a fine silt matrix (Hubert, 1965). The fine silt and clay fraction is composed mainly of illite, quartz and hematite with minor amounts of feldspar, chlorite and chamosite (Lajoie and Chagnon, 1973).

The thin bedded turbidites are tan, grey or red in color. Their thickness ranges from 2-30 cm, but it averages 10 cm. The bed thickness is consistent laterally, but rare beds contain lenses up to five times the original bed thickness, scoured into the underlying mudstone.

The soles of the turbidites are commonly fluted. The beds usually show distribution grading but rarely are all Bouma divisions visible. The most common sequence observed is BCE but many of the beds show no sedimentary structures.

Petrologically, the thin bedded turbidites may contain up to 55% quartz, 25% glauconite, 5% rock fragments, 7% feldspar, 19% cement, 6% matrix and 7% miscellaneous minerals. The quartz fraction is made up of two varieties: monocrystalline, which commonly shows undulose extinction, and polycrystalline. The amount of monocrystalline quartz always exceeds that of the polycrystalline quartz. The feldspars show a high degree of sausseritization. Glauconite occurs replacing sedimentary grains, replacing the matrix, and as well rounded grains. The rock fragments are mainly granitic and gneissic. The cement is usually silica, but

minor amounts of carbonate occur. The miscellaneous components are authigenic opaques, collophane, zircon and biotite. The opaques are commonly associated with the glauconite, either concentrated along cleavage traces or the grain boundary.

The turbidites are poorly to moderately sorted. The grain size is up to coarse sand and the grains are angular to rounded, but most are subrounded.

In unit 26, pink and grey limestone conglomerates are interbedded with the red mudstone. Most of the conglomerate is concentrated in lenses up to 3 m x 70 cm scoured into the underlying mudstone. The lenses thin, and the clast size of the conglomerate decreases laterally. The thickness changes as much as eight times in some cases. The conglomerates rarely show scour marks.

Both types of conglomerate exhibit either distribution or coarse tail grading. Some of the conglomerate lenses show no sedimentary structures, but their finer grained lateral equivalents commonly show cross stratification up to 20 cm thick. The finer grained, upper 4-10 cm of other conglomerates show parallel and cross lamination.

The clast size of the pink conglomerates is up to 7 x 2 cm, whereas it is only up to 1.5 x 0.5 cm in the grey conglomerates. The clasts are well rounded but commonly

show stylolitized boundaries. The pink limestone conglomerates are composed only of limestone clasts, whereas the grey limestone conglomerates contain limestone, quartz, and feldspar. The matrix of the pink conglomerate is red mudstone which imparts the pink color. The matrix of the grey conglomerate is composed of very coarse grained quartz, feldspar, shale and glauconite. In both types of conglomerates the limestone clasts contain shell and trilobite fragments.

The Massive Sandstone Facies

The massive sandstone facies (Figure 3-3) is the major constituent of the massive sandstone units (16, 18, and 25). The massive sandstone beds are up to 12 m thick, and range in grain size from medium sand to very fine pebble. They are usually buff to rust in color due to the weathering of secondary pyrite.

The massive sandstones have flat or scoured bases which rarely exhibit giant, deltoid shaped, flutes that measure up to 75 x 35 cm (Figure 3-4). Where the massive sandstones overlie each other the base is either amalgamated to the bed below, or flat. In the latter case, spectacular

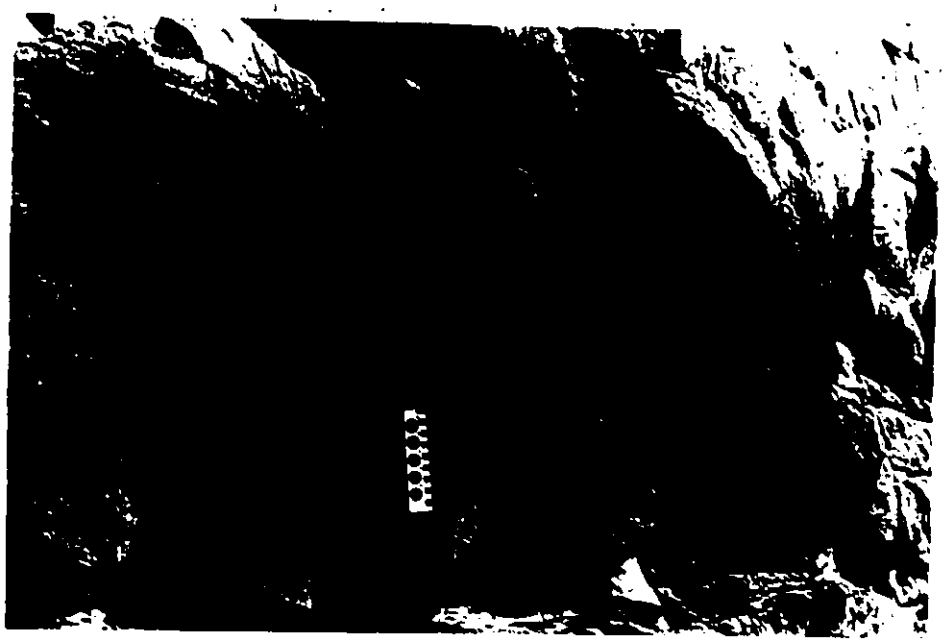

Figure 3-3 Massive sandstone bed in unit 16, Plage Victor. Scale is 18 cm long. Top of photo is stratigraphic top.

Figure 3-4 Giant flutes on the base of a massive sandstone bed in unit 18 at Demi Lieu. Figure is 1.59 m tall.

loading is developed.

The massive sandstones always exhibit coarse tail grading. Sedimentary structures are uncommon, except for cross stratification, which occurs in calcareous lenses that are at the base or top of the beds. The cross stratified lenses may be up to 1.5 m x 0.5 m, in some cases the stratification is accentuated by aligned shale and collophane clasts. Calcareous lenses up to 54 x 36 cm containing only shale and collophane clasts and no cross stratification are common. These may contain calcitic, spherulitic nodules (Figure 3-5) and fluid escape features, as well. In plan view they look like oblate ellipsoids and have been referred to as concretions (Hubert, 1965, 1973).

Fluid escape features are common in the thick bedded massive sandstones. Dish structures are more common than pillar or sheet structures. No relationship between any of the fluid escape features was observed.

The dish structures always occur in calcareous lenses that are found in the upper half of the beds. They are poorly formed and, in some cases, look more like disrupted parallel laminations. Near the bases of some lenses faint parallel laminations can be seen passing upwards into wavy laminations and then disrupted lamination (Figure 3-6).

Pillars are uncommon, but two types were recognized:

Figure 3-5 Photomicrograph of a spherulitic calcite nodule (sample P57, crossed nicols, 30x). Note extinction crosses.

Figure 3-6 Calcareous lens in massive sandstone bed showing transition from parallel laminations to undulating laminations. Top of photo is stratigraphic top.

type D (Lowe, 1975) which were up to 2 x 0.5 cm, and type B (Lowe, 1975) which were up to 25 x 1 cm and oriented obliquely to the bedding plane. The type B pillars were found in coarser grained beds than type D.

Sheet structures are rare. One spectacular example (bed 16-1-14 at Demi Lieu) has radiating sheet structures that extend up to 40 cm from a nodal point and are up to 1 cm wide (Figure 3-7).

Amalgamation is very common and is denoted by a change in grain size and normal grading. A peculiar feature of the massive sandstones which may be related to amalgamation is the presence of weathered-out horizons spaced irregularly throughout the bed. These horizons are up to 3 cm wide and can be traced from 1-10 m. There is no change in composition or grain size across these horizons.

The tops of the massive sandstones are generally sharp. However, some examples show a decrease in the degree of induration in the top. These examples are usually overlain by fine grained shaley sandstone.

Petrologically, the massive sandstones contain up to 70% quartz, 8% feldspars, 4% rock fragments, 3% glauconite, 3% cement and 1% miscellaneous.

Undulose monocrystalline quartz was more common than polycrystalline quartz. Overgrowths were seen on the

Figure 3-7 Radiating sheet structures on the top of a massive sandstone bed in unit 16, Demi Lieu. Scale is 18 cm long.

Figure 3-8 Pebbly sandstone in unit 16, Demi Lieu, showing well graded base and irregularly spaced weathered out horizons. Stratigraphic top to the right.

quartz in several examples. The few rock fragments recognized were chert and shale. However, the degree of recrystallization severely obscured grain boundaries, so that granitic and gneissic fragments may have been mistaken for quartz or feldspar grains. The feldspars showed a high degree of sausseritization. Glauconite occurred as rounded grains and interstitially. Sparry calcite seemed to be the main cement but this may have been secondary void fillings. The sandstones are moderately to well sorted and the grains are sub to well rounded.

The Pebbly Sandstone Facies

The pebbly sandstone facies (Walker, 1978) (Figure 3-8) is uncommon in the section, only occurring in units 16 and 18. The pebbly sandstones are grey and white in color and generally thick bedded (2-2.5 m); however, they may be as thin as 53 cm.

The pebbly sandstones always occur as lenses scoured into the underlying beds. They are always found interbedded with the massive sandstone facies in the middle of the massive sandstone units. They are never seen scouring into or directly overlying each other. The bases of the lenses

can be flat to gently undulating or show flame structures (Figure 3-8). The thinner lateral equivalents of the lenses are flat and in one case a giant, deltoid shaped, flute 1 m x 50 cm was seen.

In contrast to the definition of Walker (1978), no sedimentary structures, other than distribution grading, is seen in the pebbly sandstone (Figure 3-8). Imbrication is well developed in this facies and field observations suggest that the AB plane of the pebbles dip to the north or upstream, when compared with paleocurrent measurements in the units.

Amalgamation is never seen in this facies. However, like the massive sandstone facies, weathered out horizons are commonly spaced irregularly throughout the bed (Figure 3-8).

The pebbly sandstones are mainly composed of quartz and shale clasts with lesser amounts of feldspar. The clasts are well rounded and measure up to 1.5 x 1 cm. The matrix consists of coarse grained quartz sand.

The outcrops of pebbly sandstone studied represent a cross section oblique to paleoflow. The lenses measure up to 20 x 3 m, and either pinch out at the edges or thin consistently and decrease in grain size laterally. These lateral equivalents can be traced up to 60 m, and locally are scoured out by a much coarser bed occupying the same stratigraphic position.

Classical Turbidites

Classical turbidites (Walker, 1978) are very common in the section. Two types were distinguished: calcareous and siliceous. The calcareous classical turbidites make up a greater part of the section than the siliceous classical turbidites. However, the calcareous classical turbidites are not found interbedded with any other facies except the red mudstone. The calcareous classical turbidites are only found in the upper part of the section, in units 27 and 28, whereas the siliceous classical turbidites occur in all the other sandstone units.

The grey, calcareous classical turbidites of unit 27 (Figure 3-9) are up to 3.2 m thick (average 25 cm). Their maximum grain size is coarse sand, but they are usually fine grained. Their bases are always sharp and flat. Flutes, grooves, and aligned trace fossils are very well developed locally, but are not common to every bed.

The calcareous wackes rarely exhibit distribution grading. Sometimes the basal 10 cm of the beds contain low angle (<10°) cross stratification. Parallel lamination, climbing ripple cross lamination, and convoluted ripple cross lamination are common to most beds. The top of the beds is always sharp.

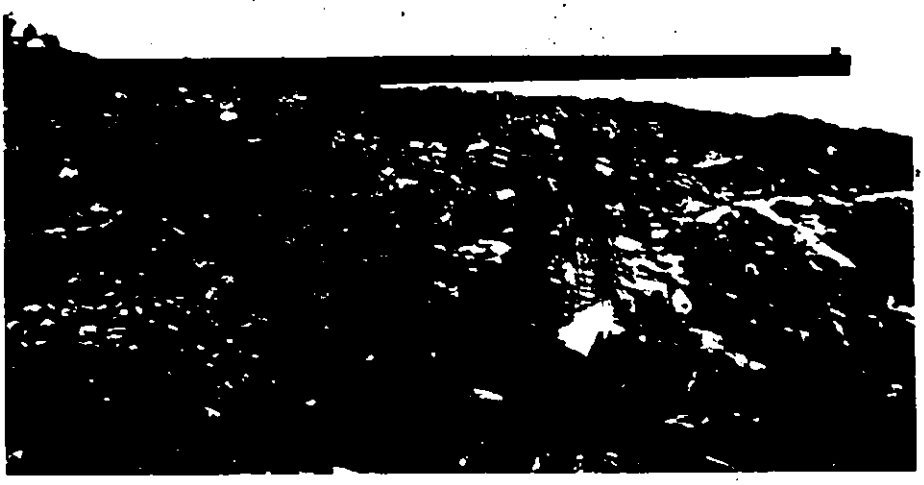

Figure 3-9 Calcareous classical turbidites in unit 27 near St. Jean-Port-Joli wharf. Stratigraphic top to the left.

Figure 3-10 Siliceous classical turbidites in unit 21 at Anse à Caronette. Stratigraphic top to the left.

Unit 28 is composed of very thin to thin bedded calcareous to dolomitic classical turbidites. They rarely show sedimentary structures.

The siliceous classical turbidites (Figure 3-10) are green to buff in color and range from 0.05-1.2 m thick. The maximum grain size is very coarse sand. They are found interbedded with the massive sandstone and slurry facies in the massive sandstone units, or only with the slurry facies in the siliceous classical turbidite units (see discussion in Chapter 4). The bases are flat and sharp or scoured and uneven. They commonly show flutes and/or grooves which sometimes show divergent current directions. The turbidites commonly exhibit distribution grading, parallel and cross lamination. Locally, parting lineation was observed in parallel laminated beds. Fluid escape features such as sheet and pillar structures are rare. The tops of the beds are sharp or gradational to the E division.

Slurry Facies

The slurry facies (Wood and Smith, 1959) is common to all noncalcareous sandstone units. The facies consists of two types of beds: slurry beds (Figure 3-11), which do

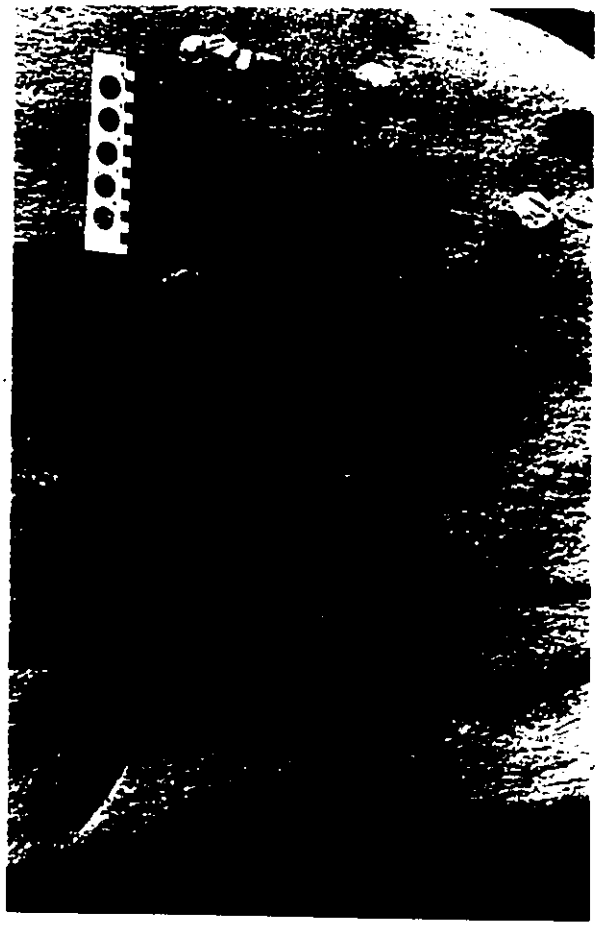

Figure 3-11 Slurry bed in unit 16, Demi-Lieu. Note the flat base, irregular, shaley parting and pseudonodules. Scale is 18 cm long.

not show internal subdivisions, and slurry-breccia beds (Figure 3-14) which are composed of a basal greywacke overlain by a breccia zone. Both types may be green, red, green and red, or red and yellow in color. They are composed of medium to very coarse grained sand in a silt to clay size matrix. The beds are usually less than 1 m thick, but some of the slurry-breccia beds are up to 3.5 m.

The slurry beds always have a sharp, flat base which is devoid of sole marks. The main part of the bed shows few features except for irregular shaley parting. Commonly the basal 5-10 cm shows normal grading. Scattered throughout the main part of the bed are pseudonodules, shale clasts and granule size grains of quartz and feldspar. The main part of the bed always grades into the overlying mudstone.

Amalgamated slurry beds are very common and in some cases several amalgamations can be seen. The amalgamations may be denoted either by a thin (1-3 cm) horizon of granule size grains which is usually graded (Figure 3-12), or by a color change. In the upper part of the beds parallel and ripple cross laminated very fine sand may be amalgamated to and show loading into the main part of the slurry bed (Figure 3-13).

There are three slurry-breccias in the section (Beds 20-1-21, 25-1-6 and 25-1-13). Bed 20-1-21 has some important

Figure 3-12 Amalgamation in a slurry bed (unit 16, Plage Victor) denoted by a thin horizon of granule size sand. Scale in cm.

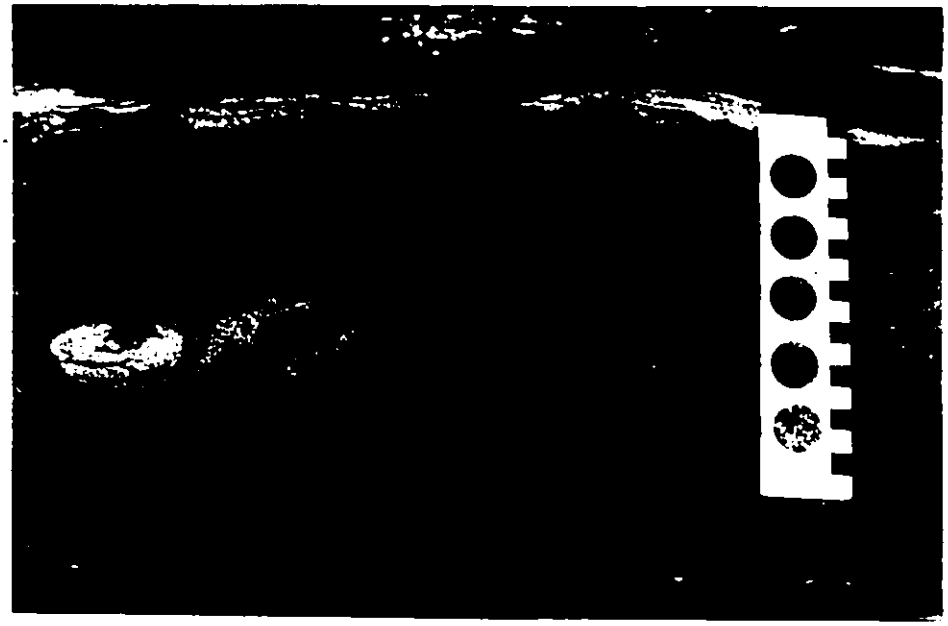

Figure 3-13 Pseudonodules which have formed from a fine grained sandstone which is amalgamated to the top of the slurry bed. Unit 16, Plage Victor. Scale in cm.

differences from the other two and therefore will be described in detail, whereas the features of the other two will be summarized.

Bed 20-1-21 (Figure 3-14) is composed of a basal, fine grained greywacke which is overlain by a heterogeneous mixture of red mudstone and yellow, medium grained sandstone. It varies from 1.1 to 3.5 m thick and can be traced laterally 210 m. The proportions of mudstone and sandstone in the upper part varies greatly from all mudstone to a sandstone-mudstone ratio of 2:1.

The basal greywacke, up to 1.2 m thick, has a flat base which has no sole marks. It is structureless, except for a few pseudonodules and poorly developed irregular parting. Laterally, the greywacke is discontinuous, disappearing abruptly in places and thinning regularly in others. Where it ends abruptly it usually has a jagged edge giving the appearance of being ripped up (Figure 3-14 d).

Above the basal greywacke is a mottled mixture of red mudstone and yellow sandstone (Figure 3-14a). Close to the greywacke, the matrix of the mixture is very fine grained red sandstone with diffuse, spindle shaped clasts (up to 70 x 10 cm) of yellow fine to medium grained sandstone. The clasts rarely show evidence of soft sediment deformation. Where there is little or no greywacke, the breccia is absent

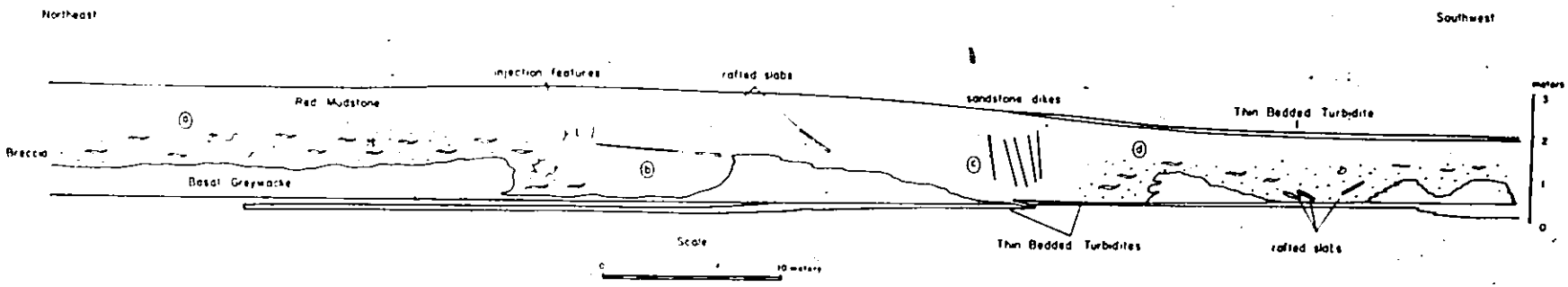

Figure 3-14 Features of the western half of the slurry breccia in bed 20 - 21 Clasts in breccia not to scale

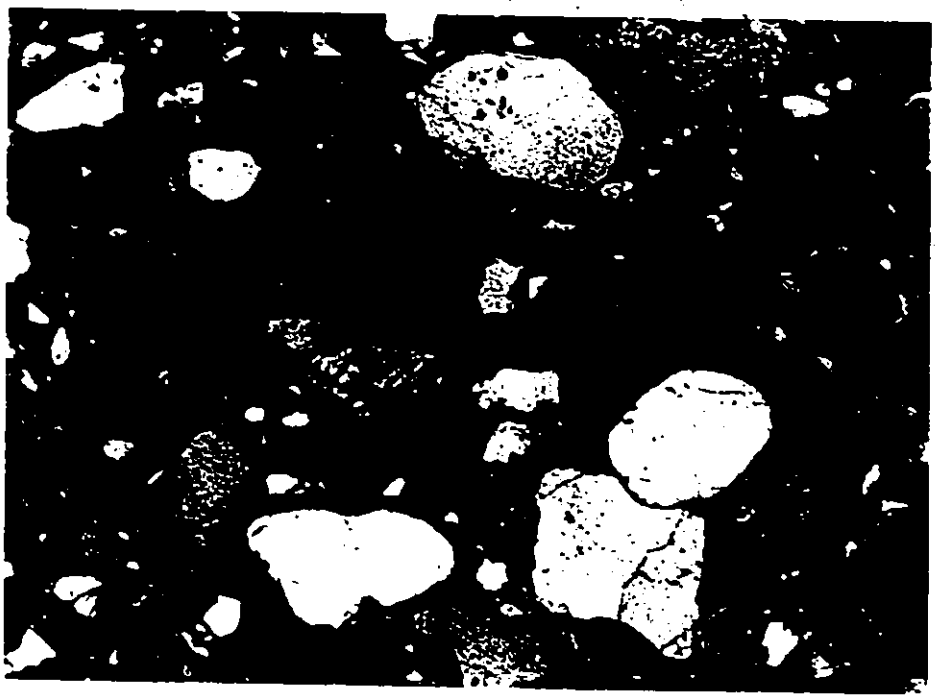

Figure 3-15 Photomicrograph of slurry facies. Note fabric developed in the matrix but haphazard arrangement of large grains (sample P11, crossed nicols, 75x)

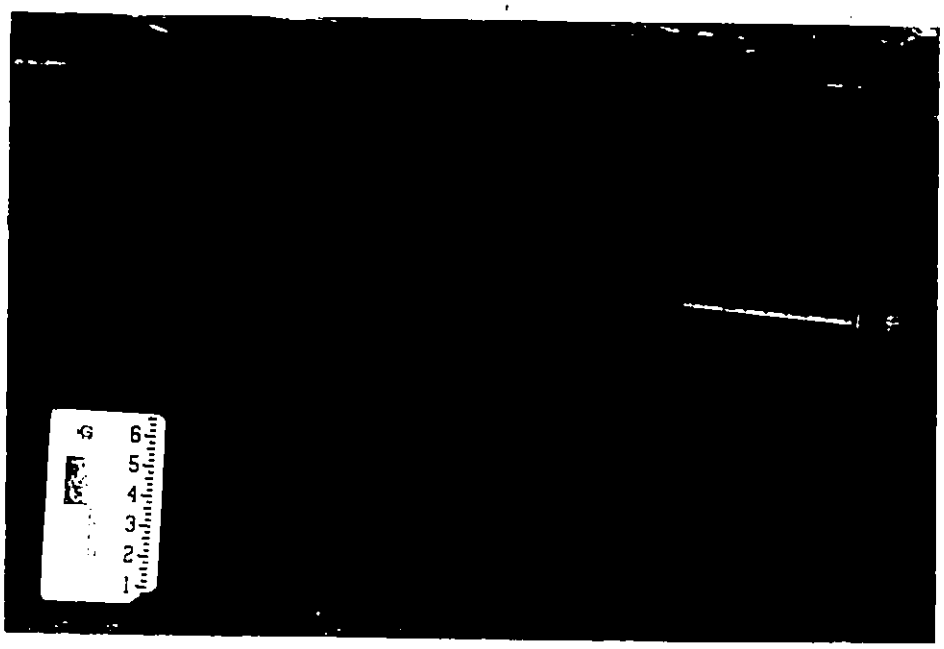

Figure 3-16 Top of pillar greywacke bed, unit 16, Demi Lieu. Note sinuosity of pillars. Scale on book in tenths of feet.

and red mudstone takes its place. Thin, sandstone dikes (Figure 3-14c) are associated with areas in which the basal greywacke is absent. However, these features are rare.

Associated with the red mudstone in this slurry-breccia bed are slabs of very fine to fine grained, parallel laminated sandstone (Figure 3-14b). They range from 1.5 x 0.15 m to 10 x 0.15 m, and dip west at an angle which varies from 5-40° to bedding.

The other two slurry-breccias (25-1-6 and 25-1-13) are similar to that described above, in that there is a discontinuous base, but the upper part is more like a slurry bed. The basal greywacke has a flat base on which there are no sole marks. The greywacke may form all or none of the bed. Normal grading is present only in the basal 5-10 cm of the western part of bed 25-1-6.

The upper part of these beds has a poor to well developed breccia. The sandstone clasts are much more poorly defined than in bed 20-1-21, and appear more like better cemented patches than clasts. Minor amounts of pseudonodules and rock fragments were observed in the breccia zone.

The petrology of the slurry and slurry-breccia beds is very similar. They contain up to 45% quartz, 5% feldspars, 2% rock fragments, 50% matrix and 5% miscellaneous. In the

quartz fraction, undulose monocrystalline quartz was more common than polycrystalline quartz. The feldspars show a high degree of sausseritization. The rock fragments were granitic and gneissic. Miscellaneous components of these beds are muscovite, biotite, glauconite, opaques and rutile. The matrix content of the slurry-breccias is lower than the slurry beds. The matrix exhibits a fabric which is parallel to bedding but the grains are scattered randomly throughout it (Figure 3-15). The grain shape ranges from angular to well rounded, but most of the grains are angular to sub-angular.

Pillar Greywacke Facies

The pillar greywackes (Figure 3-16) are characterized by a profusion of fluid escape pillar structures. They only occur in unit 16 overlying massive sandstone beds. These dark grey greywackes are medium to very coarse grained and have a maximum thickness of 2.5 m.

The soles of the pillar greywackes are flat to undulating and featureless. No grading or sedimentary structures are found in these beds. Rarely, trough cross stratified, very coarse sandstone lenses are present. (Bed 16-1-18 at Demi Lieu). These lenses are up to 26 cm thick and 1 m

Figure 3-17 Penecontemporaneous deformation of cross stratified lens in pillar greywacke, unit 16, Demi Lieu.

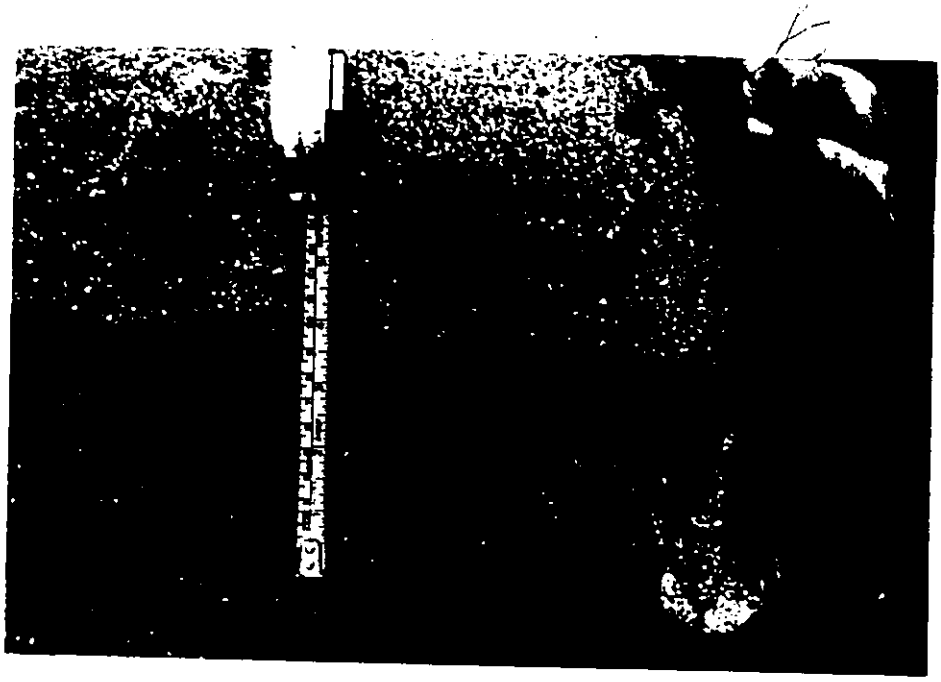

Figure 3-18 Large and small pillars truncated by sandstone lens in pillar greywacke, unit 16, Demi Lieu.

long. Some of the lenses show dramatically warped cross strata indicating penecontemporaneous deformation (Figure 3-17).

The pillars found in these beds are either thin, wispy and irregular (up to 0.5 x 0.5 x 10 cm), or thick and straight (up to 2 x 3 x 15 cm). They are most similar to the type B pillars of Lowe (1975). Neither type shows organization or preferred orientation. The ends of the pillars cannot always be seen, but in bed 16-1-18 at Demi Lieu, both types of pillars can be seen terminating against the very coarse sandstone lenses (Figure 3-18).

Thin sections cut perpendicular to bedding show that the grain size of the sand inside the pillars is greater than that outside them. Furthermore, the micas which are common in the finer grained sediment are aligned parallel to the axis of the pillars (Figure 3-19). Modal analysis of this facies is considered invalid because of the heterogeneity of the thin sections studied.

The Slump Facies

Two slump horizons were found in the section. They differ both in the types of deformational structures in them and the way in which they formed.

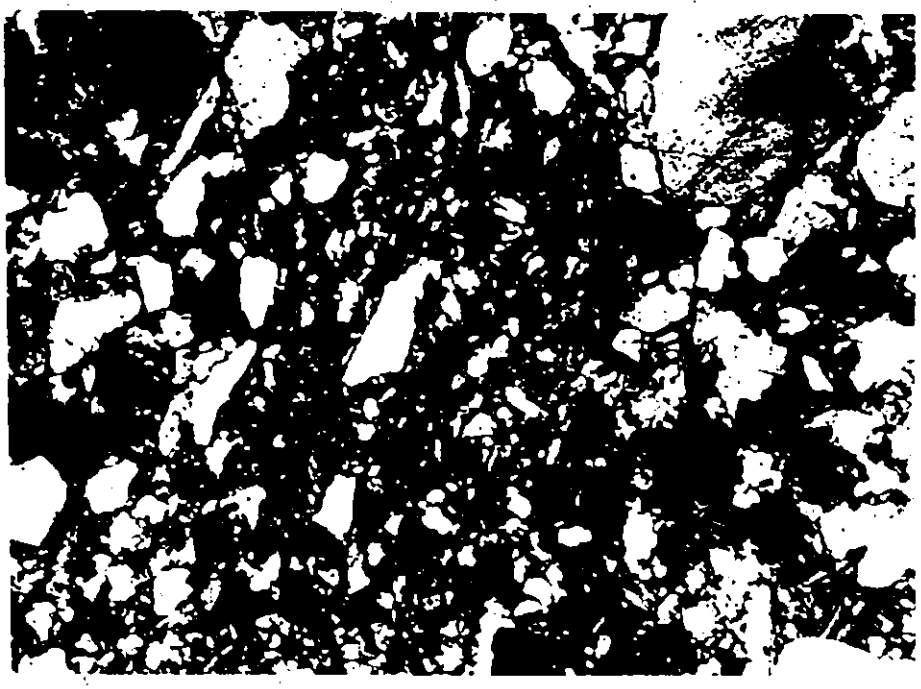

Figure 3-19 Photomicrograph of pillar greywacke facies showing grain alignment in finer grained material outside of pillar (sample P4, crossed nicols, 75x).

Figure 3-20 Reverse fault which truncates red mudstone-fine grained sandstone slump, "Pointe à Confusion". Note tectonic folding in foreground.

At the top of unit 26 at "Point à Confusion", a red mudstone buff, fine grained sandstone slump occurs. Associated with this is a high angle reverse fault which places a very thick bedded massive sandstone on top of the red mudstones and classical turbidites (Figure 3-20).

The reverse fault cuts the slump horizon obliquely, so that it cannot be traced west of the fault. The red mudstones which underlie the massive sandstone west of the fault, exhibit tectonic parasitic folds which have an amplitude of 1 m, are overturned to the north and all plunge east. Where the slump horizon begins, near the fault, the slump consists of rolled up clasts of buff, fine grained sandstone in a red mudstone matrix (Figure 3-21). As the horizon is traced east the number of rolled up clasts decreases, but isoclinally folded fine grained sandstone beds become more common and the folds become more continuous. They have fold axes which strike and plunge east (Figure 3-22).

The top of unit 27 is marked by a calcisiltite-shale slump. It is composed of grey to light brown, 3-10 cm thick calcisiltite beds and black shale. It is up to 3.5 m thick and can be traced laterally approximately 330 m around a syncline-anticline pair (see map in pocket). The eastern end of the slump pinches out approximately 10 m from the

Figure 3-21 Roll up structures in red mudstone-fine grained sandstone, "Point à Confusion". Top of photo is stratigraphic top.

Figure 3-22 Isoclinal folds in red mudstone-fine grained sandstone slump, "Pointe à Confusion". Photo taken east of Figure 3-21. Scale is 18 cm long.

Figure 3-23 Intraformational folding in the calcisiltite slump at the top of unit 27, west of the St. Jean-Port-Joli wharf.

beach, whereas in the west the horizon ends at the St. Jean-Port-Joli Reverse Fault.

At the base of the slump there is very little disturbance of the underlying beds. The calcisiltite beds are arranged in packets which are stacked on each other and show varying amounts of discordance with the underlying strata (Figure 3-23). These packets also occur as isoclinal folds completely detached from the underlying strata. Slump folds are ubiquitous in the horizon, occurring randomly throughout the packets or as parasitic folds on larger scale anticlines. The axes of these slump folds have random orientations.

Some tectonic parasitic folding is associated with the syncline-anticline pair, but the attitudes of these axes are much more regular than those of the slump folds. Along the north limb of the syncline there are no folds in the overlying and underlying very thin bedded turbidites, which would have been expected if the slump horizon were tectonically induced.

Pebbly Mudstone Facies

The pebbly mudstone facies (Crowell, 1957) (Figure 3-24)

occurs only in horizon 27-2-3. It is relatively consistent in thickness (2.8 m) and can be traced laterally for 270 m. It is interbedded with red mudstone.

This horizon has four distinct parts: (1) a basal green mudstone; (2) parallel laminated sandstone with limestone conglomerate-filled scours at the base; (3) green and red mudstone with scattered limestone clasts and (4) parallel laminated and cross laminated sandstone with limestone conglomerate-filled scours at the base. The reader is referred to Figure 3-24 in order to follow the succeeding discussion.

The basal part of the pebbly mudstone consists of laminated green mudstone, which locally contains westerly dipping slabs of laminated red and green mudstone (up to 70 x 10 cm) and grey limestone (up to 35 x 5 cm) (Figure 3-24a). The basal green mudstone can be found sporadically in the western half of the bed. The effects of deformation in it diminish as it is traced east, from west dipping slabs to only disrupted laminae. A few small limestone pebbles are scattered through this part.

The parallel laminated sandstone-limestone conglomerate part overlies the basal green mudstone and is up to 58 cm thick. The limestone conglomerate is always located in lenses which are scoured into the underlying green mudstone.

Northeast

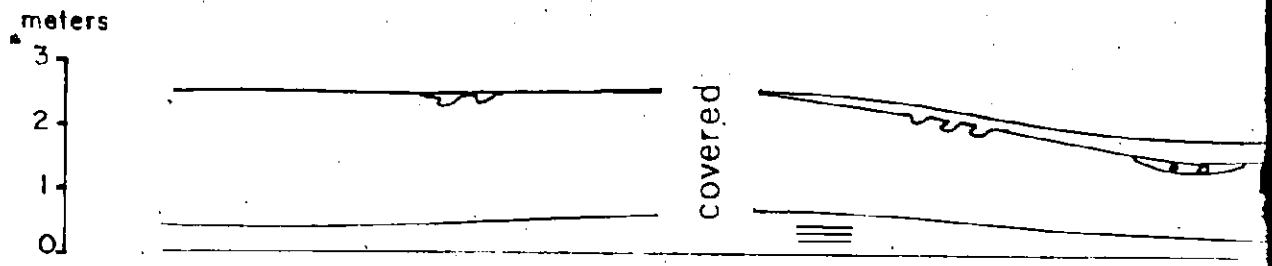

thin be

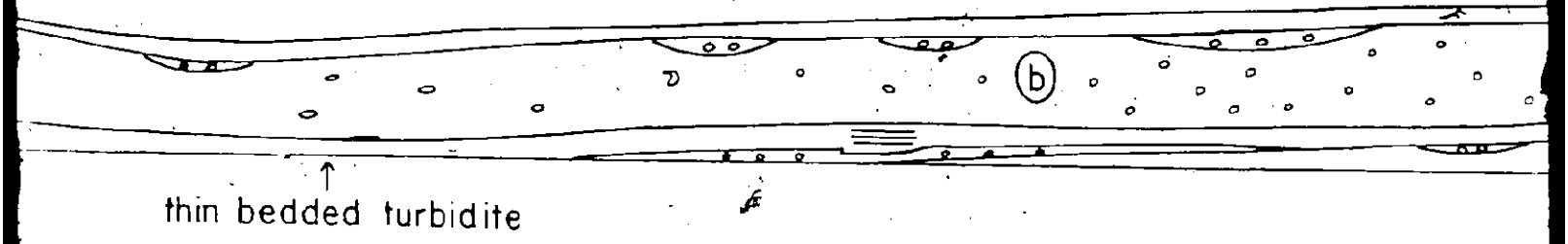

thin bedded turbidite

Scale

0 10 20 30 meters

Figure 3-24 Features of the pebbly mudstone ho

2 of

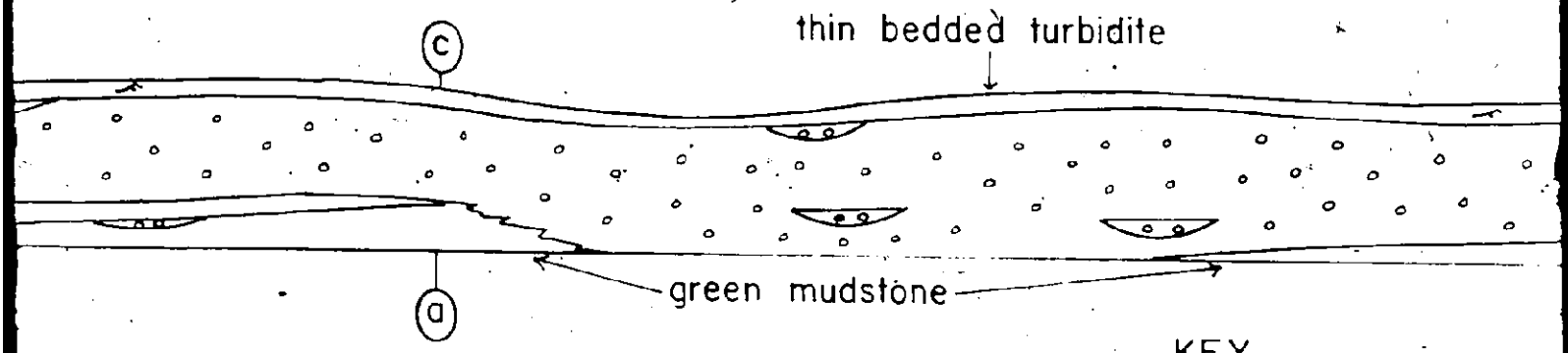

KEY

- load casts
- limestone clasts
- parallel laminations
- imbricated mudstone slabs
- ripple cross lamination

eters

dstone horizon, bed 27-2-3.

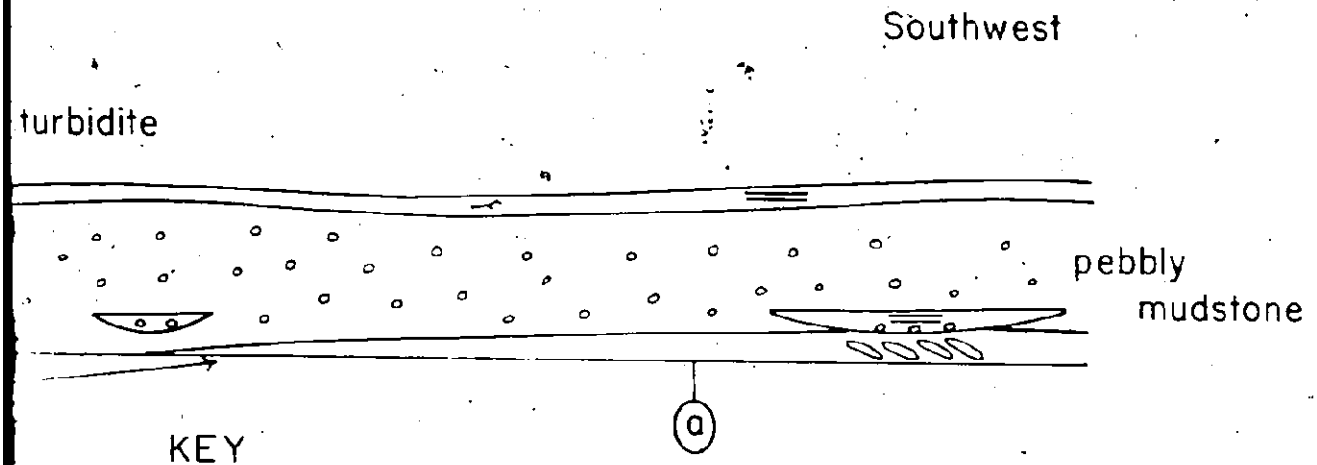

KEY

load casts

limestone clasts

parallel laminations

imbricated mudstone slabs

ripple cross lamination

The limestone clasts are up to 25 x 4 cm and show no particular orientation. The thickness of the limestone conglomerate lenses is up to 21 cm. The parallel laminated sandstone in the top of this part ranges from 20-50 cm thick. The grain size of this sandstone coarsens eastward from fine to coarse sand. In the western end of the bed the parallel laminated sandstone-limestone conglomerate occurs irregularly as lenses just above the base of the bed, whereas in the eastern half of the exposure it is continuous and relatively constant in thickness. The number of limestone conglomerate lenses decreases eastward until they are no longer present.

The main part (Figure 3-24b) of the pebbly mudstone horizon is composed of red and green mudstone with grey limestone, sandstone and shale clasts scattered haphazardly throughout the bed. This part is mainly green in color, but in the eastern end a red color is more persistent. Limestone dominates the clast lithologies, but the number of clasts decreases eastward as does the dominance of limestone. The limestone clasts are well rounded and show no soft sediment deformation, whereas the sandstone, and particularly the shale clasts, show some roll up structures. The maximum clast size of the limestone is 23 x 7 cm and the maximum size of the shale clasts is 60 x 15 cm. This part of the pebbly mudstone ranges from 1.3-2 m thick.

The top of the pebbly mudstone is a buff to red, parallel and cross laminated fine grained sandstone, which has grey limestone-conglomerate lenses associated with its base (Figure 3-24c). The thickness is up to 47 cm and it thins eastward until only 5 cm thick lenses of it are loaded into the main part. The top of the parallel laminated sandstone grades into red mudstone. This part of the pebbly mudstone shows a marked similarity to the lower parallel laminated sandstone-limestone conglomerate part.

CHAPTER 4

FACIES RELATIONSHIPS OF THE SANDSTONE UNITS

Introduction

The most striking feature of the study area is the alternation of the sandstone and mudstone units (Figure 2-5). The sandstone units are defined as those units which have a sandstone-shale ratio greater than 2:1 and are thicker than 10 m. There are two types recognized in the field: the massive sandstone units (units 16, 18, and 25) in which the massive sandstone facies forms an integral part, and the classical turbidite units (units 20, 21, 23, 27 and 29) which consist of siliceous or calcareous turbidites.

The Massive Sandstone Units

The massive sandstone facies forms the "core" of units 16, 18 and 25. Units 16 and 25 differ from unit 18 in thick-

ness, component facies, and facies sequence within the units. Units 16 and 25 are approximately 35 m thick, whereas unit 18 ranges from 30-90 m thick. All the units are repeated by faulting, so that a downcurrent as well as a transverse cross section of the units can be seen. The vector means of paleocurrent indicators for these units are approximately normal to the strike of the beds (Chapter 2).

Unit 16

Unit 16 shows no well developed trend in grain size or thickness from base to top. Comparison of coarse layer thickness (Stanley and Bouma, 1964) versus bed number shows that unit 16 at Plage Victor has an irregular profile, whereas at Demi Lieu it has a symmetric profile with the centre having the thickest beds (Figure 4-1a,b).

The most important feature of this unit is its facies sequence, which has four divisions: the lower slurry facies division, the massive sandstone facies division, the pillar greywacke facies division and the upper slurry facies division. The breaks between these facies can be seen in Figure 4-1a,b.

The slurry facies division is composed mainly of slurry beds, but classical turbidites are commonly associated with them. The classical turbidites generally scour into the

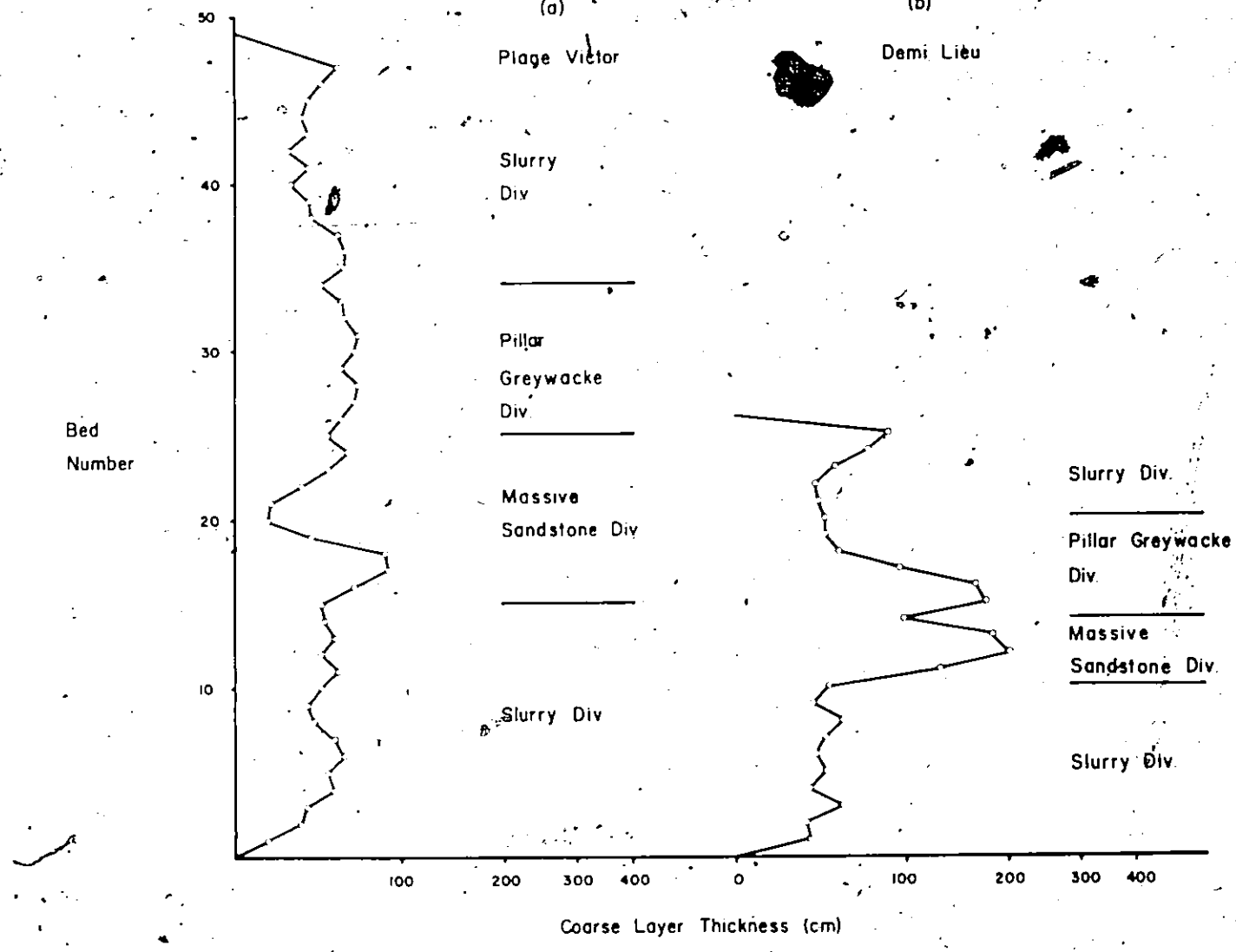

Figure 4-1 Coarse layer thickness vs. number plot, Unit 16, (3 point moving average).

underlying slurry bed, but this is not always the case. The slurry division has an abrupt but flat contact with the underlying red mudstone unit. The slurry beds are laterally continuous. The thickness of this division does not change along strike or downcurrent.

The massive sandstone division is made up of massive and pebbly sandstones. Both facies vary greatly in thickness along strike. When the massive sandstone beds are thick they are commonly amalgamated, but they tend to break up into thinner beds along strike. Shallow channelling, up to 0.5 m, can be seen at Demi Lieu, which also explains some of the discontinuity. The base of this division is scoured into the underlying slurry division. Locally, as at Plage Victor, a sandstone-shale breccia is developed along the contact. This is associated with a thick amalgamated massive sandstone which cannot be traced more than 10 m along strike. The breccia has a flat, continuous base above which is a 20-40 cm thick zone of irregularly shaped shale blocks. It is never associated with the pebbly sandstones.

The pillar greywacke division has a sharp flat contact with the underlying massive sandstone division. The individual beds are laterally continuous. At Plage Victor the beds may be separated by a thin shale bed, but at Demi Lieu they are thicker bedded, amalgamated and the pillars

are much better developed. The beds at the top of this division thin and fine upwards and are succeeded by green siltstones and red mudstones.

The upper slurry division looks like an abbreviated version of the three divisions below it. The contact between this division and the pillar greywacke division is gradational. At Plage Victor the division consists of slurry beds and classical turbidites. The top of the division is marked by a slurry which has a classical turbidite lying abruptly on top of it. At Demi Lieu the division consists of slurry beds, classical turbidites and pillar greywackes which have a massive sandstone scoured into the top of the sequence. The upper contact of this division with the overlying red mudstones is sharp and flat.

Unit 18

Unit 18 is repeated by the Demi Lieu Fault. Where it crops out at Pointe Caronette it is approximately three times its thickness at Plage Victor (Chapter 2). Like the other massive sandstone units, it can be divided into several facies divisions. At Plage Victor it only shows the slurry and massive sandstone divisions, whereas at Pointe Caronette there is a slurry division, a massive sandstone division, a classical turbidite division and another massive

sandstone division (in that order). There is no overall trend in bed thickness or grain size, but minor trends 5-10 meters thick can be seen. Excluding the slurry division, the maximum bed thickness of these minor cycles decreases from the base of the lower massive sandstone division to the top of the classical turbidite division, and it increases upwards from the top of the classical turbidite division to the top of the upper massive sandstone division.

The slurry division has a sharp, flat base which overlies the red mudstone of unit 17. It has a sandstone-shale ratio of approximately 1:1 and shows no trend in bed thickness or grain size. There are some thin bedded classical turbidites interbedded with the slurry beds, but there are also thicker classical turbidites which are scoured into the slurry beds, or overlie them with a sharp, flat contact. In the cases where the classical turbidite is scoured into the slurry bed, the turbidite contains the A, B, and C Bouma divisions, whereas it is structureless in the cases where there is a sharp, flat contact.

The contact between the massive sandstone division and the slurry division is erosional. In places it is channellized, whereas in others it consists of a sandstone-shale breccia which may pass laterally into thin bedded turbidites or amalgamated massive sandstones.

At the base of the lower massive sandstone division on Pointe Caronette a channel scours approximately 3.5 m into thin bedded turbidites (Figure 4-2a). The bottom of the channel is flat and has no breccia associated with it. The side of the channel is inclined approximately 25° to bedding and has grooves associated with it that are oriented 167-347°. The channel is filled with very coarse grained, amalgamated, massive sandstones that show no vertical trends in bed thickness or grain size.

The thin bedded turbidites which are truncated by the channel pass laterally (to the west) into a sandstone-shale breccia (Figure 4-2e-g). The turbidites seem to coarsen along strike as the breccia is approached. In some cases it is possible to see that this coarsening is the result of scouring by the coarser sand associated with the breccia (Figure 4-2f). With this change in grain size, the beds become irregular and break up into the breccia. The breccia is composed of very coarse grained to very fine pebble, sandstone and shale blocks. The base of the breccia is marked by a 20-30 cm thick sandstone horizon which, except for a one meter gap, is continuous across the outcrop. A few scour marks were observed on the sole of this sandstone, but they are ambiguous as far as indicating paleoflow. Although the base tends to be flat, measurement of the distances

NE

a

thin-bedded turbidites

gre

e

1 of

Figure 4-2 Sandstone
Pointe Ca

Scale:

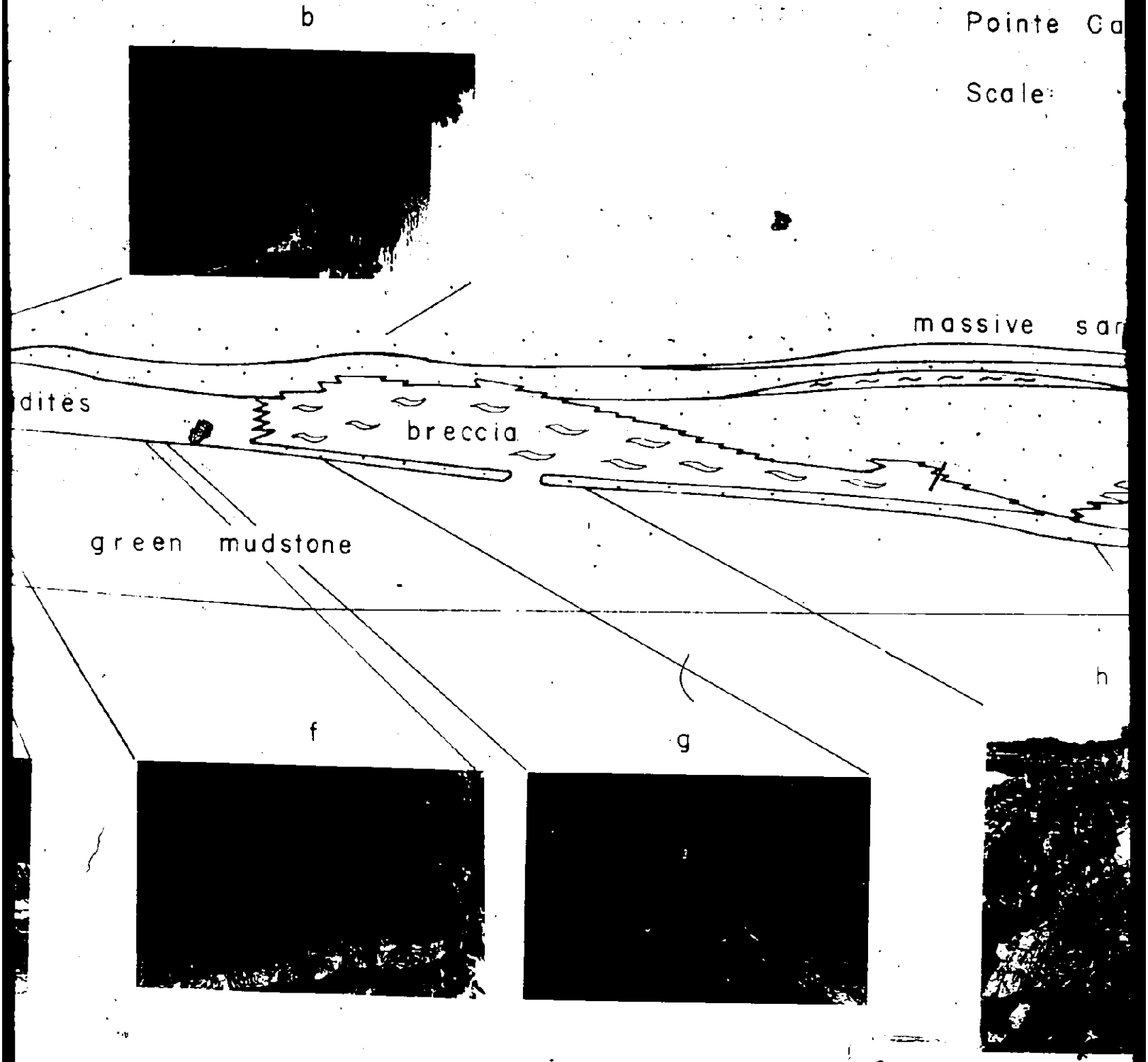

ndstone - shale breccia in unit 18,
inte Caronette.

ale:

0 10 meters

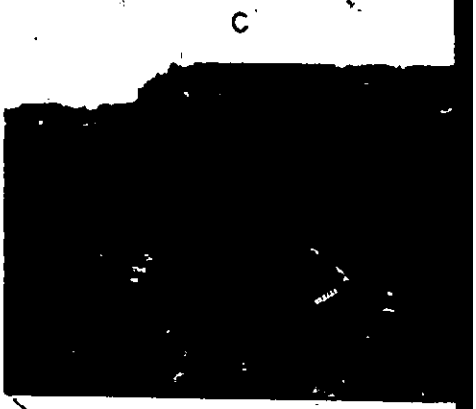

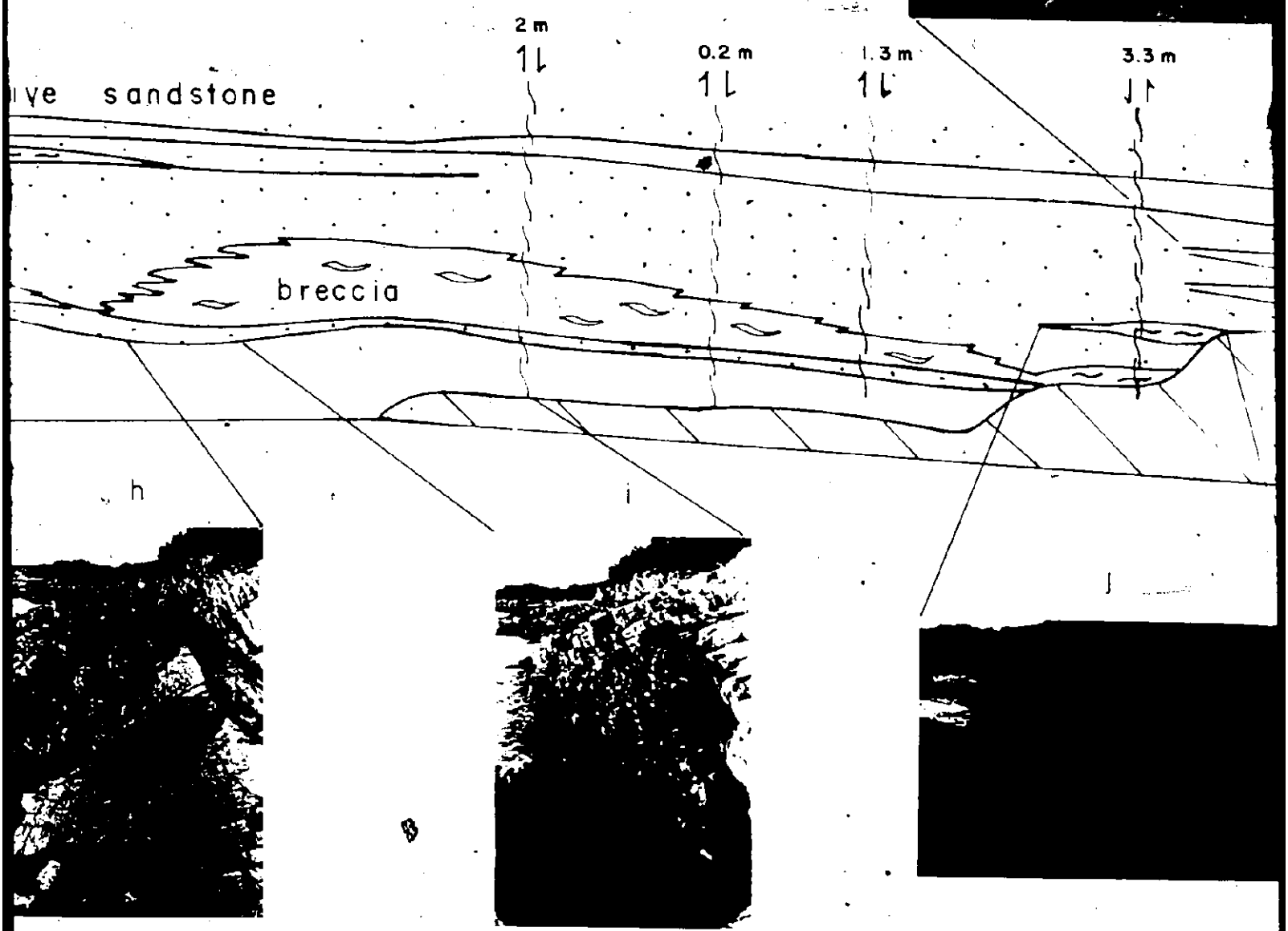

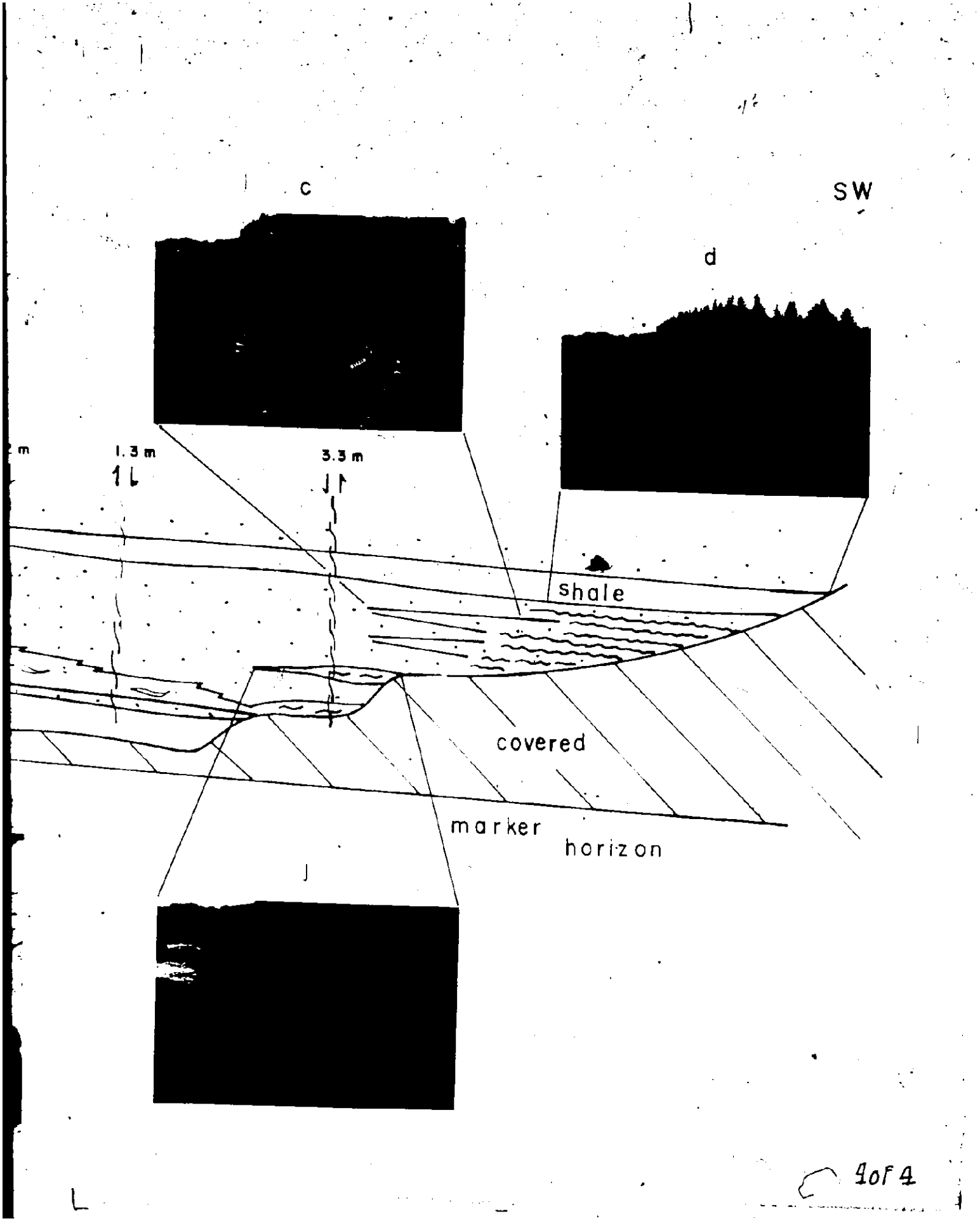
c
SW
d
m
1.3 m
3.3 m
shale
covered
marker
horizon

between it and an underlying slurry bed decrease westward, indicating that some of the sediments which underlie the breccia were eroded prior to deposition of the breccia.

The bulk of the breccia consists of irregularly shaped sandstone blocks in a green shale matrix. The sandstone-shale ratio of the breccia is greater than or equal to 2:1. The long axes of the sandstone blocks (up to 4 m) are oriented subparallel to bedding. The maximum thickness of the blocks is approximately 1.5 m. No roll up structures were observed in the sandstone blocks, although deformed laminae were noted in some of the shale blocks.

The breccia underlies amalgamated sandstone lenses which occur below the more continuous bedded sandstones forming the main body of the massive sandstone division. These massive sandstone lenses have a wedge shaped, thinning downdip profile (Figure 4-2b). They are composed of the same grain size range of material as sandstone blocks in the breccia. The contact between the breccia and the sandstone lenses is jagged. The amount of shale between the sandstone blocks decreases as the contact is approached. Likewise the size of the sandstone blocks decreases as the contact is approached. The breccia passes quickly into the massive sandstone and back into the breccia in a distance of 65 m (Figure 4-2i), as the zone is traced west. In the west end

of the exposure the breccia again passes into massive sandstone. However, further west the whole massive sandstone bed can be seen breaking up into breccia (Figure 4-2j). The first indication of this is the appearance of wedge shaped (along strike profile) beds of massive sandstone. The amount of shale between these beds increases westward until bedding becomes very irregular and finally breaks up into breccia (Figure 4-2c,d).

A similar sandstone-shale breccia also occurs at the contact between the massive sandstone and slurry divisions at Plage Victor. Much of this breccia is covered by talus so a complete study was impossible.

The main characteristics of the breccia at Plage Victor are essentially the same as described above, but with minor differences in the base and the lateral changes of the breccia. The base consists of elongate lenses of very coarse to granule size sandstones, which have thin overlapping feather edges. In places the base seems scoured into the underlying mudstone. The breccia can be traced over 100 m. In the west it ends abruptly just below the channelled edge of the overlying massive sandstones. There seems to be no erosional contact between the red mudstone and the sandstone-shale breccia, as the two are interbedded and a few sandstone stringers can be seen up to 3 m away from the end of the breccia.

The massive sandstone, which overlies the breccia, is scoured into the breccia, and grooves along its channel margin can be seen. As at Point Caronette the breccia passes laterally into lensoid massive sandstones.
At the eastern end of these massive sandstone lenses the beds can be seen passing into thin bedded turbidites.
Several of these massive sandstone lenses are stacked on top of each other and are separated by a sandstone-shale mixture which looks much like a small scale version of the sandstone-shale breccia. This feature was also observed at the Pointe Caronette occurrence.

Other than the occurrence of the sandstone-shale breccia, there is little difference between the upper and lower massive sandstone divisions. Beds are laterally discontinuous and it is easier to follow an amalgamated group of beds along strike than one bed. Likewise there is very poor bed for bed correlation between the Plage Victor and Pointe Caronette sections. Fluid escape features are common to most of the massive sandstone beds.. The contact between the upper massive sandstone division and the classical turbidite division is erosional.

The classical turbidite division has a sharp flat base overlying the lower massive sandstone division. The beds are continuous on outcrop scale, but they do not occur at

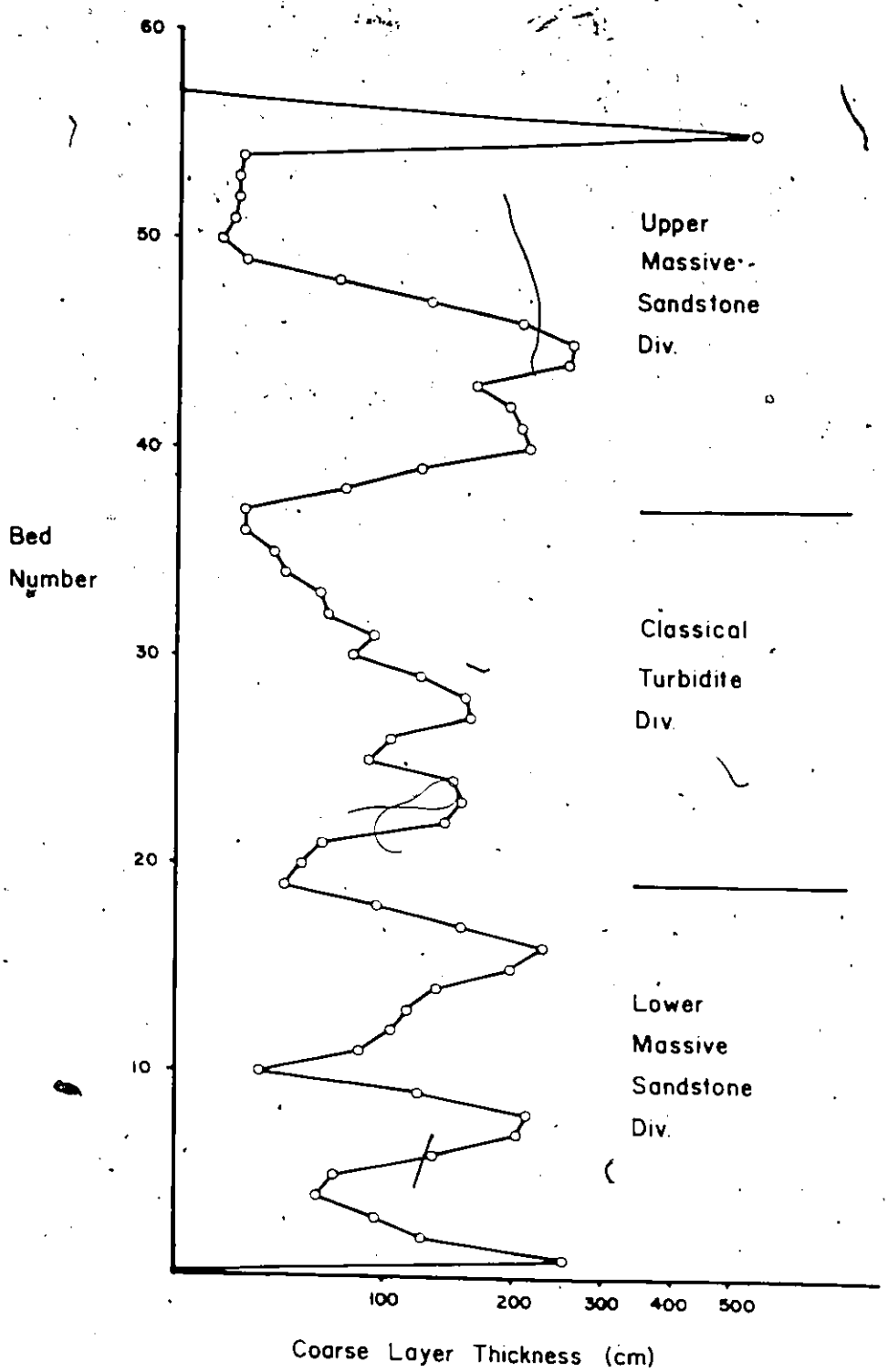

Figure 4-3: Coarse layer thickness vs. bed number plot, Unit 18, Pte. Caronette. (3 point moving average)

Figure 4-4 Thinning and fining upward sequence in classical turbidites which is cut out by a massive sandstone bed. Unit 18, Pointe Caronette.

Plage Victor: The symmetrical profile of the coarse layer versus bed number (Figure 4-3) is not evident in the field. The base of the minor trends is usually a massive sandstone and the thickness of the classical turbidites tends to decrease upwards until another thick massive sandstone bed cuts out the top (Figure 4-4).

Unit 25

Like Unit 16 there is no overall trend in grain size or bed thickness. Coarse layer thickness versus bed number plots (Figure 4-5) are irregular. Unit 16 only has three facies divisions: the slurry division, the classical turbidite division and the massive sandstone division. Only the break between the classical turbidite and massive sandstone divisions can be recognized on the coarse layer thickness versus bed number plots.

The slurry has a sharp, flat contact with the underlying red mudstone unit. The slurry beds are interbedded with thick mudstone beds (up to 2 m thick) and classical turbidites.

The individual beds seem to be more continuous laterally and downcurrent than their counterparts in the other facies divisions of this unit.

The slurry division is distinguished from the classical turbidite division by a change in the sandstone-shale ratio

from 1:2 to greater than 2:1. In the eastern, upcurrent outcrops this division shows a thinning and fining upward sequence and slurry beds are found only at the base of this division. Here the division has a sharp, flat base. As the division is traced west and downcurrent it thickens, and the number of slurry beds in the division increases until there is about a 1:1 ratio between the classical turbidites and the slurry beds. The type of base this division has in the western outcrop depends on the type of bed at its base. If it is a classical turbidite then it is scoured, whereas if it is a slurry bed it is a sharp flat contact. No trend in grain size or bed thickness is discernible in these sections.

The massive sandstone division makes up the upper half of the unit. It has a scoured to sharp, flat base. It does not show any trend in grain size or bed thickness, except in the upper 5-10 meters where there is a thinning and fining upward sequence. Individual beds are discontinuous, only the thickest beds can be traced any great distance, but even these thin and break up into thinner beds along strike and downcurrent. Fluid escape features (mainly pillars and dishes) are common to most of the massive sandstone beds in the division.

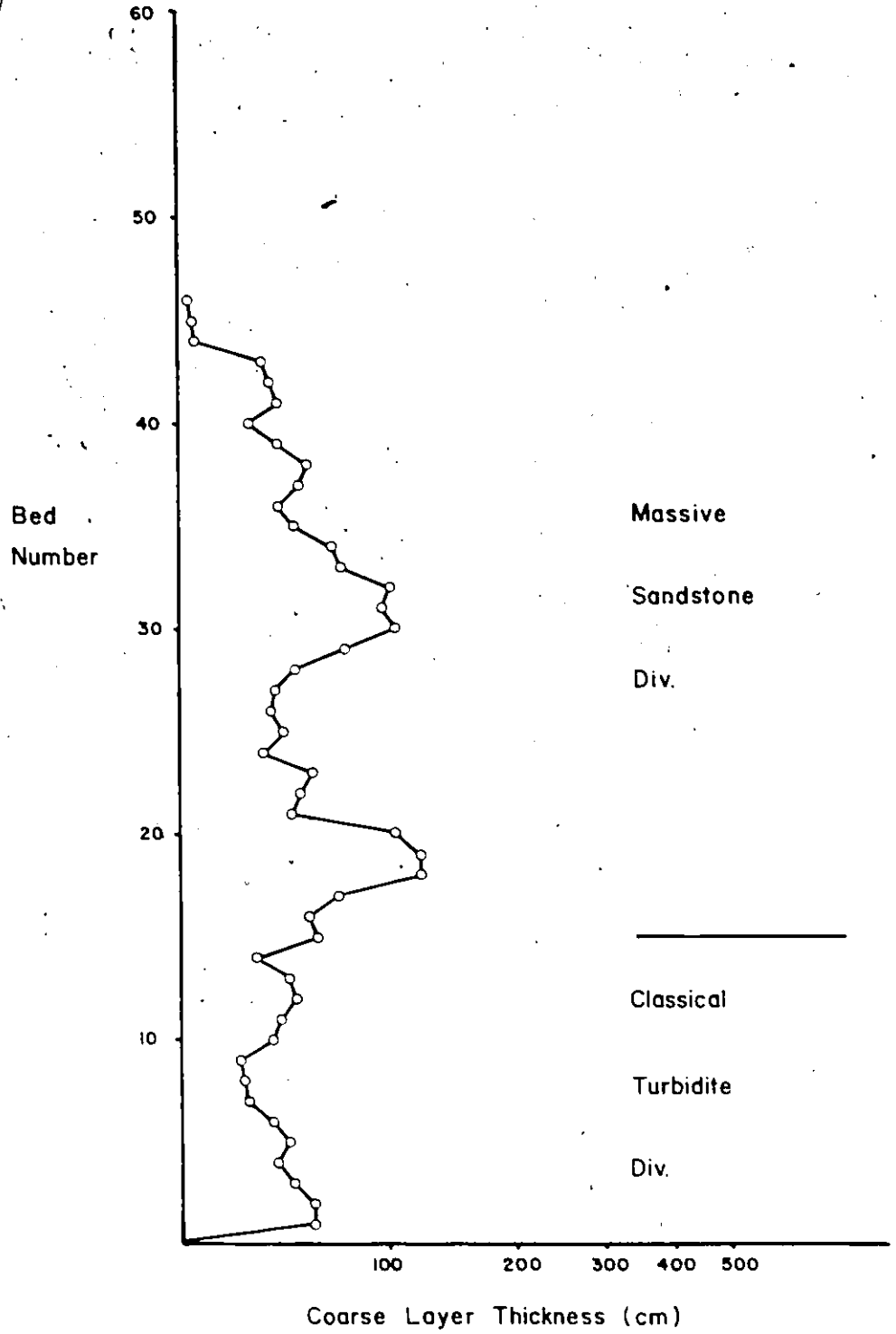

Figure 4-5: Coarse layer thickness vs. bed number plot, Unit 25. (3 point moving average)

The Classical Turbidite Units

Two types of classical turbidite units were distinguished in the field: siliceous turbidites which formed units from 10-25 m thick (units 20, 21, 23 and 29), and calcareous classical turbidites which formed two units (27 and 28) that are 100 m and 34 m thick.

The Siliceous Classical Turbidite Units (Units 20, 21, 23 and 29)

Both the units and the individual beds are very continuous and change little in thickness or character over distances up to 1 km (limit of exposure). Generally the units are composed of the classical turbidite facies and the slurry facies, but unit A (Anse aux Sauvages, Central Zone, map in pocket) is an exception, as it contains the massive sandstone facies as well. A more detailed description of the turbidites can be seen in Chapter 3.

The classical turbidites outnumber the slurry and slurry breccia beds from 2:1 to 7:1. The magnitude of this ratio cannot be related to stratigraphic position or bed thickness. The units do not show any trend in grain size or bed thickness vertically.

Channelling is not characteristic of these units. It

can only be seen in unit A at Anse aux Sauvages. The channel is about 8 m deep and can be traced approximately 70 m from the margin eastward. It has a flat base which is not marked by any type of breccia. The margin of the channel is stepped, the steeper parts truncating sandstones outside the channel, whereas the flatter parts are subparallel to bedding (Figure 4-6). The channel has a slightly asymmetric profile, i.e. it shallows east. Except at the base, a clay drape marks the channel margin.

The channel is filled by massive sandstones and classical turbidites. No vertical trends in grain size or bed thickness are evident. The grain size of the sandstones ranges from medium to very coarse sand, although calcareous lenses in the massive sandstones commonly contain pebble size clasts. Massive sandstone beds dominate the lower and upper part of the channel fill. In the lower part of the channel, the top of the massive sandstone passes laterally into classical turbidites. The classical turbidites and slurry beds in the middle of the channel fill thin westward, and at the channel margin they form feather edge pinch outs. The massive sandstone at the top of the channel fill thins both east and west. The number of amalgamations that are discernible decreases both to the east and west. The massive sandstones are scoured into the underlying classical

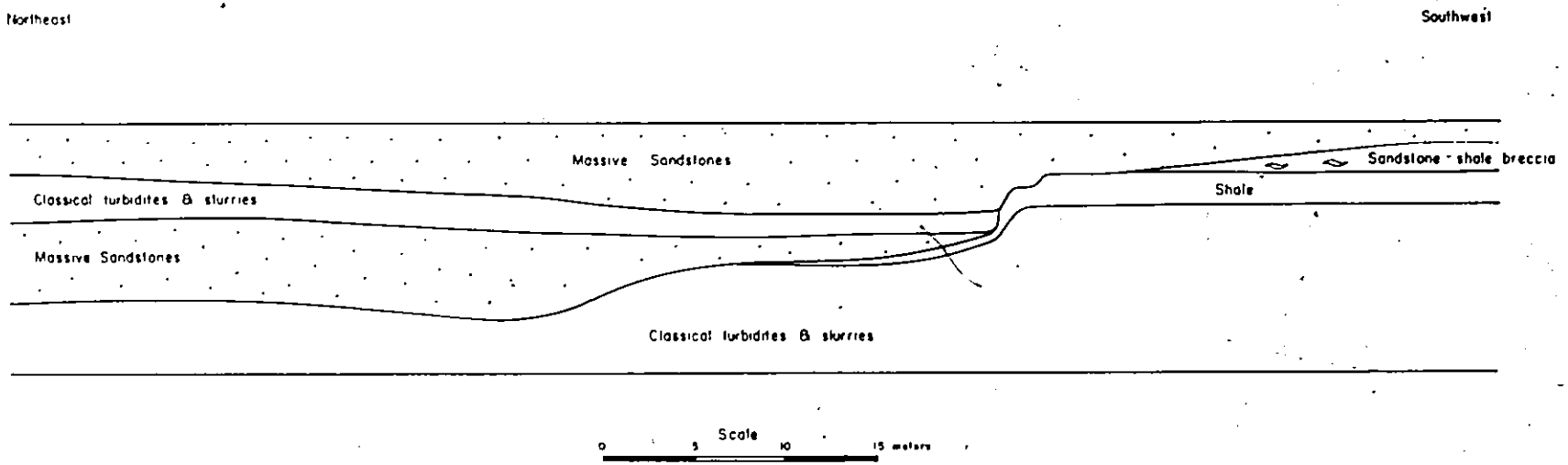

Figure 4-6 Channel in unit A, Anse aux Sauvages

turbidites and slurry beds.

Near the top of the channel margin there is approximately 2 m of grey finely laminated siltstone and shale which overlies the classical turbidites outside the channel. At the top of these siltstones and shales near the channel margin is a thin zone of very coarse sandstone and shale breccia which thickens to the west. The continuity of the sandstone stringers in the breccia increases westward.

Rib and furrow structure found within the channel indicates a direction of 160° compared to 172° for the same structure outside the channel. Grooves on the channel wall are oriented 035-215°.

Units 27 and 28: Calcareous Classical Turbidites

Unit 27 shows no vertical trend in grain size or bed thickness. It is 100 m thick and is internally homogeneous. At the base calcareous classical turbidites are interbedded with red mudstone, whereas at the top they are interbedded with grey or black shale. The base of the unit is marked by a pebbly mudstone horizon, and the top is marked by a calcisiltite slump (Chapter 3). The beds are laterally continuous but lack of complete exposure prevents study of the thickness of the unit along strike.

Unit 28 is 34 m thick and is primarily very thin to

thin bedded calcareous to dolomitic siltstones and very fine sandstones interbedded with black shale. Except for the calcisiltite slump, there is gradation from thick turbidites of the top of unit 27 to the thin and very thin bedded turbidites of unit 28.

Facies Transitions

To study the nature of the facies transitions in units 16-25 a tally matrix (Table 4-1) was compiled. A difference probability matrix (observed minus predicted) was then calculated to check the randomness of these transitions (Table 4-2). An arbitrary cut off point of +0.2 was chosen to distinguish those transitions which occurred more commonly than random.

The transitions which occurred more commonly than random were the red mudstone-slurry, slurry-classical turbidite and the massive sandstone-classical turbidite. These are the transitions which typify the slurry division and the massive sandstone division of the massive sandstone units. However, it is important to note that the transition from the classical turbidite facies to any other facies is random. There is no strong link between the massive sandstone

facies and any preceding facies.

The transitions which are least likely to occur are the red mudstone-massive sandstone and the massive sandstone-slurry.

	Red Mudstone	Slurry	Classical Turbidite	Massive Sandstone	
Red Mudstone	-	3	3	0	6
Slurry	0	-	14	3	17
Classical Turbidite	5	14	-	10	29
Massive Sandstone	1	0	12	-	13
	6	17	29	13	65

Table 4-1 Facies transition tally matrix for the red mudstone, slurry, classical turbidite and massive sandstone facies of units 16-25.

	Red Mudstone	Slurry	Classical Turbidite	Massive Sandstone
Red Mudstone	0	+0.21	+0.01	-0.22
Slurry	-0.13	0	+0.22	-0.09
Classical Turbidite	0	+0.01	0	-0.02
Massive Sandstone	-0.04	-0.33	+0.36	0

Table 4-2 Difference probability matrix (observed minus expected) for the red mudstone, slurry, classical turbidite and massive sandstone facies of units 16-25. Positive values are those transitions which occur more commonly than random, negative values are those which occur less commonly than random. Important positive values have solid underlining and important negative values have dashed underlining.

CHAPTER 5

PEBBLY MUDSTONE, SLURRY BEDS AND SLURRY BRECCIAS: EXAMPLES OF COARSE AND FINE GRAINED DEBRIS FLOW DEPOSITS

Introduction

The evolution of a sediment gravity flow (Middleton and Hampton, 1973, 1976) can be envisaged as a continuum of processes which can be divided into three stages: initiation, long distance transport and late stage modification (Walker, 1978) (Figure 5-1). It would be unlikely to see indications of all three stages in one deposit because the mechanisms operative during each stage obscure the effects of those from the previous stage. This is especially evident in those flows which have undergone a substantial amount of late stage modification.

There are two main mechanisms of support which can operate during long distance transport: fluid turbulence and matrix strength. A great deal more work has been done on fluid turbulence than on matrix strength. Knowledge of the role of matrix strength in subaqueous debris flows

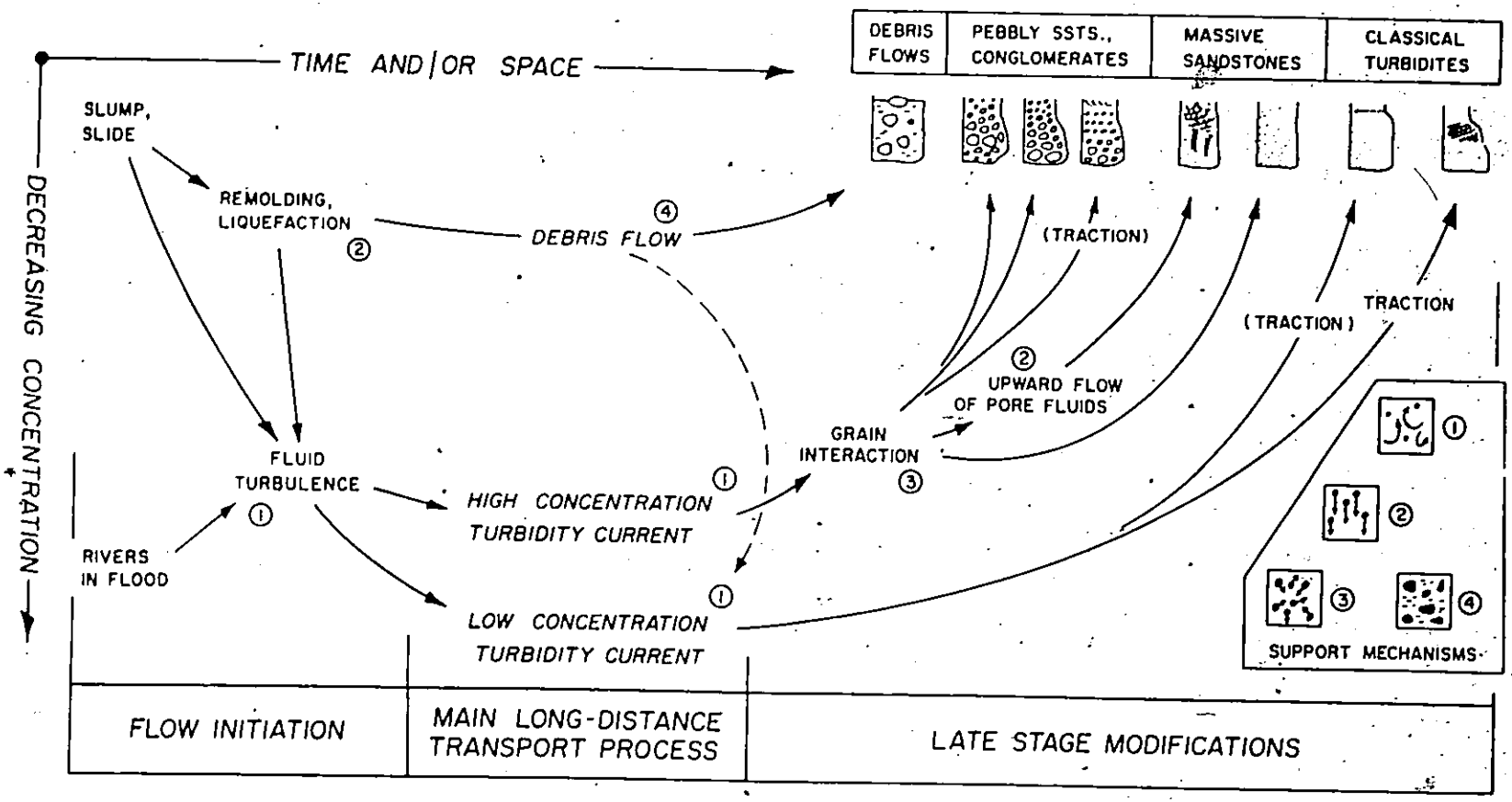

Figure 5-1 The stages in the evolution of a sediment gravity flow and the support mechanisms operative in them (from Walker, 1978, Fig. 4).

mainly stems from the extrapolation of subaerial debris flow theory (Johnson, 1970) to subaqueous environments, e.g. Hampton (1972).

Debris flows can be divided into two categories: coarse grained and fine grained. Coarse grained varieties should be more analogous with subaerial debris flows because they undergo less late stage modification than the fine grained flows. Based on the subaerial debris flow characteristics, one would expect subaqueous examples to show a bimodal or multimodal grain size distribution, with the larger clasts set randomly in a finer grained matrix (Johnson, 1970). Hampton (1972) and Carter (1975) have reinterpreted the pebbly mudstones of Crowell (1957) as coarse grained debris flow deposits. Other coarse grained deposits interpreted as having formed from debris flows are the Devonian megabreccias of Australia and Alberta (Mountjoy and Playford, 1972) and the Ordovician megabreccias of Western Newfoundland (Delong and Middleton, 1978). However, these last two examples differ from the description presented above by their low matrix content.

Recognition of fine grained debris flows has been less obvious. Morris (1971) suggested that the slurry beds (after Wood and Smith, 1959) of the Ouachita Mountains were deposited from fine grained debris flows. A similar inter-

pretation for the slurry beds of Tourelle Formation (Ordovician, Quebec) was proposed by Hiscott (1977).

Hampton (1972) pointed out the similarity that would exist between fine grained debris flow deposits and sandstones deposited by other subaqueous processes. He suggested that the fine grained debris flow deposits would be characterized by: (1) texture - fine grained (or coarser) sand with low clay content (although clay content could also be high); (2) a coarse grained layer sharply or gradationally surrounded by finer grained layers (i.e. the development of inverse or inverse/normal grading; (3) "laminar flow" fabric - parallel clast fabric, could be present.

Subaqueous debris flow deposits with some of these characteristics have been recognized interbedded with lacustrine sediments associated with the Devonian Karlskaret alluvial fan of Norway (Larsen and Steele, 1978). Grading in these deposits may be normal (distribution and coarse tail), inverse or inverse/normal. The grain size distribution of these sediments is multimodal.

The Pebbly Mudstone

The pebbly mudstone horizon (27-1-32) consists of four beds of which only the third bed is a pebbly mudstone (sensu stricto). The third bed is characterized by the presence of pebble to cobble size clasts set randomly in a structureless matrix which is consistent with criteria for coarse grained debris flow deposits.

As originally defined by Crowell (1957), the pebbly mudstones were deposits which resulted from loading of coarse sediments onto very fine grained sediments and subsequent downslope movement. No great distance of transport was implied. In contrast, the pebbly mudstone in this section is closely associated with classical turbidites. This suggests that the sediment gravity flow which deposited the pebbly mudstone moved as far into the basin as the turbidity currents which deposited the classical turbidites.

Although the four beds of the pebbly mudstone horizon have been considered in one context, the differences in the processes which deposited them suggests that they are four different events with little or no genetic link. The only link between the beds seems to be the limestone clasts which occur in the conglomeratic lenses at the bases of the turbidites, in the pebbly mudstone and rarely in the mudstone at the base of the horizon.

The strike of the outcrop is oblique to the direction of movement inferred by the vector mean of the paleo-current directions for the beds above and below this horizon. Thus the cross section seen only represents a small fraction of the actual length (or even width) of this horizon. No interpretations of particular aspects of the horizon are attempted, since these may only be local variations and no other examples were seen with which a comparison could be drawn.

Slurry and Slurry-Breccia Beds

The slurry and slurry-breccia beds (Chapter 3) differ in detail, but have the following features in common:

(1) a flat, featureless sole;

(2) high matrix content in which larger grains are randomly oriented;

(3) varying amounts of pseudonodules, shale clasts and granules of quartz, feldspar and rock fragments scattered throughout;

(4) they are commonly composed of two or more parts denoted by a change from massive greywacke to sandstone-mudstone breccia or simply an amalgamation.

Both these types of beds are considered to have been

deposited from the same type of sediment gravity flow. Deposition under different conditions is thought to have formed the variations in the characteristics of the deposits.

The high amount of matrix, the poorly sorted nature, and the presence of outsized clasts (from granules to slabs) suggest that deposition may have been from subaqueous debris flows. But the division of many of the beds into two or more parts suggests that deposition occurred in stages.

Deposition in stages, from a two layer turbidity current, is envisaged by Skipper and Middleton (1975) as having formed the type III greywackes (Enos, 1969a) of the Cloridorme Formation. The type III greywackes have three divisions: (1) a basal division consisting of limestone or quartz granule to pebble conglomerate, or coarse sand greywacke or calcareous wacke which may exhibit cross lamination, parallel lamination or upstreamed inclined lamination; (2) a second division consisting of spindle - or globular-shaped calcareous nodules in a muddy matrix, and (3) an upper division of siltstone or shale.

The two layer turbidity current consisted of a thin coarse grained lower layer and a thick upper layer of sand, silt and clay. The basal division was deposited from the lower layer and traction formed the sedimentary structures present in it. The upper layer was deposited from a series

of liquefied sediment flows. As the coarser sediment from each flow settled onto the bed it sank into it forming the pseudonodules.

The following discussion evaluates the ability of the two types of sediment gravity flows proposed to explain the main characteristics of the slurry and slurry-breccia beds.

The flat, featureless sole could have been formed by either type of flow. Flutes are not characteristic of the soles of debris flow deposits, but they are common to those of the type III greywackes. However, the main control over the development of scour marks is the "severity" of the flow (Allen, 1969). The flows which deposited these beds may not have been erosive enough to cause scouring.

The very poor sorting and high proportion of matrix in the basal greywacke of the slurry-breccias and in the slurry beds could also be found in either type of flow. This would depend on the initial grain size distribution of the sediment before incorporation into the flow.

Normal grading is not seen in the basal division of the type III greywackes, but it is common to subaqueous debris flow deposits. In the two layer turbidity currents, deposition is thought to have occurred too slowly for grading to form (Skipper and Middleton, 1975). The normal grading in the subaqueous debris flow deposits suggests that

deposition occurred from suspension and that the high matrix content was never great enough to retard movement of grains past each other (Larsen and Steele, 1978, p.54). This would suggest that matrix strength became a more important factor in the latter stages of flow. This would have prevented the formation of the 'quick' beds from which the abundance of pseudonodules in the second division of the type III greywackes were derived.

Pseudonodules are common in the slurry beds but do not dominate them as in the type III greywackes. They are most common in the upper part of the beds, either unrelated to any feature or associated with amalgamations. The position of the pseudonodules in the top of the bed suggests that they are late stage features, and that liquefaction only played a minor role in the deposition of the bed as a whole.

The amalgamations seen in the slurry beds suggest that deposition did occur in pulses. However, as proposed above, the matrix strength of the beds was strong enough to withstand any great amount of liquefaction which would have formed an abundance of pseudonodules.

The discontinuous nature of the basal greywacke in the slurry-breccias may represent "pull apart" (Hampton, 1972), which occurs in low water content debris flows. This would not be expected to form during deposition from a

turbidity current.

The close association of the breccia of the slurry-breccia with the underlying basal greywacke suggests that the breccia is derived from the underlying greywacke. This might represent debris ripped off the front of the debris flow and modified by shearing farther back in the flow. Alternatively, the breccia may have been formed by liquefaction in the same manner that the pseudonodules formed in the second division of the type III greywackes. But the shape of the sandstone clasts is not characteristic of the loading which formed the pseudonodules in the second division. The breccia should have developed as a continuous horizon throughout the bed if it had formed in the same manner as the second division of the type III greywackes.

The rafted slabs of thin bedded turbidite are consistent with a debris flow interpretation. But if their density was approximately the same as the surrounding matrix, they could also have been rafted in by a turbidity current. Their large size would also enable them to float in a matrix that may have been weak.

It is evident from the foregoing discussion that liquefaction has only played a minor role in the deposition of the slurry beds and slurry-breccias, although it may have been important locally. The characteristics of these beds fit

the criteria suggested for fine grained debris flows and they also compare well with other examples in the literature. Whether matrix strength was the main mechanism of support throughout the transportational history remains to be seen. But it is evident that it was important in the late stage of the transportation of the sediments.

A review of the features of the individual beds (Chapter 3) shows that beds 25-1-6 and 25-1-13 (slurry-breccias) have features which seem transitional between the slurry-breccia 20-1-21 and the slurry beds. This does not mean that the beds represent various stages in the development of one debris flow. Rather, it indicates that the same mechanism(s) were operative but under different conditions. These are discussed below.

Hampton (1972) reports that low water content (<70 weight %) debris flows are characterized by blocks which have pulled away from the main part of the flow. Debris was eroded from the front of the flow and incorporated into a dilute turbulent cloud. In medium content (70-75 weight %) debris flows the shape of the debris flow was more variable and a large cloud, denser than for the high water content flows, covered most of the flow. For flows with greater than 75 weight % water, flow was chaotic and the turbulent cloud was very large and dense. In this case thorough mixing

occurred between the ambient fluid and the debris flow.

The differences observed in the slurry beds and slurry-breccias may be the result of the difference in the amount of water in the debris flows. The slurry-breccias may have been formed by low water content debris flows, in which the discontinuity in the basal greywacke may represent "pull apart". The breccia in these beds may represent debris that was eroded off the front of the debris flow. The slurry beds may represent deposition from moderate to high water content debris flows. A more diluted debris flow would enable easier settling of the grains to occur and therefore form a graded base. The parallel laminations and ripples seen at the top of some of the slurry beds are traction features associated with the dilute tail of the turbulent cloud, which accompanies and is derived from the debris flow.

CHAPTER 6

INTERPRETATIONS

Introduction

The main purpose of this chapter is to summarize the descriptions of the lithologic units and their component facies or facies divisions. This will provide a framework for interpretation of the depositional environment of the sediments and allow comparison with existing facies models. The interpretation will then be compared with regional studies of the Quebec Complex to provide further insight into the type of basin the sediments were deposited in.

The Massive Sandstone Units

Two important queries arise from the study of the massive sandstone units: what do the facies divisions represent, and why does the slurry division always precede deposition of the massive sandstone division?

Four facies divisions were recognized in these units: slurry, classical turbidite, massive sandstone and pillar greywacke.

The slurry division has a sharp, flat contact with the underlying red mudstone unit; it is laterally continuous and shows little variation in thickness along strike. The individual beds show the same characteristics. There is no vertical trend in grain size or bed thickness. Classical turbidites are always interbedded with or are scoured into the slurry beds.

The classical turbidite division in unit 25 is only distinguished from the slurry division, which it overlies, by a change in the sandstone-shale ratio. It passes laterally from only classical turbidites to interbedded classical turbidites and slurry beds. Because of this and its stratigraphic position directly below the massive sandstone division, it is considered to occupy the same sedimentological "niche" as the slurry division.

The massive sandstone division always forms an important part of the massive sandstone units. Its base is either marked by channelling or small scale scouring, or it can be sharp and flat. The thickness of the division does not change over distances of 1-2 km, e.g. unit 25, but there are exceptions, e.g. unit 18. Individual beds

tend to be discontinuous. The beds in the thickest unit (18) show more scouring and amalgamation than do the massive sandstones of the other units (16 and 25).

The sandstone-shale breccia in the channel at the base of unit 18 has a flat base, which may be composed of thin sandstone lenses or one relatively continuous sandstone horizon, which blankets the channel base as well as extending outside it. The breccia is composed of large, irregularly shaped sandstone blocks whose long axes are subparallel to bedding. The breccia passes laterally into or scours out thin bedded turbidites outside the channel, or into amalgamated massive sandstone lenses towards the channel axis. The massive sandstones have a thinning downdip profile. They may pass laterally into rubbly or even bedded thin turbidites.

The pillar greywacke division can be considered part of the massive sandstone division because it is similar to the massive sandstone facies. It is thick and massive bedded, can have a flat or scoured base, and shows fluid escape features. In unit 16, its only occurrence, it is part of a thinning and fining upward sequence at the top of the massive sandstone division.

The beds of the slurry division were deposited on an area of very low relief, which enabled the formation of

extensive sheets of sand. The slurry beds were deposited from debris flows (Chapter 5). Some of the classical turbidites which are interbedded with the slurry beds may have been deposited from turbidity currents which were generated by the debris flows (Hampton, 1972). The classical turbidites which can be seen scouring into the slurry beds are the deposits of more erosive flows, which may signify the approach of the sandstones forming the massive sandstone division.

The beds of the massive sandstone division were deposited in a braided channel system. This is clearly shown by the nested channels seen at the base of the massive sandstone division in unit 18 at Pointe Caronette, the abundant scouring and amalgamation seen in the massive sandstone beds and the lenticularity and lateral discontinuity of the massive sandstones and pebbly sandstones. Channel crossover is probably responsible for the change in thickness of unit 18 between Plage Victor and Pointe Caronette.

Deposition of the massive sandstone division began abruptly. This is suggested by the lack of thickening and coarsening upwards sequence below the division, and the scoured contact between the massive sandstone and slurry divisions. The upper contact of the massive sandstone division with the overlying red mudstone unit is sharp, or

marked by a 'starved' thinning and fining upward sequence. This indicates that the decrease of sediment supply to the braided channel system was rapid.

The change from abundant scouring and amalgamation of the massive sandstone beds (e.g. unit 18) to sharp, flat basal contacts (e.g. unit 25), and the lateral passage of amalgamated beds into thin bedded sandstones, is related to the distance from the active channel supplying the sediment. Less scouring occurs in the distal ends of the channel system, and the sandstones begin to assume a character similar to that of classical turbidites.

The sandstone-shale breccia is a channel phenomenon. The breccia is in part derived from erosion of the channel base, but also is made up of sediment deposited by the sediment gravity flows which formed the channel. The development of the breccia depends on the amount of shale present, as can be seen from the increase in block size and amount of shale away from the channel axis. Loading only plays a minor role in the formation of the breccia. It is thought to be responsible for the irregular to pock marked surface of some of the sandstone blocks. The sandstone blocks were not lithified before incorporation into the breccia because they have an irregular outline, they do not show rolling up and their long axes are subparallel to bedding. However,

they were not entirely cohesionless as there seems to be no mixing of the sandstone and shale. The amalgamated sandstone lenses in the channel axis represent the bulk of the channel fill. The thinning downdip profile is possibly the result of bypassing by subsequent flows. These subsequent flows "leapfrog" or shingle (Enos, 1969a) the previous deposits, and deposit a sheet of sand which thickens downstream at first, but then thins at the distal end.

The facies relationships (Tables 4-1, 4-2) show that the massive sandstone facies is preceded either by the slurry or classical turbidite facies. The transition from either of these facies to the massive sandstone facies is random. It is also important to note that the slurry facies is never found overlying the massive sandstone facies. This suggests that the slurry facies is in some manner linked to initial progradation of the braided channel system in which the massive sandstone facies was deposited.

Channelling of any great depth only occurs at the base of the massive sandstone division. The channel excavation processes which formed the sandstone-shale breccia could possibly be one way in which the debris flows which deposited the slurry beds originated. Random slumping associated with channel deterioration after abandonment (Hiscott, 1977) is not thought to have formed the debris flows, because this

would not explain why the slurry beds dominate the base rather than the top of the massive sandstone units, or why they are not interbedded with the red mudstone facies.

As a whole, the slurry division is interpreted as a precursor of the massive sandstone division. The slurry and classical turbidite facies which make it up represent an initial increase in sandstone deposition before the braided channel system prograded into the depositional site.

The Classical Turbidite Units

The calcareous and siliceous classical turbidite units differ from classical turbidite sequences predicted by submarine fan models in that they are not characterized by coarsening and thickening upward trends. Apart from the obvious petrographic differences, the units differ greatly in their paleocurrent directions. The calcareous classical turbidites have a vector mean of 90°, whereas the vector mean of the siliceous classical turbidites and massive sandstone units is 140°.

The siliceous classical turbidite units (20, 21, 23 and 29) are composed of members of the classical turbidite and

slurry facies. The units are laterally continuous and regularly bedded. They show no internal vertical trends in bed thickness or grain size.

The lateral continuity and thickness regularity of the siliceous classical turbidite units suggests that they were deposited in an area of very low relief. The lack of vertical trend in grain size or bed thickness indicates random deposition of the beds.

The calcareous classical turbidite units (27 and 28) are composed solely of classical turbidites. The only trend in bed thickness and grain size is found in the upper part of unit 27 and unit 28. There is a decrease in the mean bed thickness and in grain size.

The calcareous classical turbidites were derived from a different source from the siliceous classical turbidites. The irregularity of the bed thickness changes in vertical sequence in unit 27 indicates random deposition. The thinning and fining upward trend in units 27 and 28 represents the demise of calcareous sedimentation in the area.

The Red Mudstone Units

The red mudstone units consist of very thick bedded mudstones which are usually structureless. Interbedded with

the mudstones are turbidites which have an average thickness of 10 cm. The turbidites are very continuous. Their petrology and paleocurrent indicators suggest they were derived from the same sources as the massive sandstone units. In unit 26 the red mudstones are interbedded with calcareous turbidites and limestone conglomerates. The red mudstone units are best developed where associated with the noncalcareous sandstone units.

There are several possibilities for the locus of deposition of the red mudstone units. The most important of these are: basin plain; at the base of a slope not associated with a submarine fan; or at the base of a slope associated with a submarine fan. If they were deposited on a submarine fan they could represent interlobe mud blankets (Walker, 1978) or interchannel deposits.

Definitive basin plain criteria are hard to establish since the characteristics will depend on the size of the basin. Characteristics such as multiprovenance and polymodal paleocurrent directions may apply to restricted basins, but not necessarily to open ocean basins. Similarly, regular and continuous bedding and the lack of a vertical trend in grain size or bed thickness not only apply to basin plain environments, but could also apply to base of slope environments. Perhaps the only thing that would not be expected in a basin plain environment would be the

regular appearance of coarse grained, thick bedded sediments.

Deposition in a base of slope, non-fan environment, might be characterized by polymodal paleocurrent directions; irregular, vertical trends in bed thickness and grain size and multiple provenance. Polymodal paleocurrent directions would develop from sediment being supplied laterally along the slope from either direction, as well as sediment transport downslope. The random interbedding of sediments from these directions would prevent development of a well defined trend in bed thickness or grain size. If the sources of these sediments were different the sediments will show multi-provenance.

If the red mudstones were deposited on a submarine fan they would be expected to be regularly interbedded with thick, coarse sediments, the sands might show channeling and/or a thinning and fining upward trend, or a thickening and coarsening upward trend, the paleocurrents may show a radial distribution, and the source of the sediments would be the same.

The red mudstone units are thought to have been deposited on a submarine fan because of:

(1) their close association with coarse sands deposited in a braided channel system;

(2) the regular and repeated facies sequence of red mudstone to slurry beds to massive sandstones to classical

turbidites to red mudstones;

(3) the radial distribution of the paleocurrent indicators;

(4) the common source of all the noncalcareous sandstones.

Submarine fan sediments which have similar characteristics to those of the red mudstone units are found in interchannel and interlobe areas. Interchannel areas are typified by thin bundles of turbidites, association with channel and levee deposits, thinning and wedging of the turbidites over short distances, and the presence of crevasse splay deposits (Mutti, 1977).

Sediments deposited in an interlobe area would be expected to be thick mudstones, very thin bedded siltstones and thin bedded turbidites, which envelope coarse sand bodies (in the case of a suprafan lobe these sandstones should be classical turbidites). A low sand/shale ratio and divergent but similar paleocurrent distributions should be found in the thin bedded turbidites and sandstone bodies.

The thin bedded turbidites in the red mudstone units were derived from the same type of source area as the massive sandstone units (except for those in unit 26, which are calcareous), and they exhibit paleocurrent indicators that are consistent with those of the sandstone units. The sand/shale ratio is low as would be expected if the red mudstones were deposited as an interlobe mud blanket. The

red mudstone units do not represent interchannel deposits because the thin bedded turbidites are too regular and continuous and they are not associated with large channels.

Slump Interpretation

The Calcisiltite Slump

To determine the direction of movement of the calcisiltite slump horizon in unit 27 the plunges of 75 slump fold axes and their senses of rotation were plotted on a Schmidt net (Hansen, 1967, 1971). To compensate for folding, the plunge of the syncline on which the horizon is located was removed before the limbs of the fold were rotated to the horizontal.

The fold axes from the north limb of the syncline are approximated by a great circle whose attitude is 062/24SE. No angle of separation is apparent between the slump folds with different senses of rotation. However, the slump folds which show counterclockwise rotation predominantly occur along the eastern half of the great circle. This suggests that the slump moved to the NNW (i.e. 318°).

The fold axes from the south limb of the syncline are approximated by a great circle whose attitude is 039/52NW.

A separation angle of 112° is evident and the senses of rotation of the folds suggest movement to the NNW (292°) down a northwest dipping paleoslope.

When the data from both limbs are combined, the results are the same as that obtained from the data of the south limb, but there is much better separation of the fold axes with different senses of rotation (Figure 6-1).

Discussion

Ideally, all the data should plot along one great circle in which the direction of movement is down the dip of the great circle, and the separation angle should bracket the direction of movement (Hansen, 1967, 1971). Furthermore, the data from each limb should mimic this, the only difference being a wider separation angle due to fewer points. The data presented agree with this except that the separate plots of the data from the fold limbs gives great circles which dip in different directions, although they both suggest that the slump moved to the northwest. The contradiction in the dips of the great circles may be due to errors in measurement of the slump fold axes.

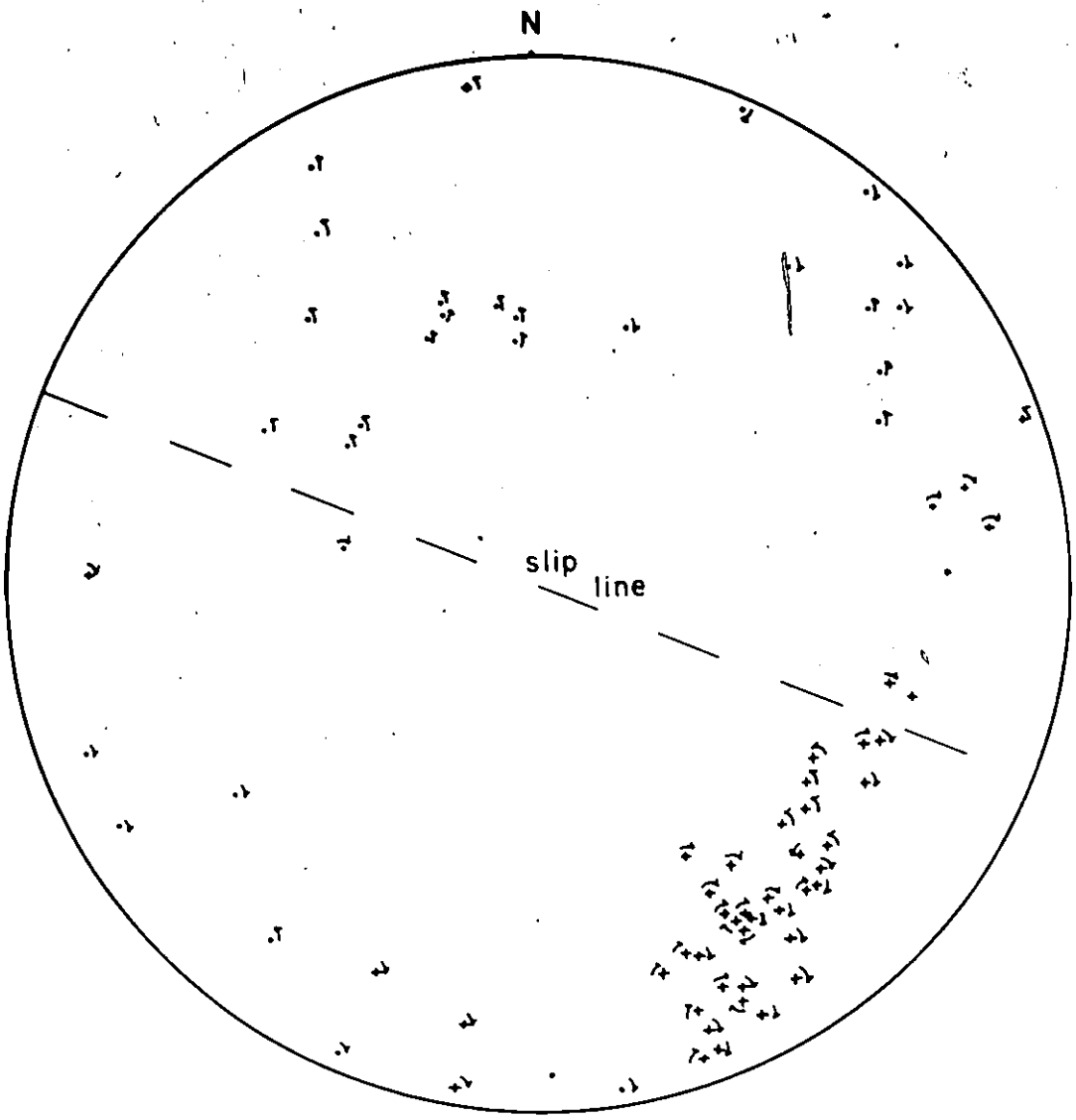

Figure 6-1: Stereoplot of fold axes in calcisiltite slump
+ - fold axis from north limb of syncline;
• - fold axis from south limb of syncline; no.= 75.

Errors in estimation of the slump movement direction, due to insufficient compensation for folding, the inclusion of parasitic folds and misidentification of the sense of rotation of the slump folds are negligible. Error in estimation of the plunge of the slump folds can have a major effect on the final position of the great circle when tectonic folding is accounted for. If the plunge is overestimated (e.g. pitch measured instead of plunge), and this overestimation is greater than the dip of the bed, then the slump fold axis will not be rotated to its correct position. This is important because if the plunge is less than the dip of the bed the slump fold axis will be rotated into the diametrically opposed quadrant and change its sense of rotation. This could explain why the data from the north limb of the syncline suggests that the slump moved up the paleoslope indicated by the dip of the great circle.

The lack of a separation angle in the data from the north limb of the syncline does not represent errors in slump fold measurement. Rather, it points out the presence of slump folds which are oriented perpendicular to the strike of the paleoslope. Such orientations have been reported in snow slides (Lajoie, 1972). They by no means preclude the use of the data since it is their sense of

rotation and the direction of plunge which are important to the method. The only reason a separation angle is obtained at all in a Hansen plot is because little or no data from the sides of the slump, where the fold axes are subparallel to the slip line, are usually evident (P.M. Clifford, pers. comm., 1977).

Other Slumps

The red mudstone-calcareous sandstone slump in unit 26 at "Point à Confusion" is interpreted as being tectonically induced. This is clearly shown by the close association of a reverse fault (Figure 3-20), the close association of tectonic parasitic folds, and the decrease in the degree of deformation as the horizon is traced away from the fault.

Shalaby (1977) has described in detail the slump horizon forming unit 3 at Plage Victor. His Hansen plot of the slump fold axes indicates that the slump moved to the southwest (233°). His discussion of the results concludes that due to polydeformation of some of the folds, the original orientations of the slump fold axes cannot be determined and therefore the Hansen plot does not mean anything.

Sequence of Deposition

The lower part of the section shows a coarsening and thickening upward sequence in units 15, 16 and 18 (Figure 2-6), which accompanies a change from calcareous to noncalcareous sedimentation. The thickness of the sandstone units above this shows no particular trend, indicating that sandstone deposition was becoming irregular. Units 26 and 27 record a switch in paleocurrent directions and the re-establishment of calcareous sedimentation in the area. The thinning and fining upward trend in units 27, 28 and 30 represents the demise of calcareous sedimentation. Unit 29 signifies the change back to noncalcareous sedimentation.

Deposition on a Submarine Fan?

The depositional history outlined above is best explained by deposition on a submarine fan. The following discussion deals with why this conclusion was reached and the type of fan on which the sediments were deposited.

Nelson and Nilsen (1974) outline two types of basins in which submarine fans develop, and point out a third type in which fan-like facies relationships could develop. The first type is a restricted basin which is characterized by

multiple source areas, well developed proximal facies, and distinct proximal to distal facies gradation. This type of fan has perhaps provided the basis of current submarine fan models. The fans of the Periadriatic Apennines (Miocene) (Ricci Lucchi, 1975) are a good example of this type. The second type are those which develop in open ocean basins. The features of this type are: one depositional source; a poorly developed suprafan; and very gradual and indistinct proximal to distal changes. The best example of this type is the Bengal Fan (Curray and Moore, 1971). Facies relationships which are similar to those developed on submarine fans could also be found in deep sea trenches and channels. These geomorphic features would be expected to contain long linear sand bodies. Smaller fans might be built out perpendicular to the trench axis, but this would not occur in mid-ocean channels. An example of this type is the Northwest Mid Atlantic Ocean Channel (Chough and Hesse, 1976).

The style of deposition of the St. Roch sediments does not agree with the characteristics of deposition in a restricted basin, as there is no well developed proximal facies and there is no distinct proximal to distal gradation in the facies. The facies relationships in the massive sandstone units are similar to those found on the upper

part of a suprafan lobe, but they are not associated with the classical turbidites of the suprafan lobe or coarser sediments of the inner fan facies. The absence of these might be explained by having the sediments deposited off the debouching mouth of an incised channel. But even so, there still should be the classical turbidites, of the newly deposited lobe, associated with it.

Deposition in a deep sea trench or mid-ocean channel is dismissed because the paleocurrent data indicate transport perpendicular to tectonic strike with which the feature would have been parallel. The calcareous sediments do not represent the channel deposits, because they are not the dominant type of sediment in the St. Roch Formation, and there is no evidence that they are channelized. Furthermore, the regional interpretation (St. Julien and Hubert, 1975) of the Quebec Appalachians suggest that the sediments were deposited on an Atlantic type continental margin (Dewey and Bird, 1970) which is not characterized by a trench or mid-ocean channel.

The poorly developed suprafan and the lack of distinct proximal to distal facies transition suggest that the St. Roch Formation sediments were deposited on a fan in an open ocean basin. It is evident that two source areas contributed to deposition in this area, and that only the

cratonic source developed the submarine fan facies associations. The calcareous sediments were transported longitudinally from a source to the west and deposited across the lower part of the fan.

Interpretation of the sediments as a submarine fan which formed in an open ocean basin explains several important features. (1) The regular alternation of the sandstone and mudstone units can be explained by switching channel systems that become covered by a mud blanket when disused. (2) The thickening upwards sequence seen in units 15, 16 and 18 is concurrent with the switch from calcareous to noncalcareous sedimentation. It indicates progradation of the braided channel system into the area. However, the lack of coarser grained facies suggests that progradation was not extensive or that no coarse material was available. (3) The consistency of the paleocurrent measurements and their radial distribution is a common feature of submarine fans. The divergence between the directions observed in the red mudstone and siliceous classical turbidite units and the massive sandstone units is due to the spreading out of the sediment gravity flows as they leave the channellized area of the fan.

Regional Geology

The primary study on the sediments of the Quebec Complex (Hubert, 1965, 1973) interprets the St. Roch Formation as the deep water lithosome of the complex, which was deposited between two continental shelves, one to the northwest and the other to the southeast. The arkosic sandstones and conglomerates (noncalcareous sandstones of this study) were interpreted as being derived from the shelf to the southeast, and the calcareous sediments were derived from the shelf to the northwest. The amount of calcareous sedimentation in the area was thought to be minimal, forming only 5% of the total thickness.

The paleocurrent data and the petrology of the calcareous sediments indicates that they were derived from a carbonate platform to the west. The noncalcareous sediments were derived from a cratonic source to the northwest. The high degree of alteration of the feldspars and the occurrence of the chamosite in the red mudstones suggests the sediments were deposited in tropical latitudes, because chamosite only forms in waters warmer than 20°C. The occurrence of glauconitic thin bedded sandstones interbedded with the red mudstone suggests that these sediments were deposited in water that was deeper than 125 m, as in the

tropical latitudes glauconite does not form at depths less than this (Porrenga, 1967).

The calcareous sediments make up 25% (134 m) of the total thickness measured. When this is combined with the thickness of calcareous sediments at Plage Victor (approximately 130 m) it forms 22% of the maximum thickness of the St. Roch Formation (1210 m).

During the Cambrian Period an Atlantic type continental margin (Dewey and Bird, 1970) probably existed along the eastern side of North America. The Quebec Complex was part of a shale-feldspathic sandstone assemblage which formed the continental rise prism of this margin (St. Julien and Hubert, 1975). The calcareous sediments in this sequence were derived from a source to the west (Osborne, 1956; Hubert, 1965, 1973; Rogers, 1968; Hubert, Lajoie and Leonard, 1970). The noncalcareous sediments were derived from the Canadian shield to the northwest (Lajoie, Heroux and Mathey, 1974; Hubert, Lajoie and Leonard, 1970).

The petrological and paleocurrent studies of the study area are in complete agreement with the regional interpretations of the sediments of the Quebec Complex of St. Julien and Hubert (1975). If the regional interpretation of the Quebec Appalachians is correct, the Atlantic type margin would facilitate the development of an open ocean basin fan

system.

From the amount of calcareous sandstones seen at Plage Victor and St. Jean-Port-Joli it is evident that the carbonate platform was a much more important source than originally thought by Hubert (1965, 1973).

The Plage Victor-St. Jean-Port-Joli area contains at least 960 m of sediment. This is almost the same as the maximum thickness estimated for the St. Roch Formation (1210 m). If none of the stratigraphic sequence is repeated to any great extent further along the St. Lawrence River, it seems very probable that the formation is much thicker than originally estimated.

REFERENCES

ALLEN, J.R.L., 1969. Erosional current marks of weakly cohesive mud beds. J. Sediment. Petrology, 39, 607-623.

BLATT, H., MIDDLETON, G.V. and MURRAY, R., 1972. Origin of Sedimentary Rocks. Prentice-Hall, Inc., 634p.

CARTER, R.M., 1975. A discussion and classification of subaqueous mass-transport with particular application to grain-flow, slurry-flow, and fluxoturbidites. Earth-Sci. Rev., 11, 145-177.

CHOUGH, S. and HESSE, R., 1976. Submarine meandering thalweg and turbidity currents flowing for 4000 km in the Northwest Atlantic Mid-Ocean Channel, Labrador Sea. Geology, 4, 529-533.

CROWELL, J.C., 1957. Origin of pebbly mudstones. Geol. Soc. Amer., Bull., 68, 993-1010.

CURRAY, J.R., 1956. The analysis of two-dimensional orientation data. Jour. Geol., 64, 117-131.

CURRAY, J.R. and MOORE, D.G., 1971. Growth of the Bengal Deep Sea Fan and denudation in the Himalayas. Geol. Soc. Amer., Bull., 82, 563-572.

DELONG, R.C. and MIDDLETON, G.V., 1978. Ordovician carbonate megabreccias at Cape Cormorant, Western Newfoundland: Submarine debris flows. Abstract submitted to Geol. Soc. Amer. Ann. Mtg., 1978.

DEWEY, J.F. and BIRD, J.M., 1970. Mountain belts and the new global tectonics. Jour. Geophys. Res., 75, 2625-2647.

ENOS, P., 1969a. Cloridorme Formation, Middle Ordovician flysch, northern Gaspé Peninsula, Quebec. Geol. Soc. Amer., Spec. Pap. 117, 66p.

ENOS, P., 1969b. Anatomy of a flysch. J. Sediment. Petrology, 39, 680-723.

FOLK, R.L., 1954. The distinction between grain size and mineralogical composition in sedimentary-rock nomenclature. Jour. Geol., 62, 344-359.

HAMPTON, M.A., 1972. The role of subaqueous debris flow in generating turbidity currents. J. Sediment. Petrology, 42, 775-793.

HAMPTON, M.A., 1975. Competence of fine-grained debris flows. J. Sediment. Petrology, 45, 834-844.

HANSEN, E., 1967. Methods of deducing slip line orientations from the geometry of folds. Yb. Carnegie Instn., Wash., 65, 387-405.

HANSEN, E., 1971. Strain Facies. Springer-Verlag, New York, 207p.

HISCOTT, R.N., 1977. Sedimentology and Regional Implications of Deep-Water Sandstones of the Tourelle Formation, Ordovician, Quebec. Ph.D. Thesis, McMaster Univ., Hamilton, Ont., 542p.

HUBERT, C., 1965. Stratigraphy of the Quebec Complex in the l'Islet-Kamouraska Area, Quebec. Unpub. Ph.D. Thesis, McGill Univ., Montreal, Quebec, 192p.

HUBERT, C., 1969. Plage Victor. In Flysch Sedimentology in the Appalachians (C. Hubert et al., editors). Geol. Assoc. Can./Mineral. Assoc. Can. Guidebook #1, 23-27.

HUBERT, C., 1973. Région de Kamouraska, La Pocatière, Saint-Jean-Port-Joli. Rapport Géologique 151, Min. des Richesses Naturelles du Québec, 205p.

HUBERT, C., LAJOIE, J. and LEONARD, M.A., 1970. Deep sea sediments in the Lower Paleozoic Quebec Supergroup. In Flysch Sedimentology in North America (J. Lajoie, editor). Geol. Assoc. Can., Spec. Pap. 7, 103-125.

JOHNSON, A.M., 1970. Physical Processes in Geology. Freeman, Cooper and Co., San Francisco, 577p.

LAJOIE, J., 1972. Slump fold axis orientation: an indication of paleoslope? J. Sediment. Petrology, 42, 584-586.

LAJOIE, J. and CHAGNON, A., 1973. Origin of red beds in a Cambrian flysch sequence, Canadian Appalachians, Quebec. Sedimentology, 20, 91-104.

LAJOIE, J., HEROUX, Y. and MATHEY, B., 1977. The Precambrian Shield and the Lower Paleozoic Shelf: the unstable provenance of the Lower Paleozoic flysch sandstones and conglomerates of the Appalachians between Beaumont and Bic, Quebec. Can. J. Earth Sci., 11, 951-963.

LARSEN, V. and STEEL, R.J., 1978. The sedimentary history of a debris flow dominated, Devonian alluvial fan - a study of textural inversion. Sedimentology, 25, 37-60.

LOWE, D.R., 1975. Water escape structures in coarse grained sediments. Sedimentology, 22, 157-204.

MIDDLETON, G.V. and HAMPTON, M.A., 1973. Sediment gravity flows: mechanics of flow and deposition. In Turbidites and Deep-water Sedimentation (G.V. Middleton and A.H. Bouma, editors). Soc. Econ. Paleontol. Mineral., Short Course, Anaheim, 1-38.

MIDDLETON, G.V. and HAMPTON, M.A., 1976. Subaqueous sediment transport and deposition by sediment gravity flows. In Marine Sediment Transport and Environmental Management (D.J. Stanley and D.J.P. Swift, editors). John Wiley and Sons, 197-218.

MORRIS, R.C., 1971. Classification and interpretation of disturbed bedding types in the Jackfork flysch rocks (Upper Mississippian), Ouachita Mountains, Arkansas. J. Sediment. Petrology, 41, 410-424.

MOUNTJOY, E.W. and PLAYFORD, P.E., 1972. Submarine megabreccia debris flows and slumped blocks of Devonian of Australia and Alberta - a comparison (abstr.). Amer. Assoc. Petrol. Geol., Bull., 56, 641.

MUTTI, E., 1974. Examples of ancient deep-sea fan deposits from circum-Mediterranean geosynclines. Soc. Econ. Paleontol. Mineral., Spec. Publ. 19, 92-105.

MUTTI, E., 1977. Distinctive thin-bedded turbidite facies and related depositional environments in the Eocene Hecho Group (south-central Pyrenees, Spain). Sedimentology, 24, 107-132.

MUTTI, E. and RICCI LUCCHI, F., 1972. Le torbidite dell' Appenino settentrionale: introduzione all'analisi di facies. Mem. Soc. Geol. Italiana, 11, 161-199.

NELSON, C.H. and NILSEN, T.H., 1974. Depositional trends of modern and ancient deep-sea fans. Soc. Econ. Paleontol. Mineral., Spec. Publ. 19, 69-91.

NORMARK, W.R., 1970. Growth patterns of deep-sea fans. Amer. Assoc. Petrol. Geol., Bull., 54, 2170-2195.

NORMARK, W.R., 1974. Submarine canyons and fan valleys: factors affecting growth patterns of deep sea fans. Soc. Econ. Paleontol. Mineral., Spec. Publ. 19, 56-68.

OSBORNE, F.F., 1956. Geology near Quebec City. Naturaliste Canadien, 83, 157-223.

PORRENGA, D.H., 1967. Glauconite and chamosite as depth indicators in the marine environment. Mar. Geol., 5, 495-501.

RAMSAY, J.G., 1961. The effects of folding upon the orientation of sedimentary structures. J. Geol., 69, 84-100.

RAO, J.S. and SENGUPTA, S., 1972. Mathematical techniques for paleocurrent analysis: treatment of data. J. Internatl. Assoc. Math. Geol., 4, 235-248.

REINECK, H.E. and SINGH, I.B., 1975. Depositional Sedimentary Environments. Springer-Verlag, New York, 439p.

RICCI LUCCHI, F., 1975. Miocene paleogeography and basin analysis in the Periadriatic Apennines. In Geology of Italy (S. Coy, editor), Tripoli, Petroleum Exploration Soc. of Libya, 5-111.

RODGERS, J., 1968. The eastern edge of the North American continent during the Cambrian and Early Ordovician. In Studies of Appalachian Geology: Northern and Maritime (E-an Zen et al., editors), Wiley Interscience, New York, 141-149.

SHALABY, H., 1977. Analyse des Structures Geometriques et Interpretation Rheologique d'un Slump Cambrien dans le Flysch de Saint-Jean-Port-Joli, Appalaches du Quebec. M.Sc. Thesis, Univ. de Montreal, 86p.

SKIPPER, K. and MIDDLETON, G.V., 1975. The sedimentary structures and depositional mechanics of certain Ordovician turbidites, Cloridorme Formation, Gaspe Peninsula, Quebec. Can. J. Earth Sci., 12, 1934-1952.

STANLEY, D.J. and BOUMA, A.H., 1964. Methodology and paleogeographic interpretation of flysch formations: a summary of studies in the Maritime Alps. In Turbidites, Developments in Sedimentology 3, (A.H. Bouma and A. Brouwer, editors), Elsevier, Amsterdam, 34-64.

ST. JULIEN, P. and HUBERT, C., 1975. Evolution of the Taconian Orogen in the Quebec Appalachians. Amer. J. Sci., 275-A, 337-362.

WALKER, R.G., 1978. Deep-water sandstone facies and ancient submarine fans: Models for exploration for stratigraphic traps. Amer. Assoc. Petrol. Geol., Bull., 62, 932-966.

WOOD, A. and SMITH, A.J., 1959. The sedimentation and sedimentary history of the Aberystwyth Grits (Upper Llandoverian). Geol. Soc. London, Quart. J., 114, 163-195.

APPENDIX 1

The equality of mean directions can be tested by calculating the homogeneity of the number of populations studied.

$$H = \frac{\left\{ \sum_{1}^{k} \frac{Ti^2}{Si^2} - \left(\sum_{1}^{k} \frac{Ti}{Si^2} \right)^2 \right\}}{\sum_{1}^{k} \frac{1}{Si^2}}$$

(Rao and Sengupta, 1972).

where: H - homogeneity

Ti - tangent of the vector mean

Si - standard deviation (derived from Fig. 3 of Curray, 1956)

k - number of populations.

A null hypothesis (H_o) is then set up and is rejected if the homogeneity (H) is significant.

H_o: The vector mean of units 16-25 is the same as the vector mean of units 26 and 27.

$$H = \frac{\left(\frac{-.6371^2}{30^2} + \frac{-4.437^2}{18^2} \right) - \left(\frac{-.6371}{30^2} + \frac{-4.437}{18^2} \right)^2}{\frac{1}{30^2} + \frac{1}{18^2}}$$

$$= 14.52$$

Therefore H_o is rejected.

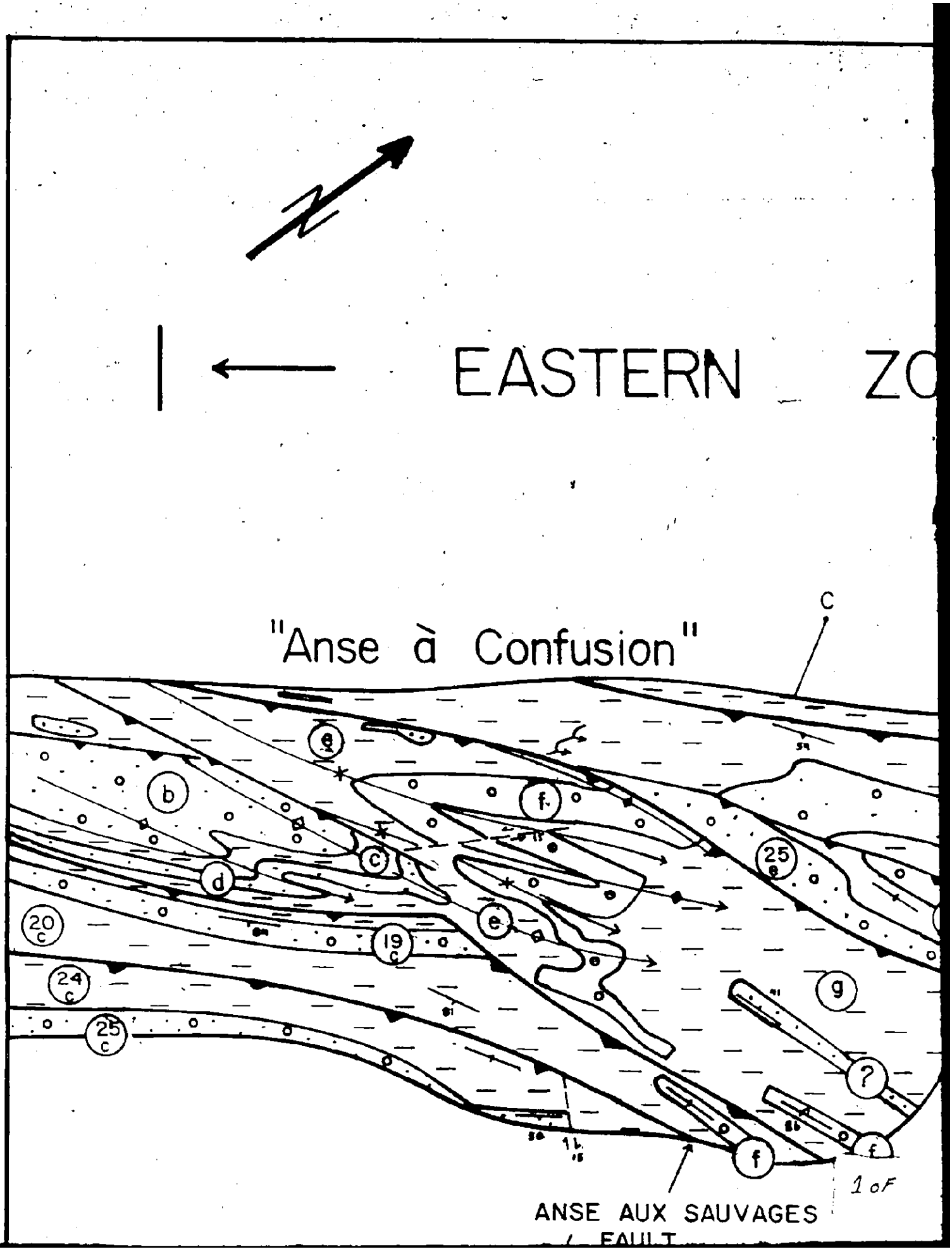
EASTERN ZO
"Anse à Confusion"
C
a
b
c
d
e
f
g
20 c
19 c
24 c
25 c
25 g
?
f
f
1 of
ANSE AUX SAUVAGES
FAULT

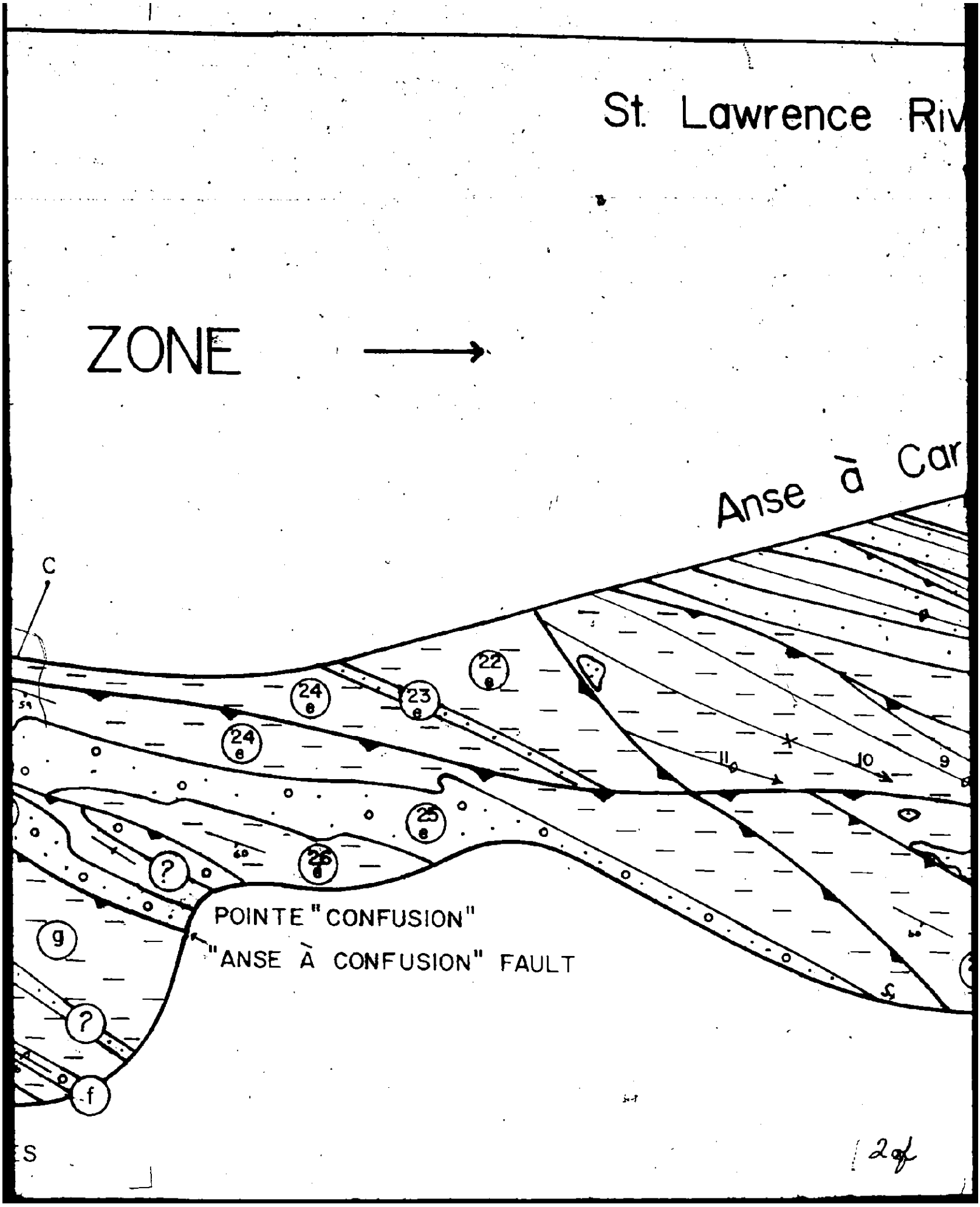
St. Lawrence Riv
ZONE
Anse à Car
C
22
e
24
e
23
e
24
e
25
e
26
e
?
11
10
9
POINTE "CONFUSION"
"ANSE À CONFUSION" FAULT
g
?
f
S

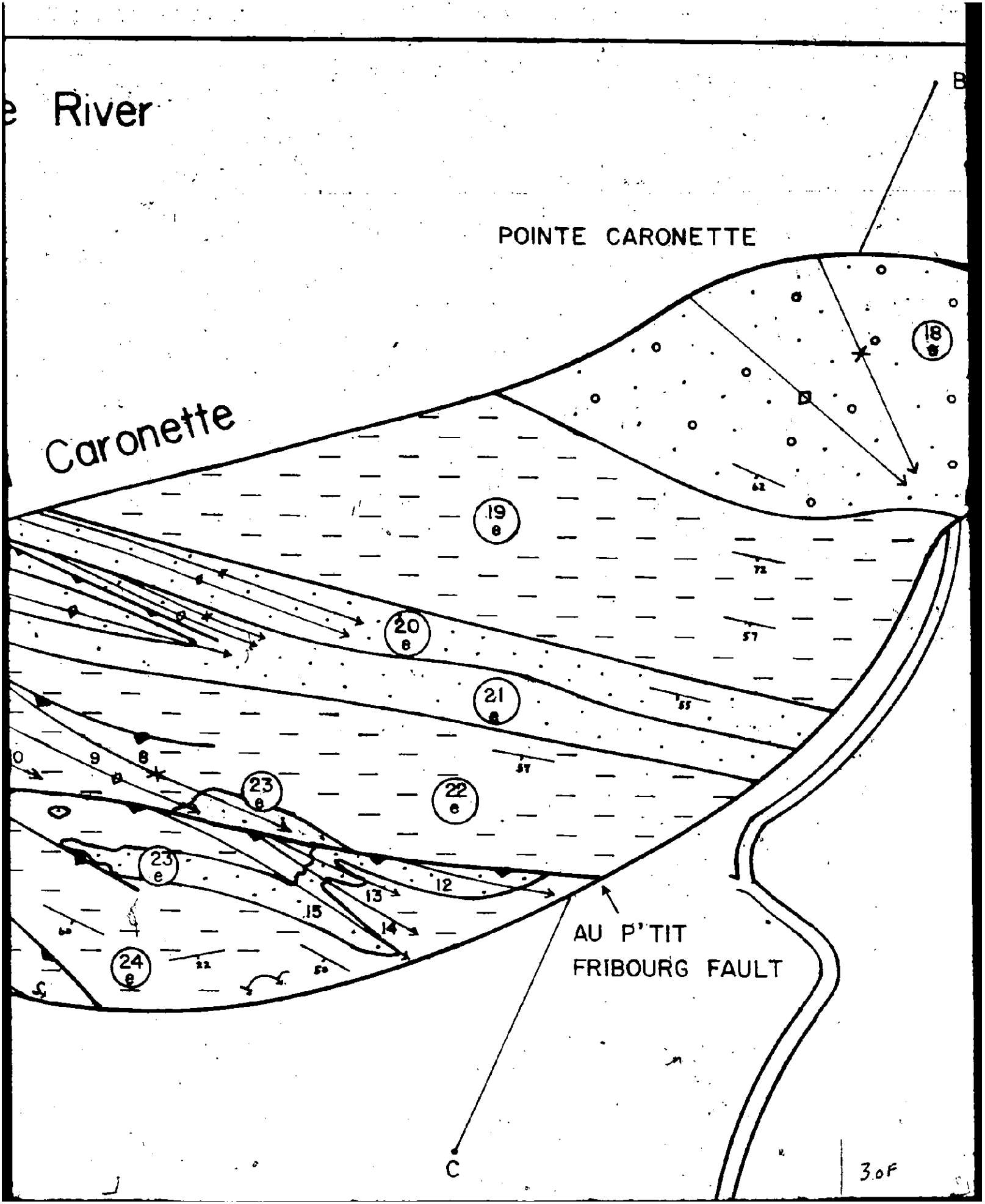
e River
POINTE CARONETTE
Caronette
18 e
19 e
20 e
21 e
22 e
23 e
23 e
24 e
AU P'TIT
FRIBOURG FAULT
C
3 of

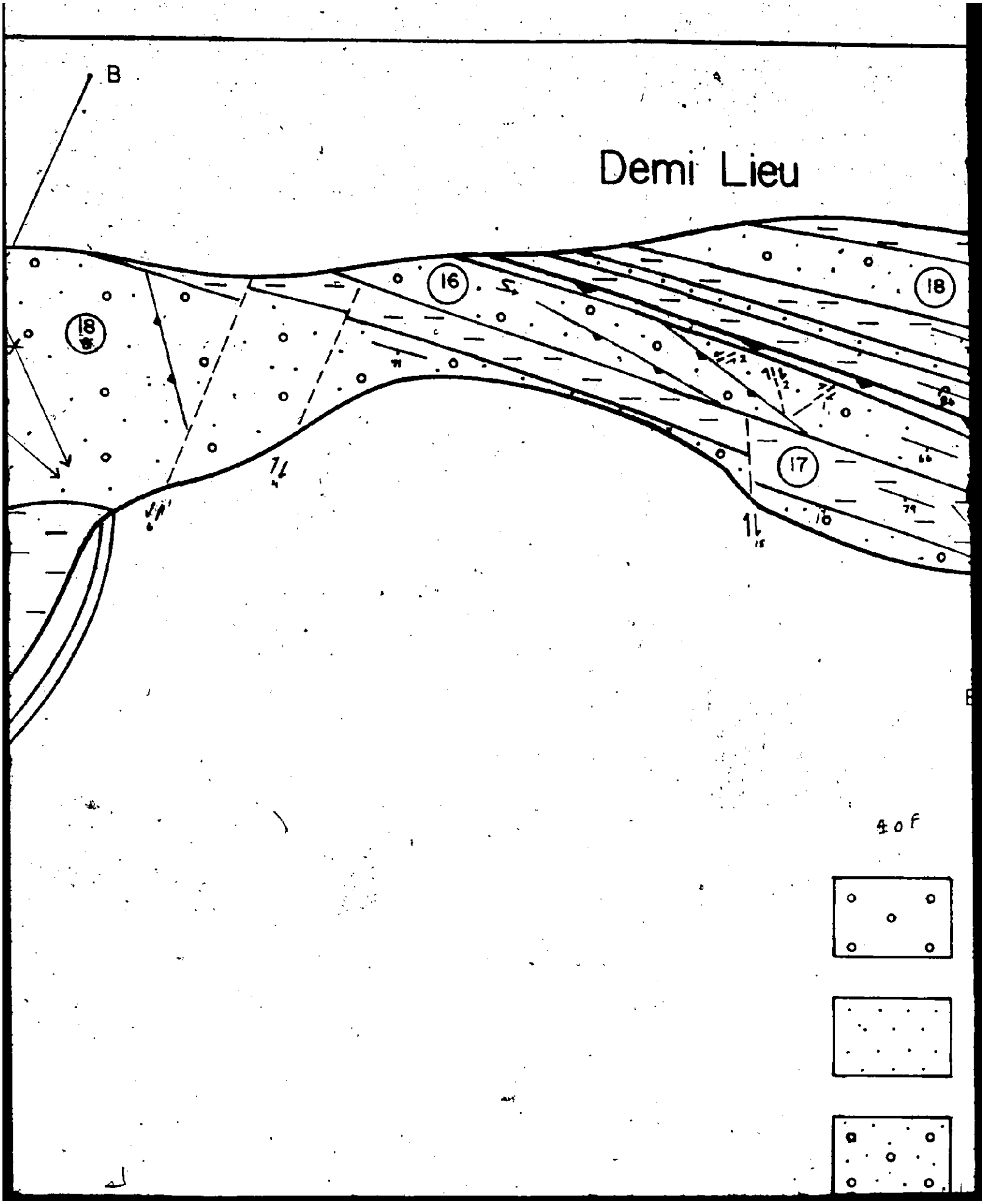
B
Demi Lieu
16
18
18
17
4 of

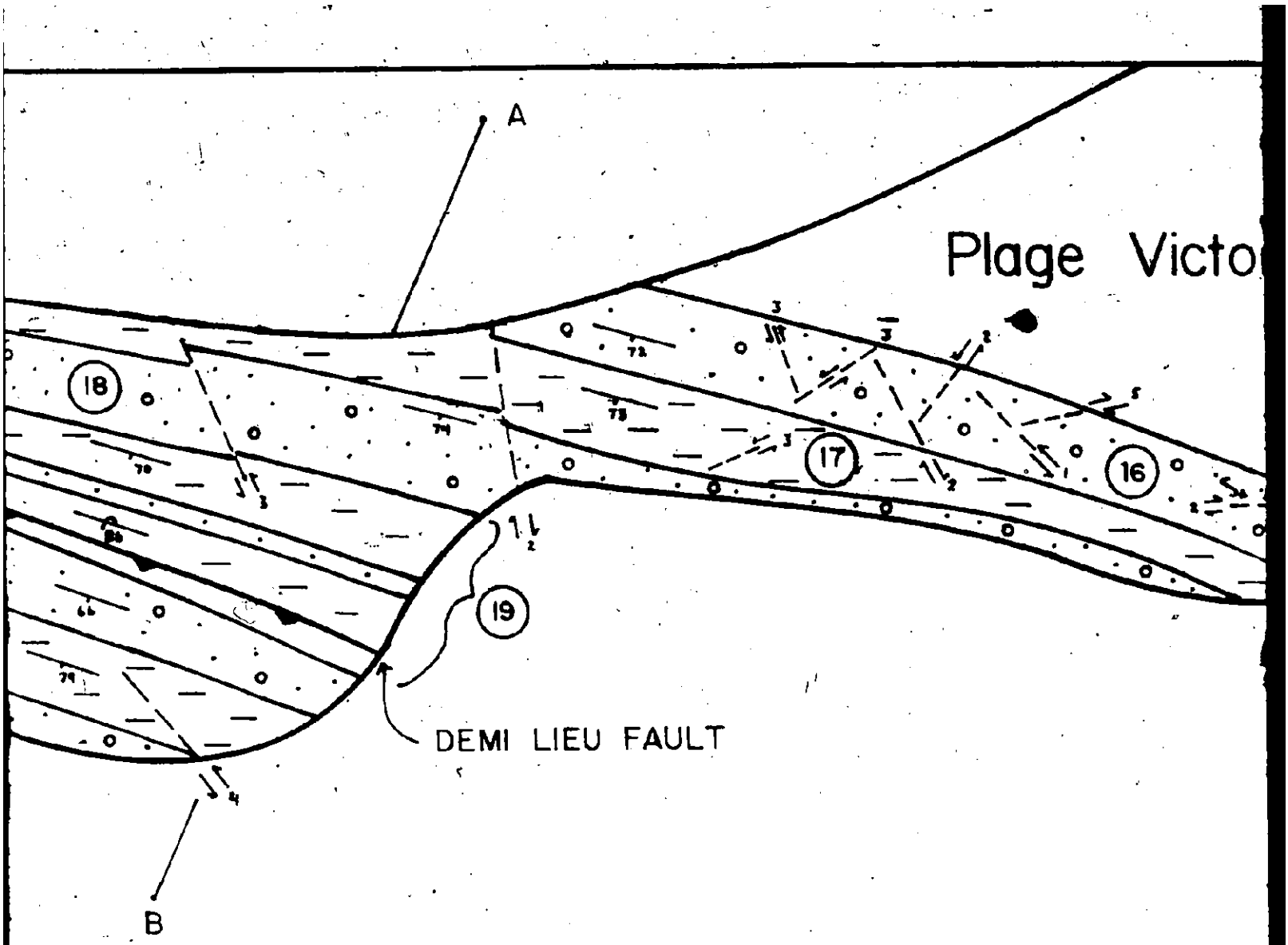

KEY

5 OF

Massive sandstones +/-
Pebbly sandstones

Classical turbidites &
Slurries

Classical turbidites, slurries,
massive & pebbly sandstones

Reverse

Transcurre
meters; u

Dip & stri
overturned

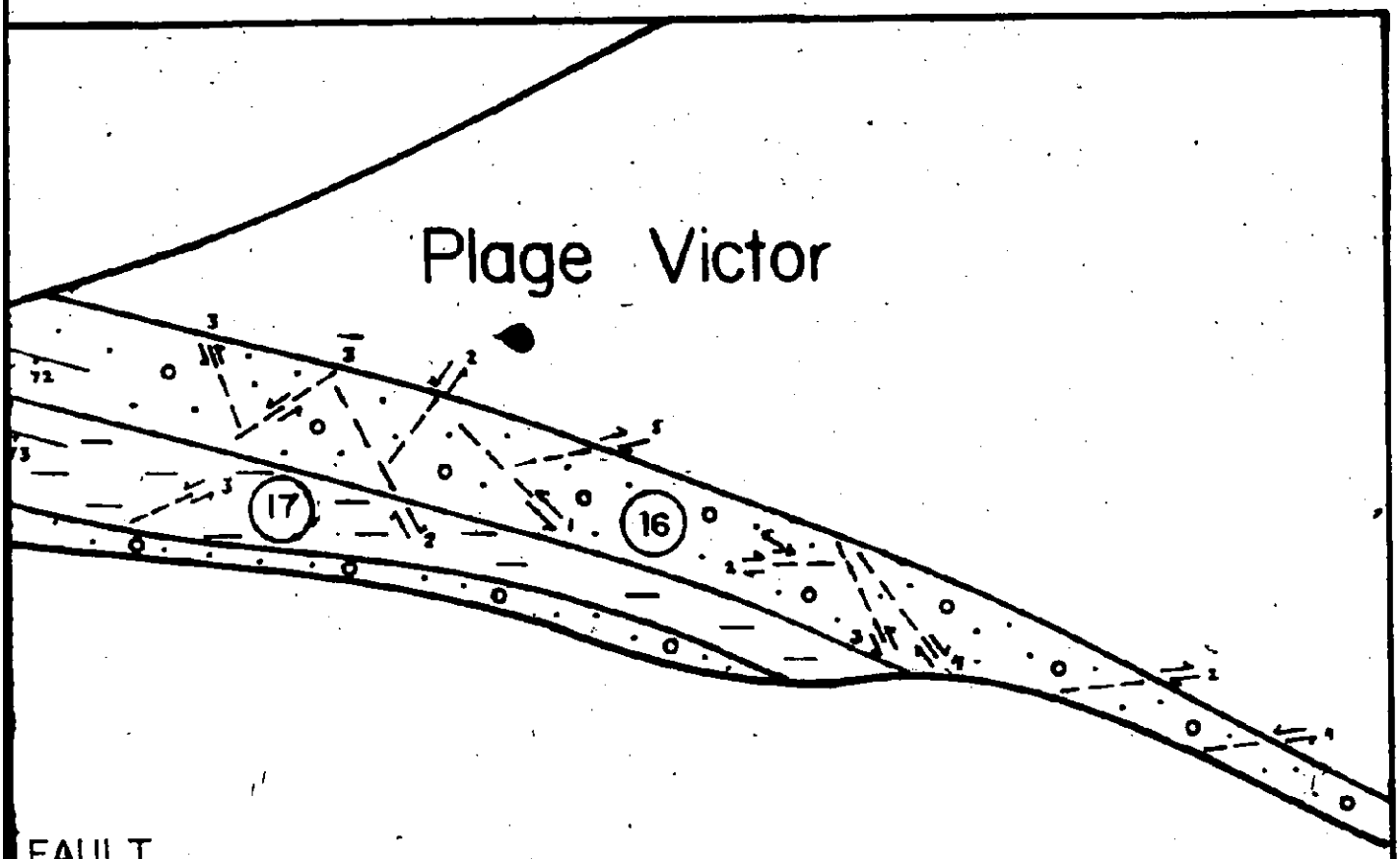

FAULT

KEY

Reverse fault

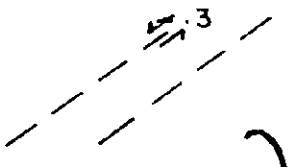

Transcurrent fault, movement in meters; undetermined

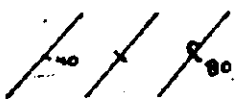

Dip & strike: upright, vertical, overturned

es,

dstones

6 o F

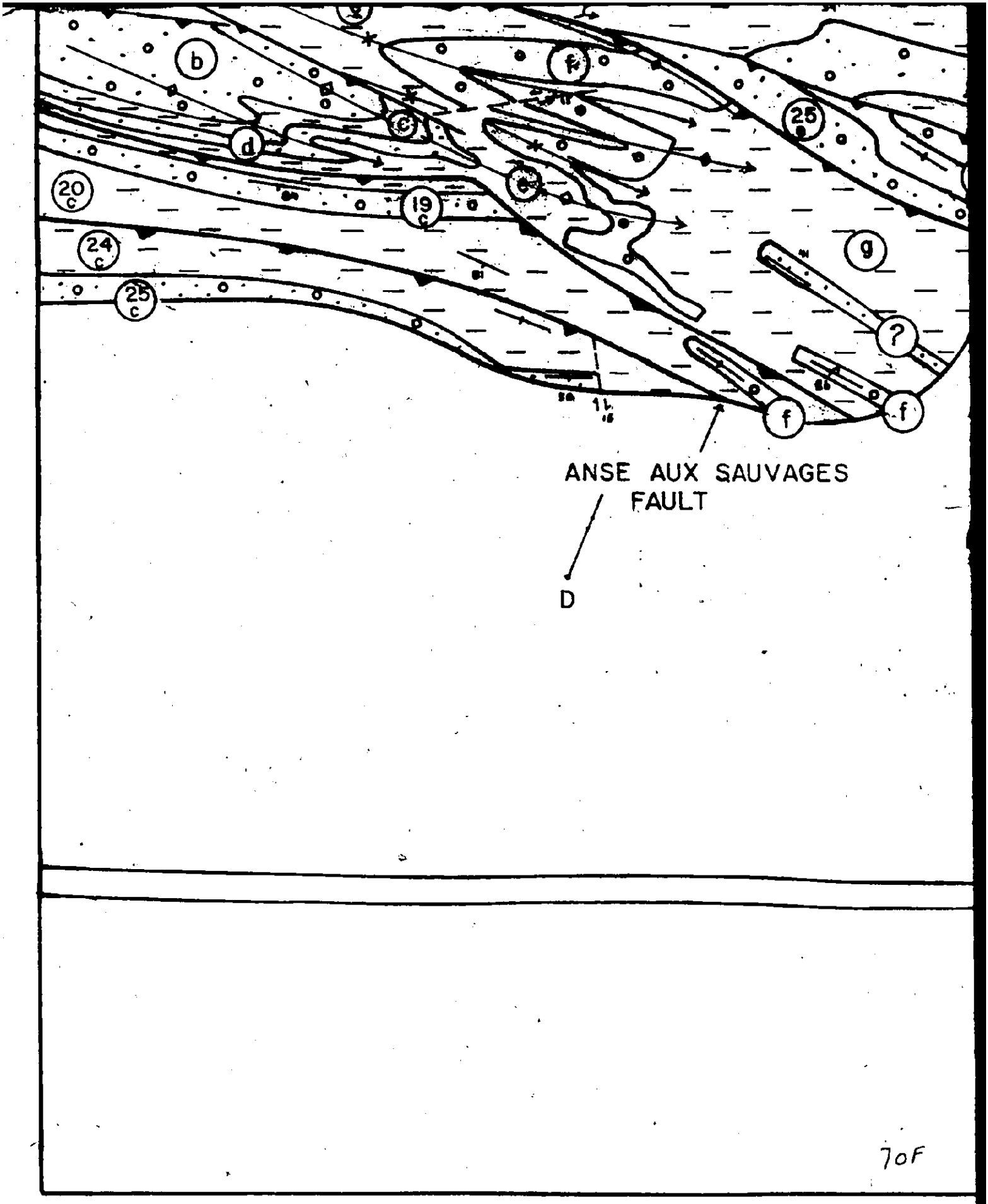
b
d
c
e
f
25
20
c
19
c
24
c
25
c
g
?
f
f
ANSE AUX SAUVAGES
FAULT
D

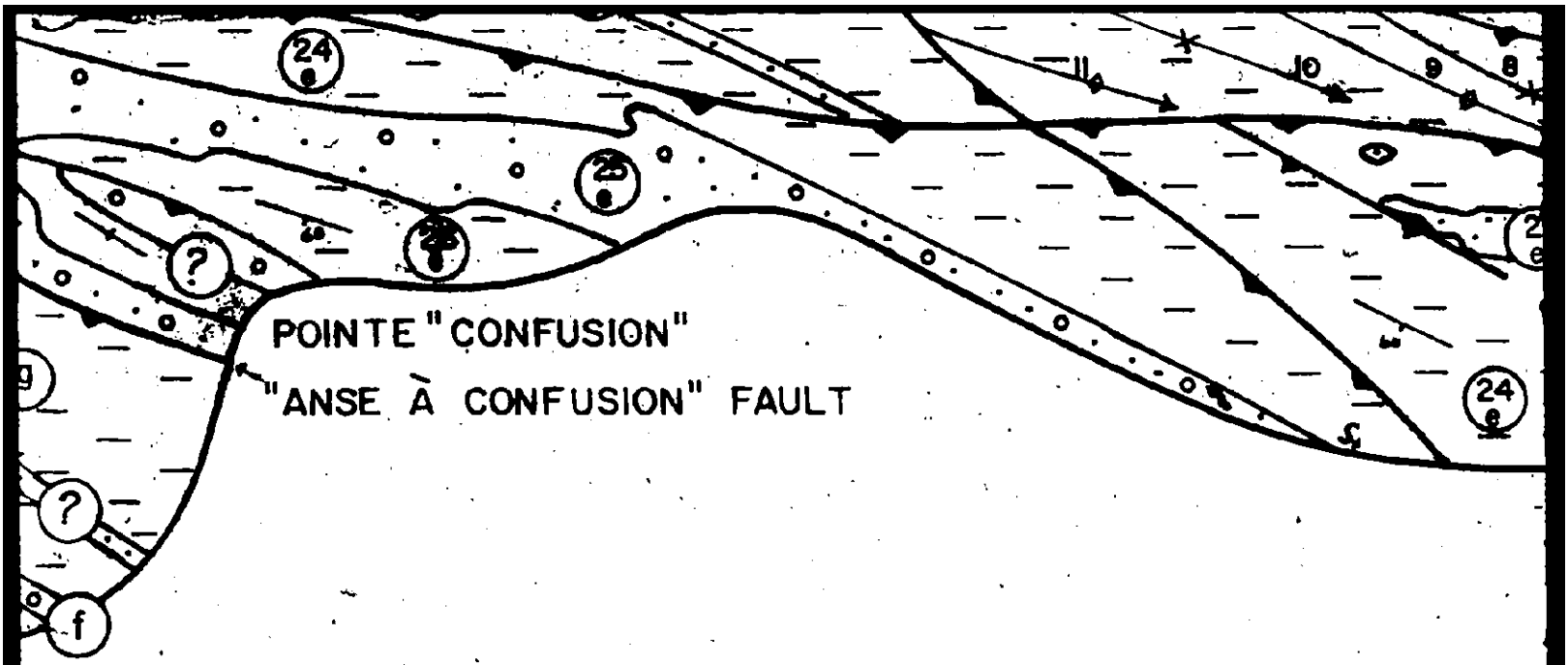

SCALE

0 50 100 150 200

Rte. 132

8 OF

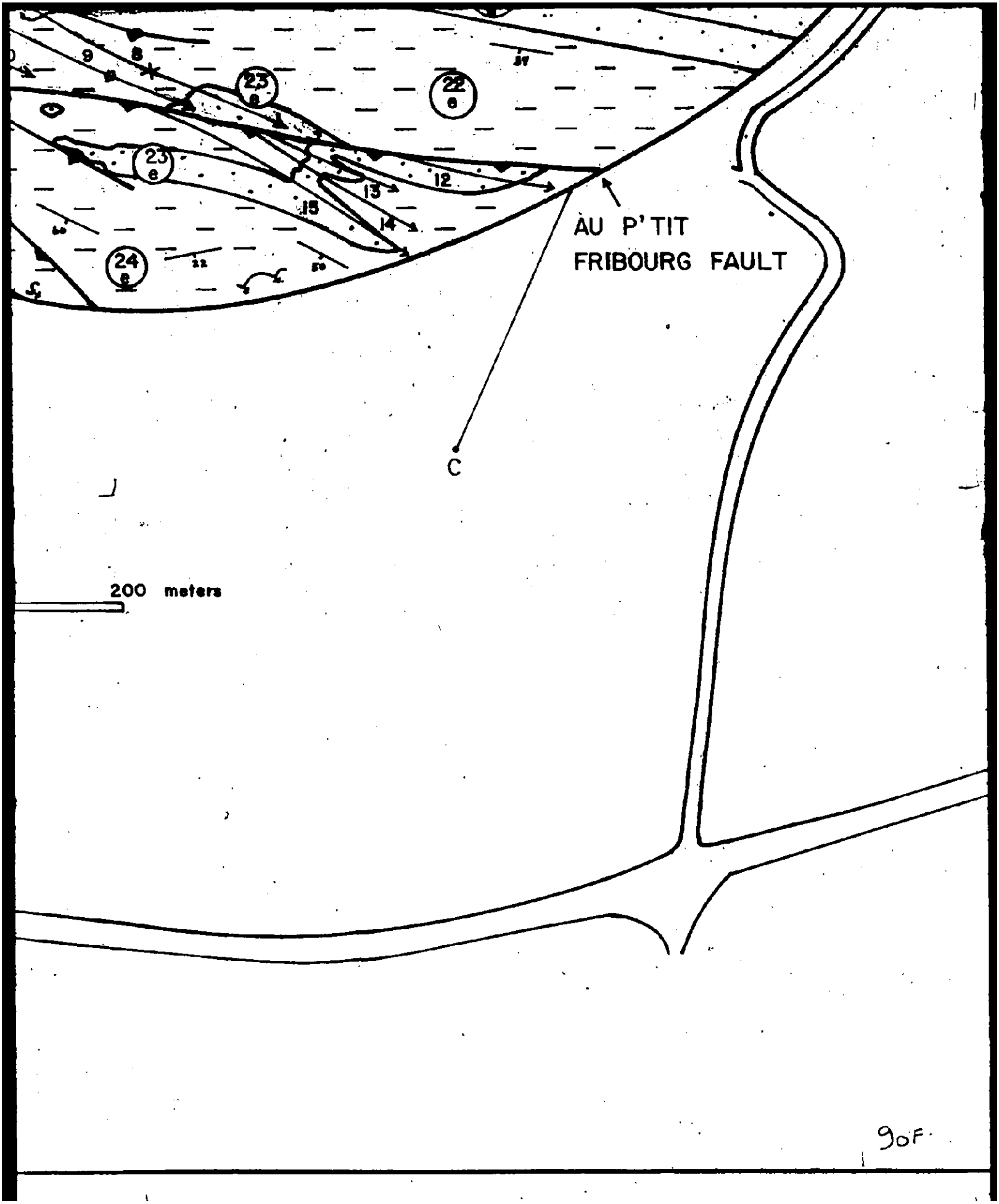
AU P'TIT
FRIBOURG FAULT
C
200 meters

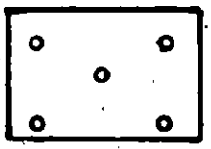

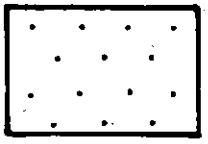

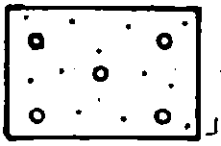

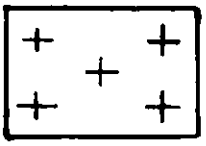

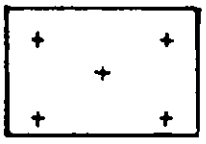

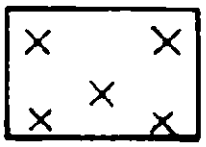

KEY

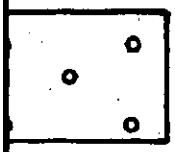

Massive sandstones +/-
Pebbly sandstones

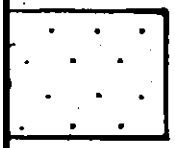

Classical turbidites &
Slurries

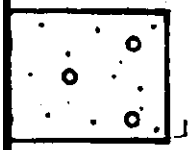

Classical turbidites, slurries,
massive & pebbly sandstones

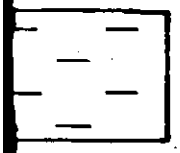

Red mudstone

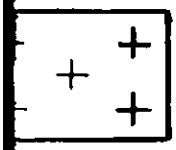

Calcareous sandstone

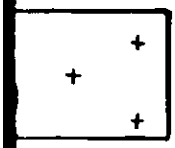

Calcareous siltstone

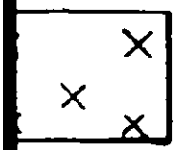

Black shale

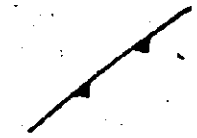

Reverse

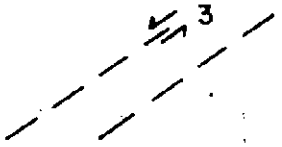

Transcurre
meters; u

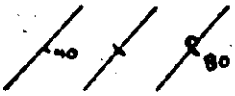

Dip & str
overturned

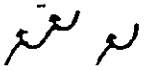

Parasitic

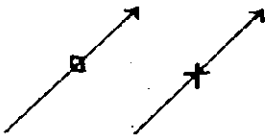

Anticline,

Structural

(16)

Unit numb

KEY

Reverse fault

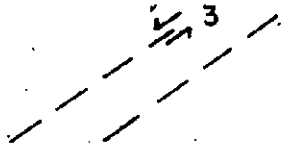

Transcurrent fault, movement in meters; undetermined

ies,
dstones

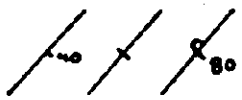

Dip & strike: upright, vertical, overturned

Parasitic folds

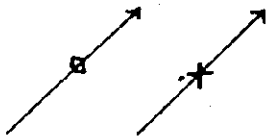

Anticline, syncline

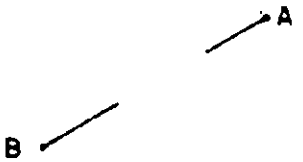

Structural cross section

Unit number

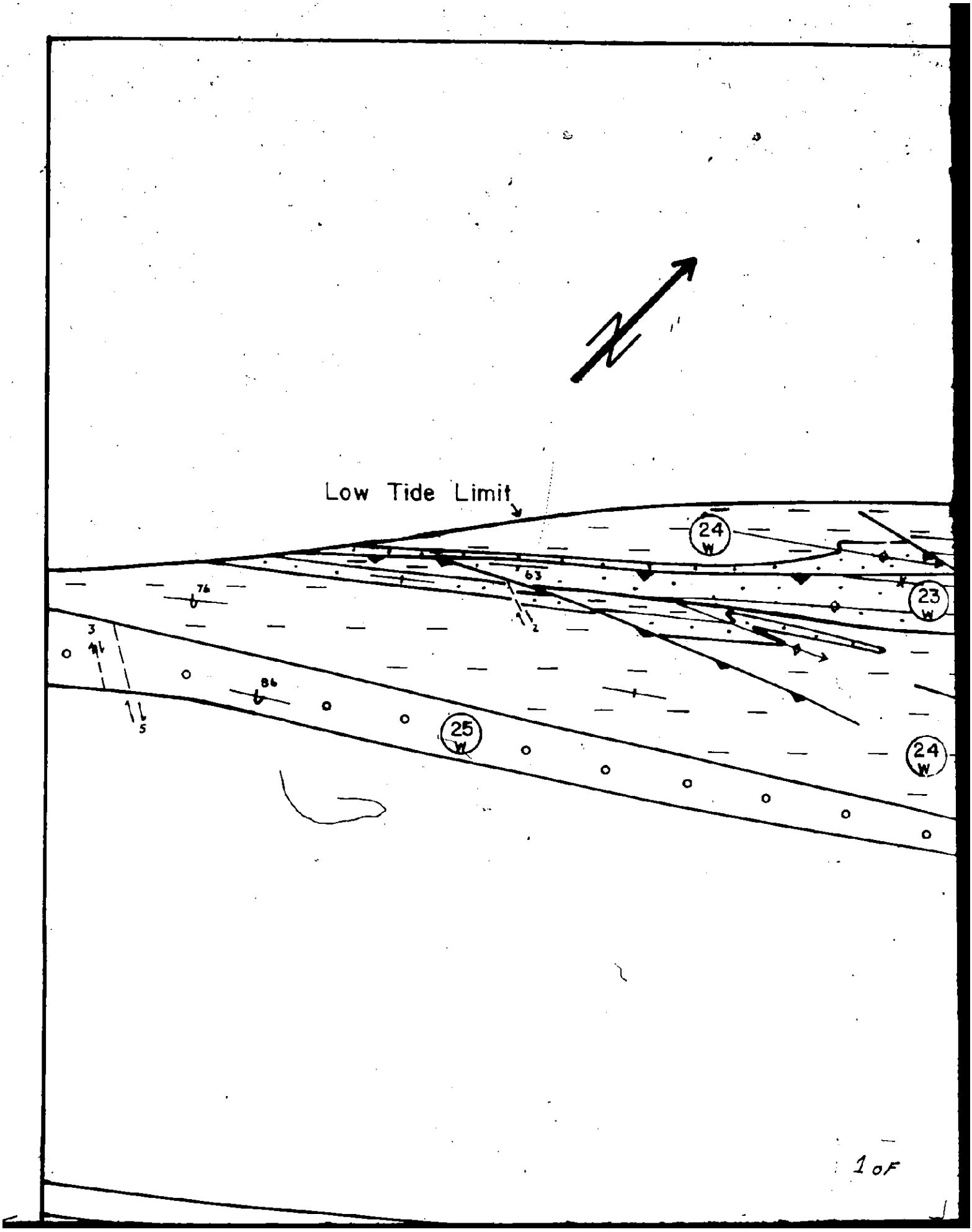

1 of

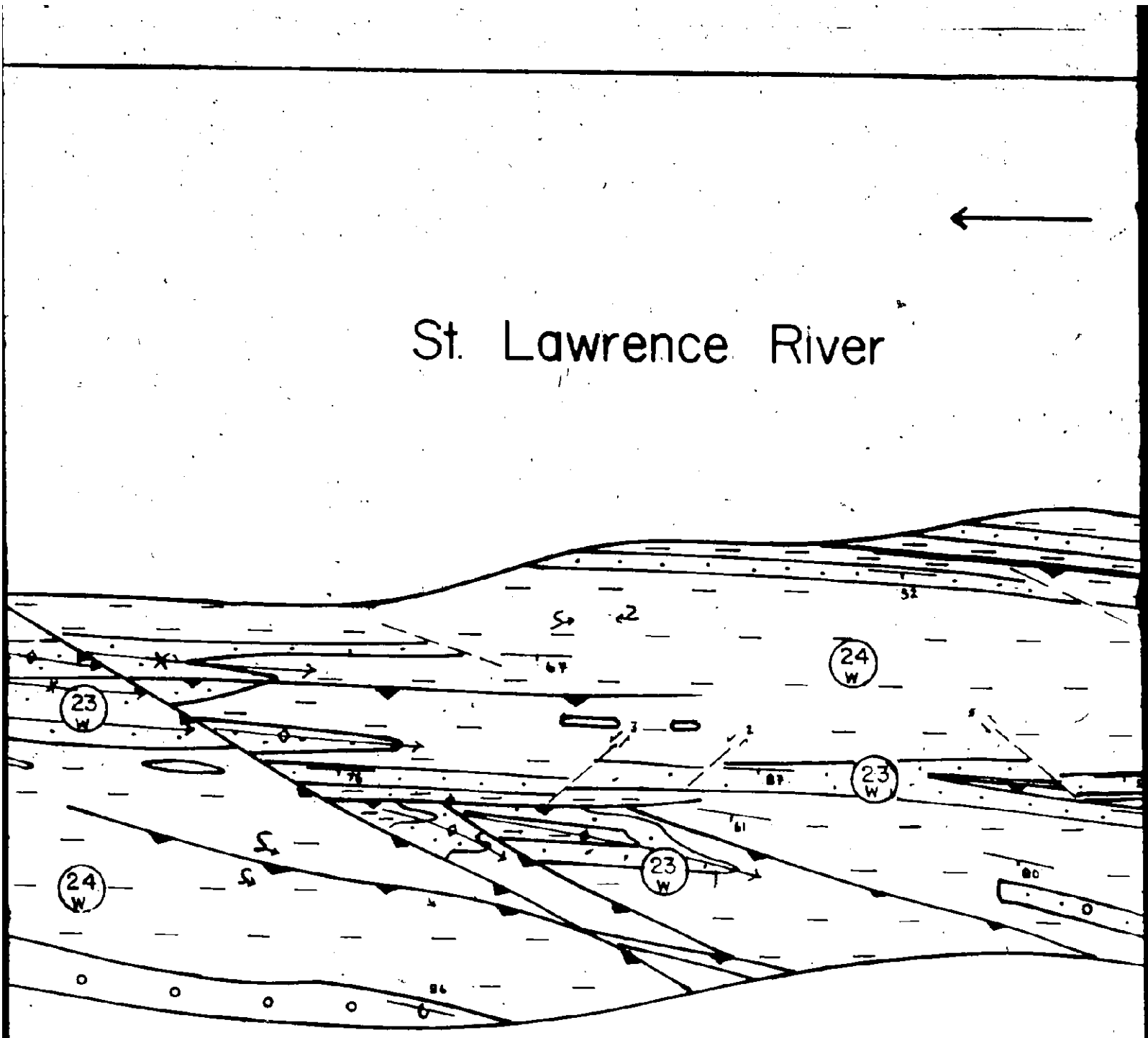
St. Lawrence River
23 W
24 W
23 W
24 W
23 W

WESTERN ZONE

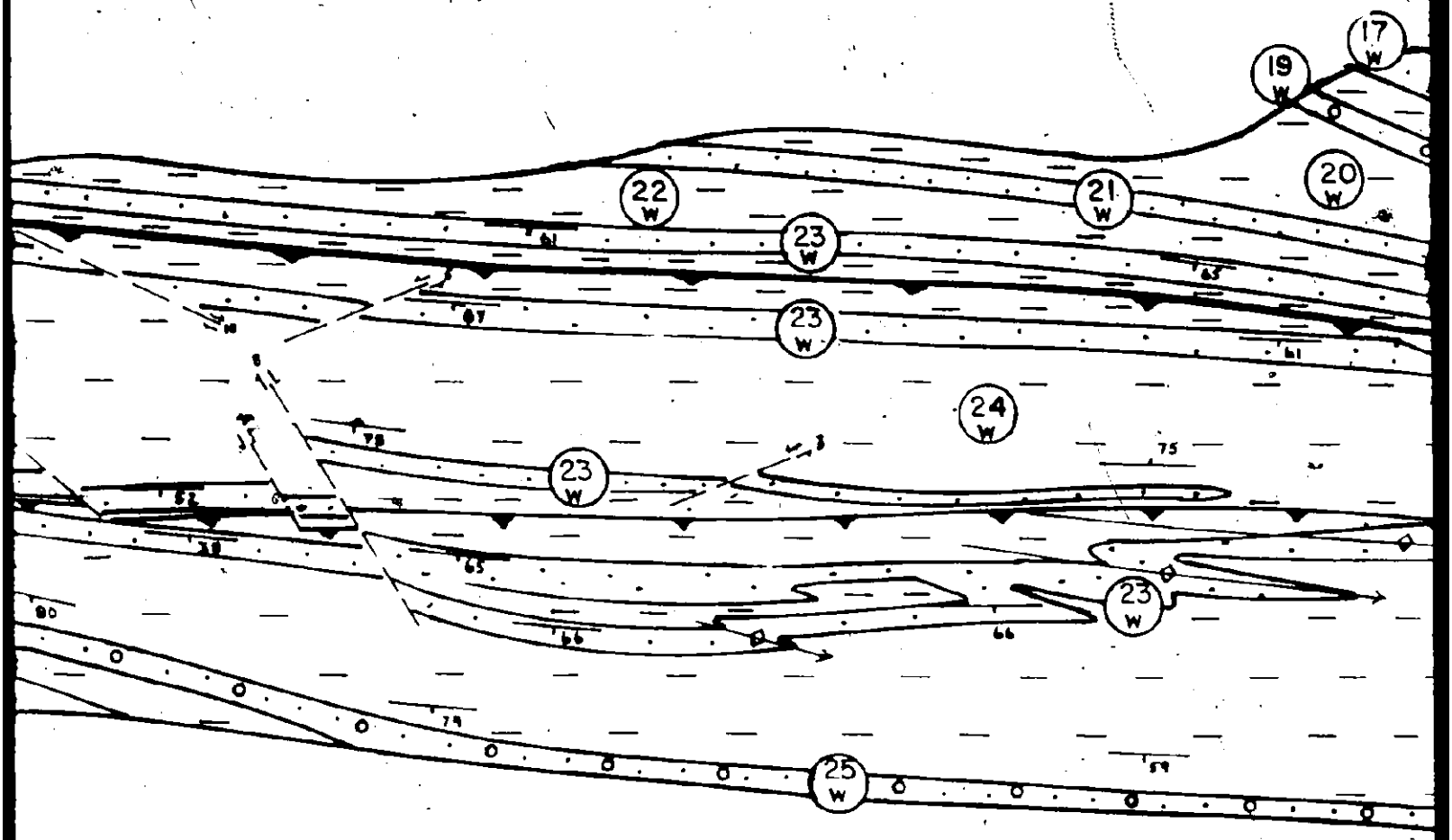

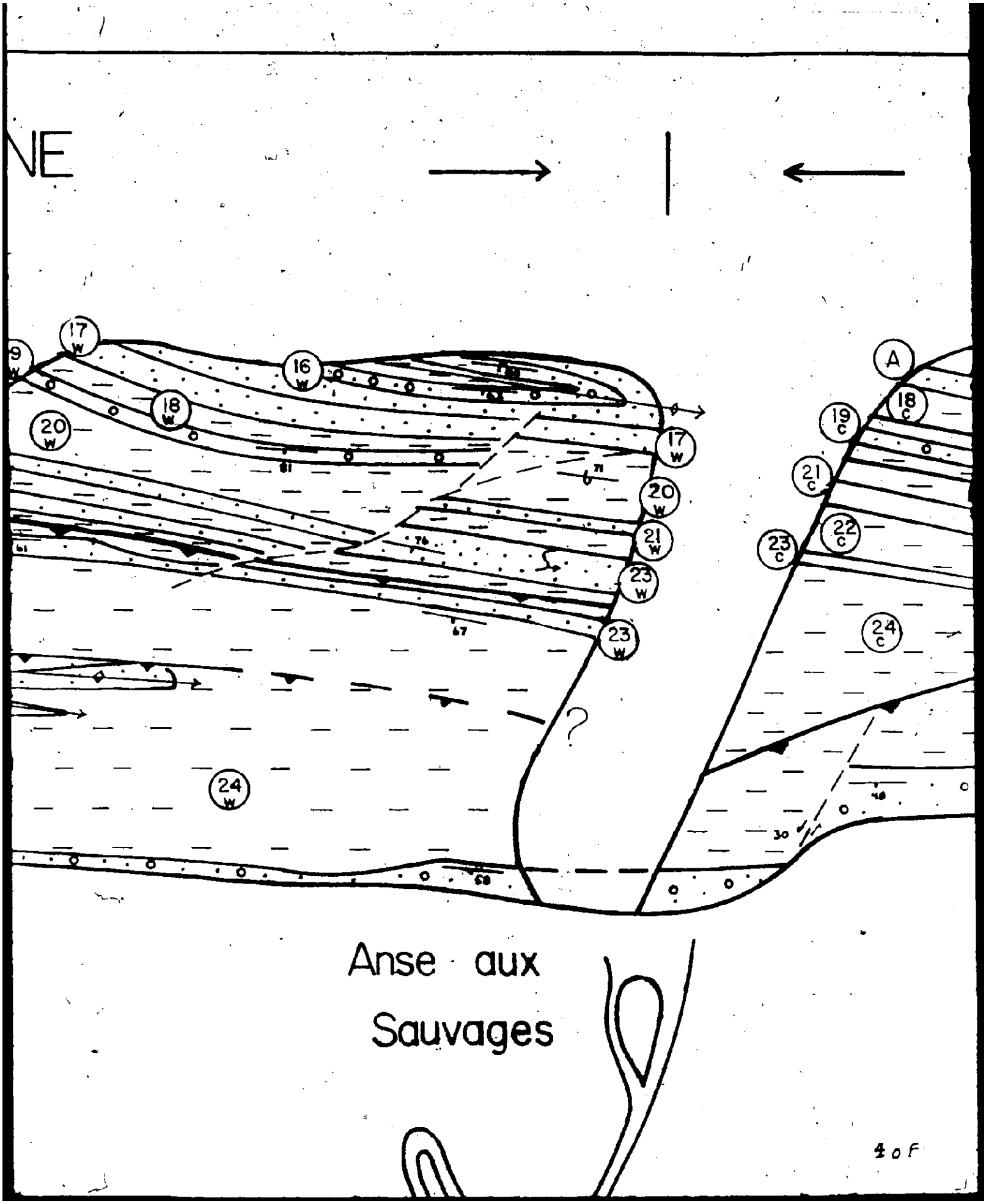
NE
17 W
16 W
18 W
20 W
17 W
20 W
21 W
23 W
23 W
24 W
A
18 C
19 C
21 C
22 C
23 C
24 C
?
Anse aux
Sauvages
4 of F

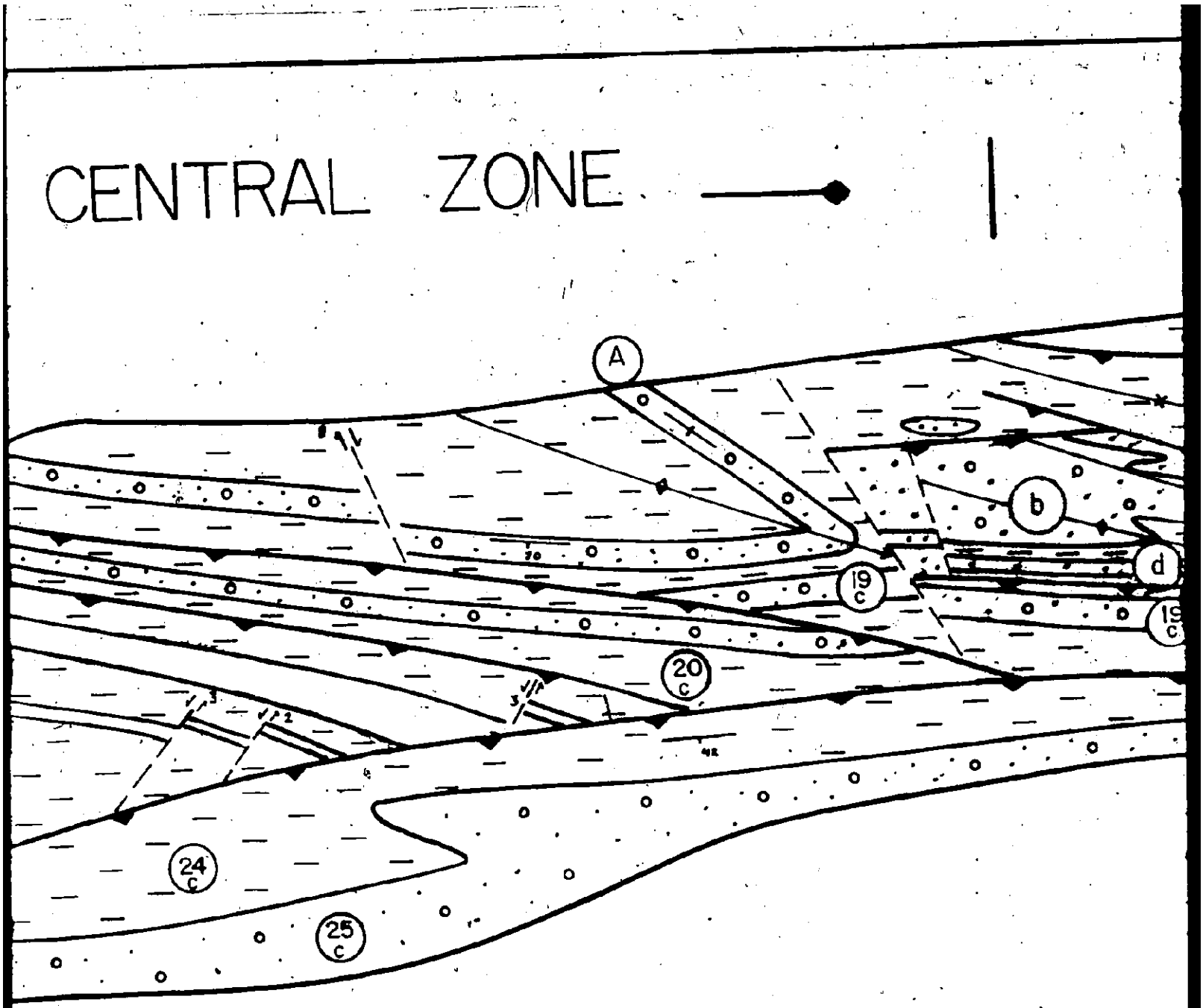
CENTRAL ZONE
A
b
d
19
C
20
C
24
C
25
C

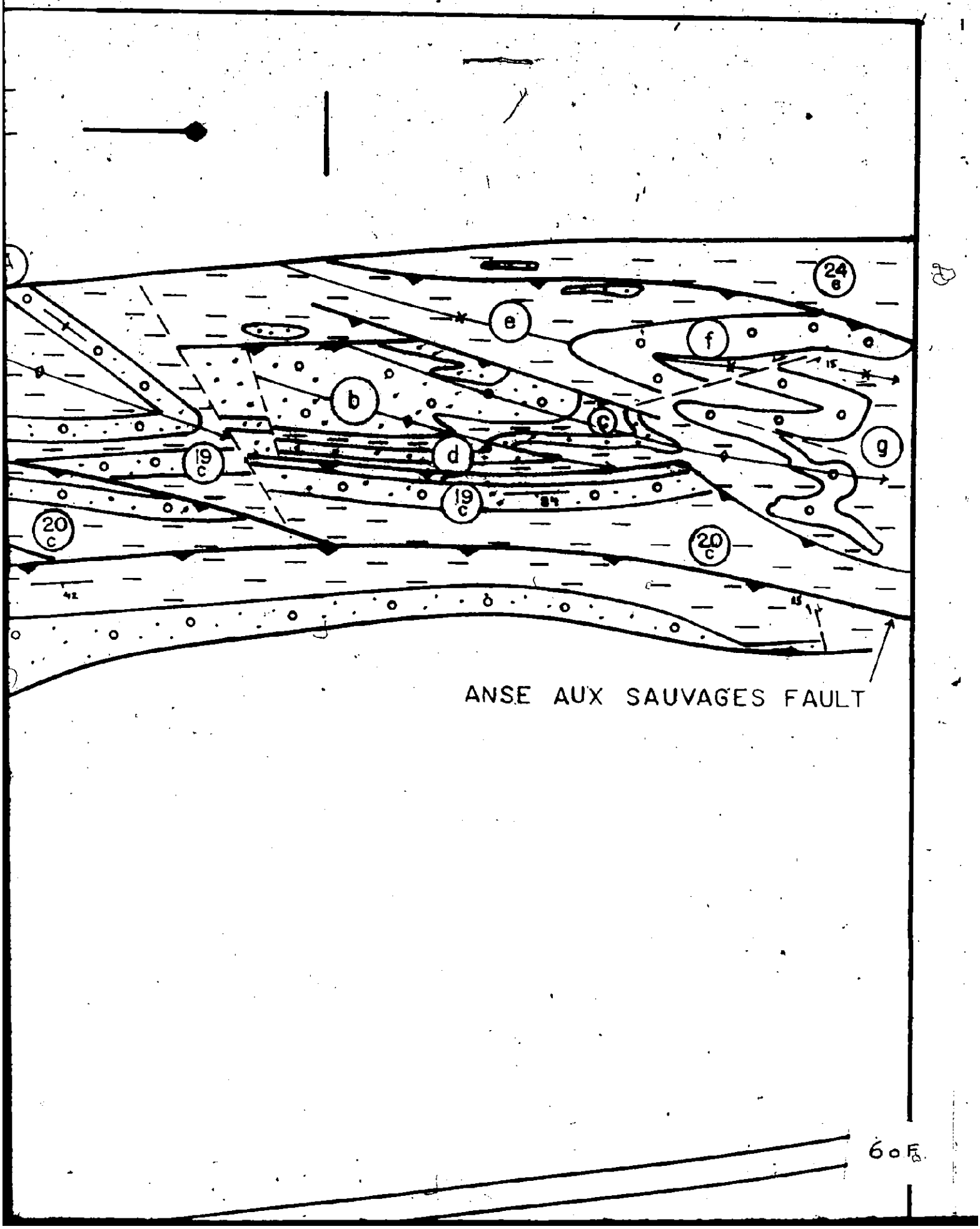
24 e
e
f
b
c
g
d
19 c
19 c
20 c
20 c
ANSE AUX SAUVAGES FAULT

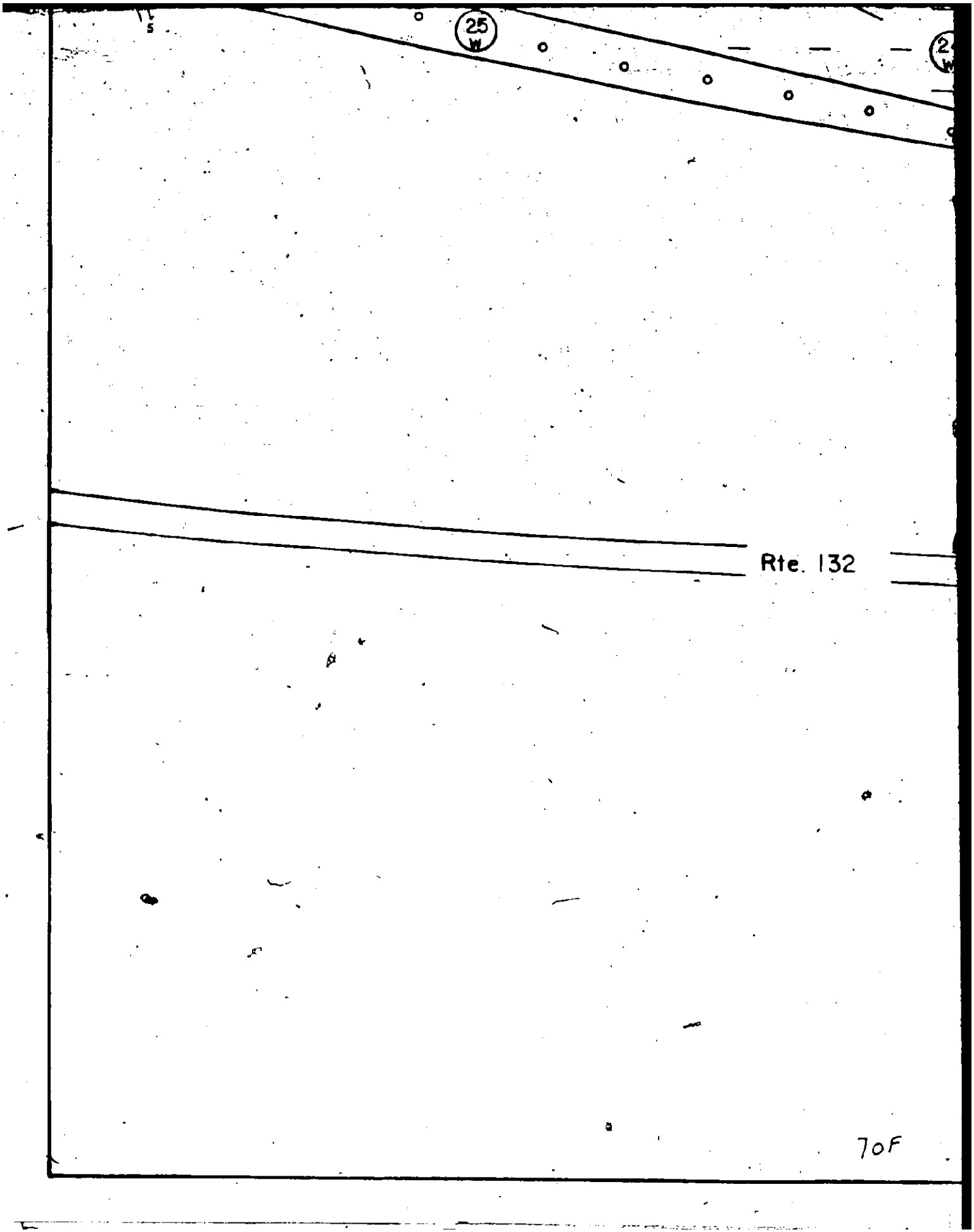
25
W
Rte. 132
7 OF

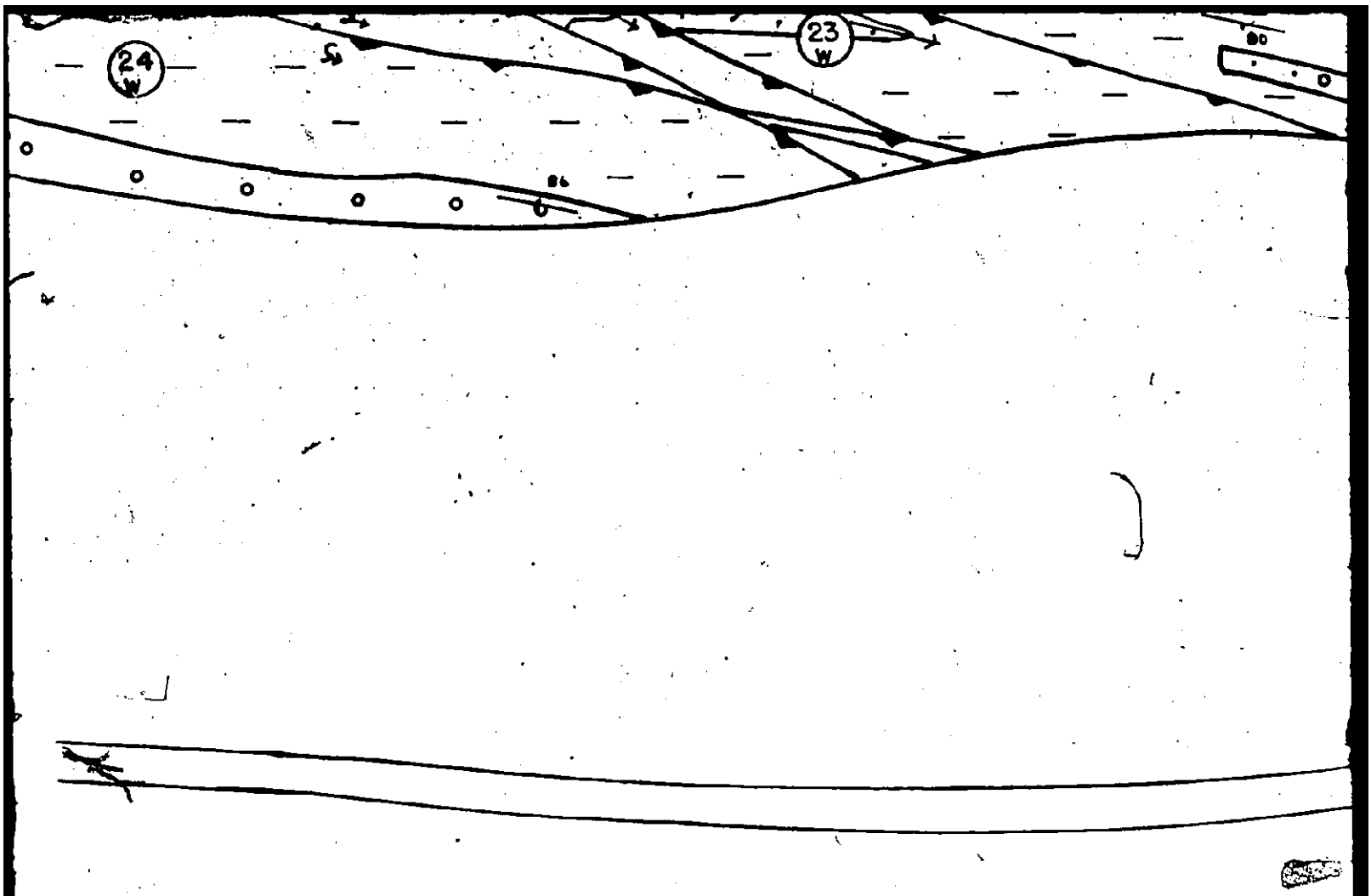
24
W
23
W

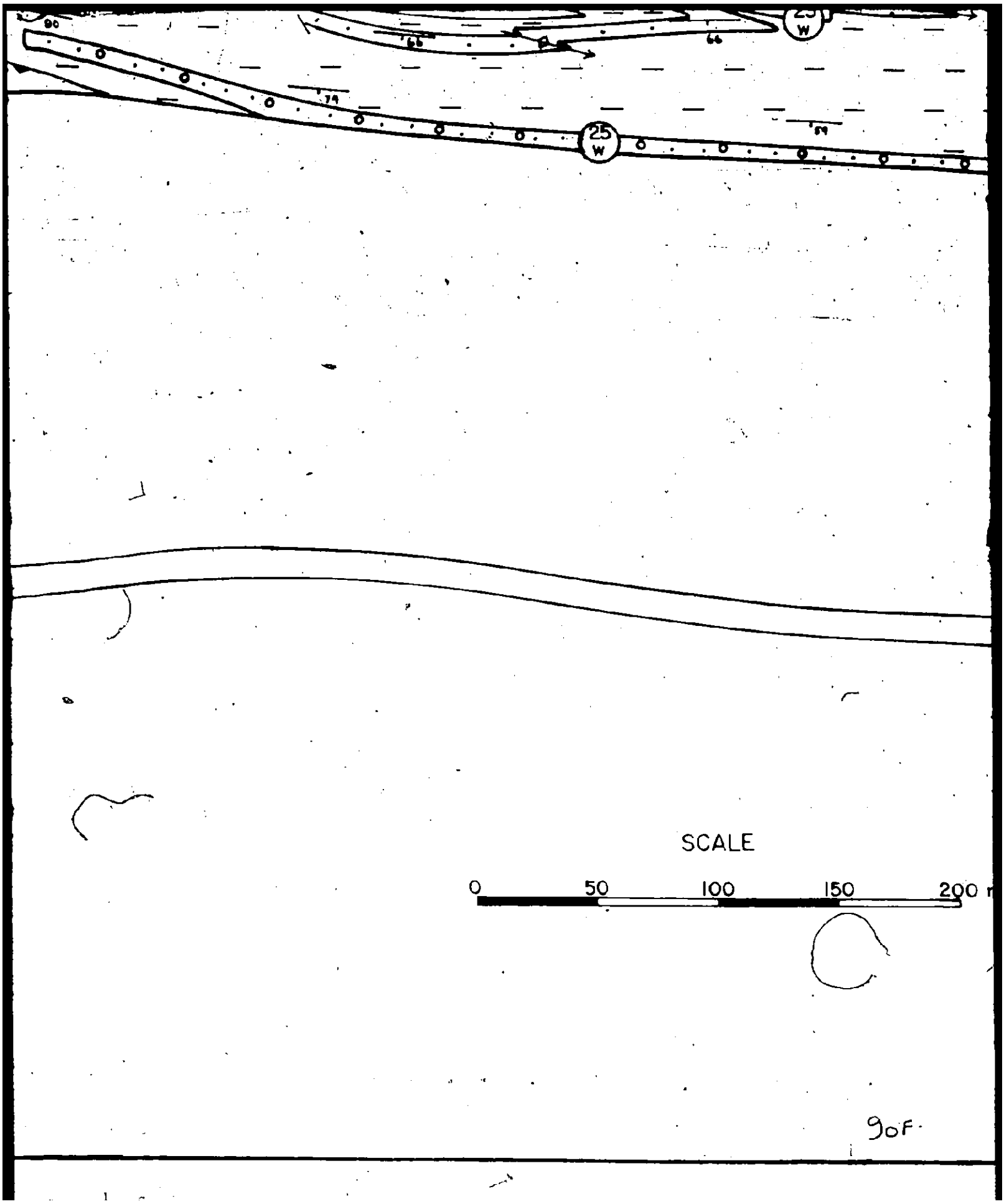
25
W
SCALE
0
50
100
150
200

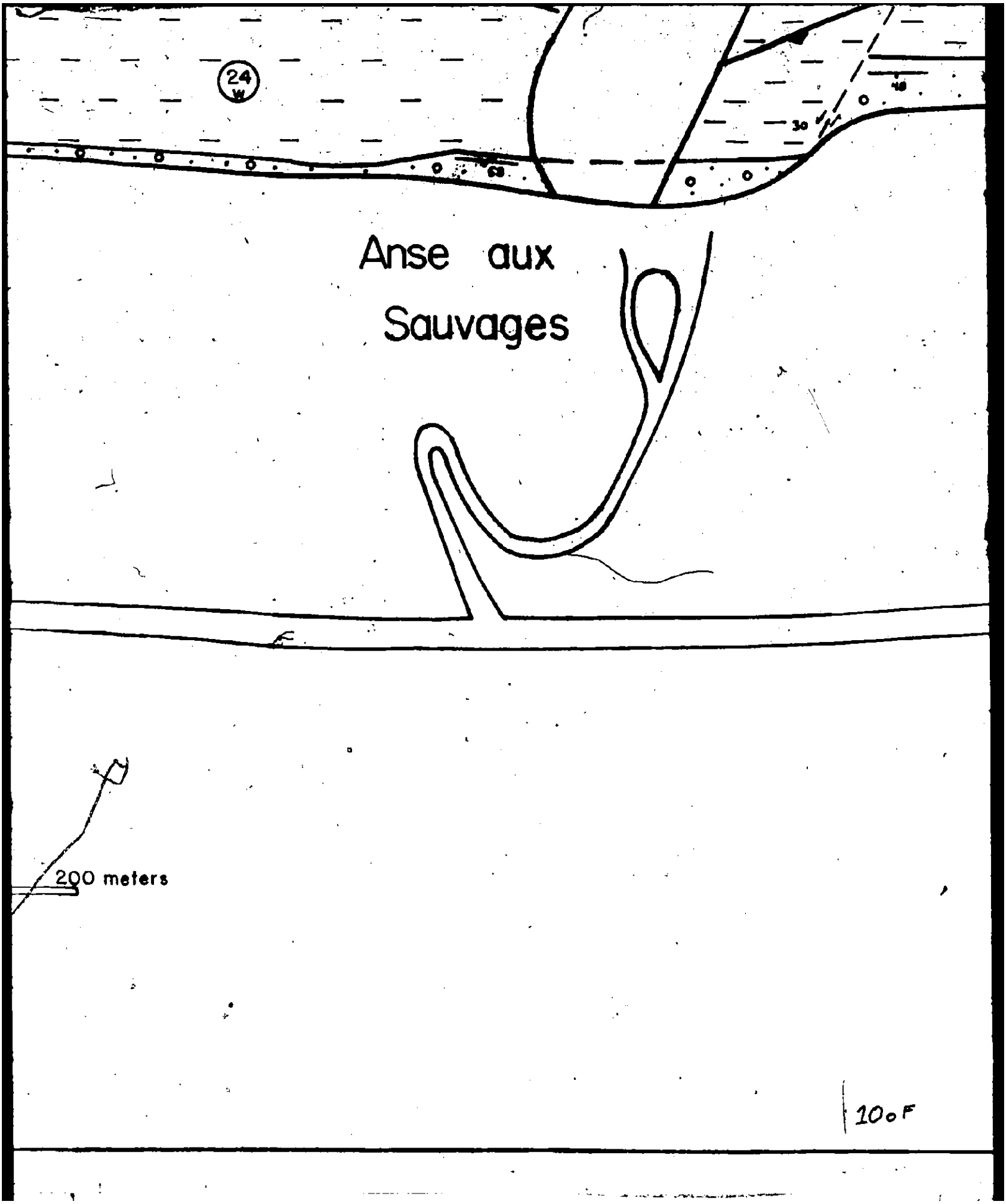
24
W
30
Anse aux
Sauvages
200 meters
100 F

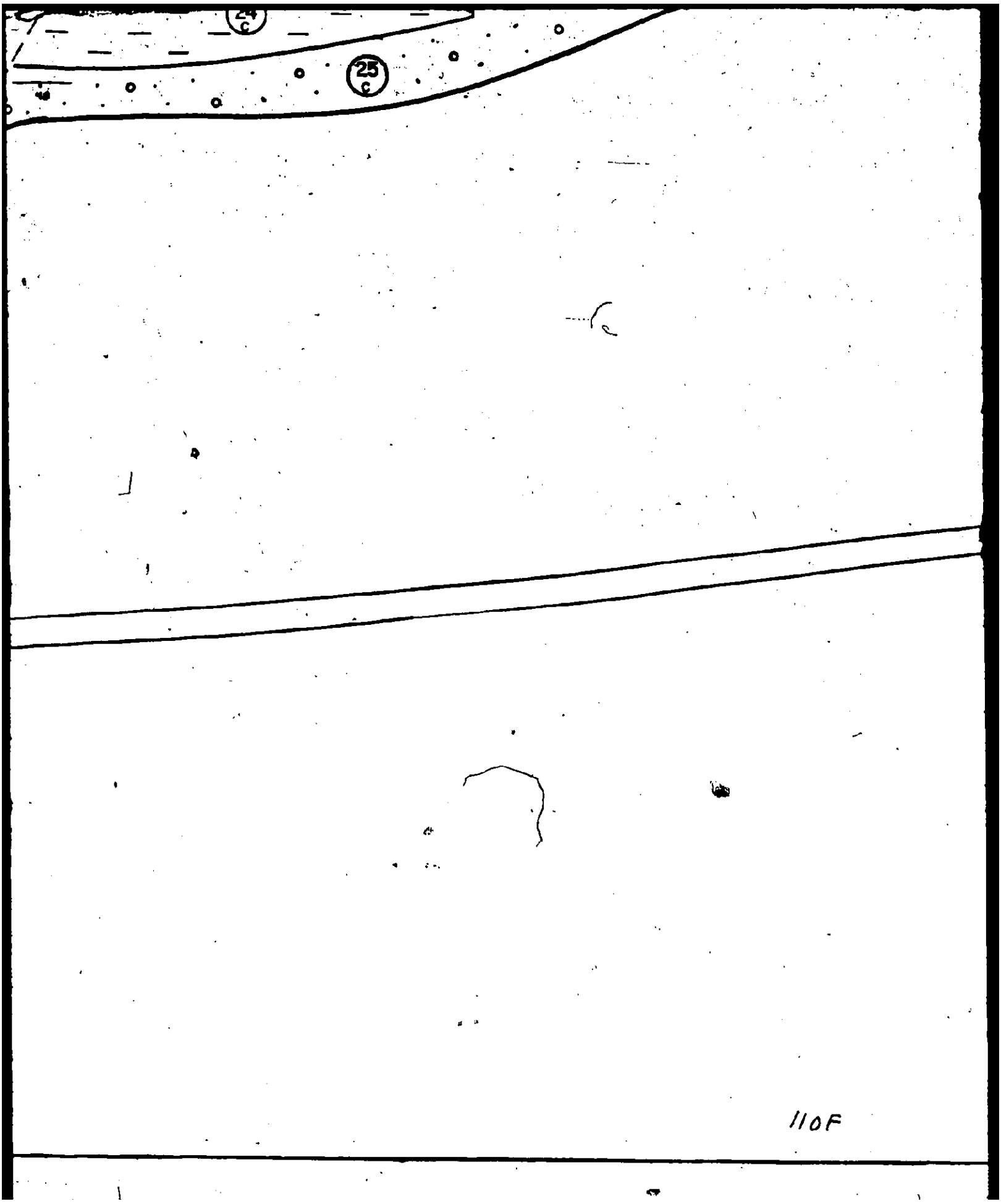

110F

ANSE AUX SAUVAGES FAULT

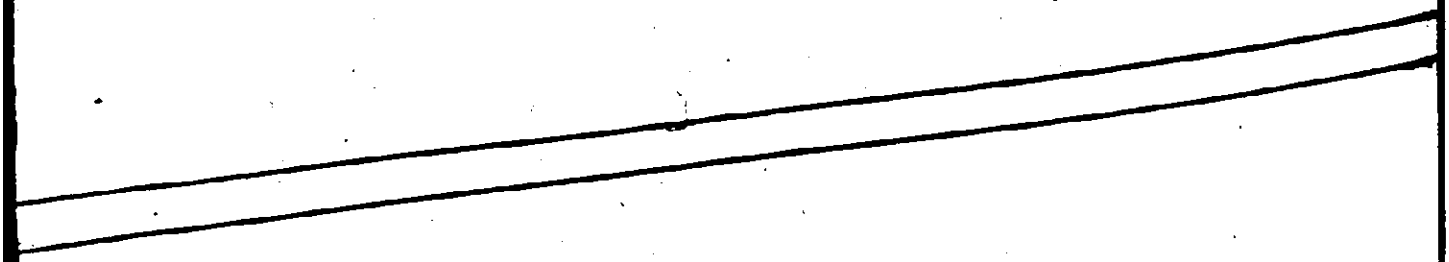

(2 of 3)

1 of

St. Lawrence River

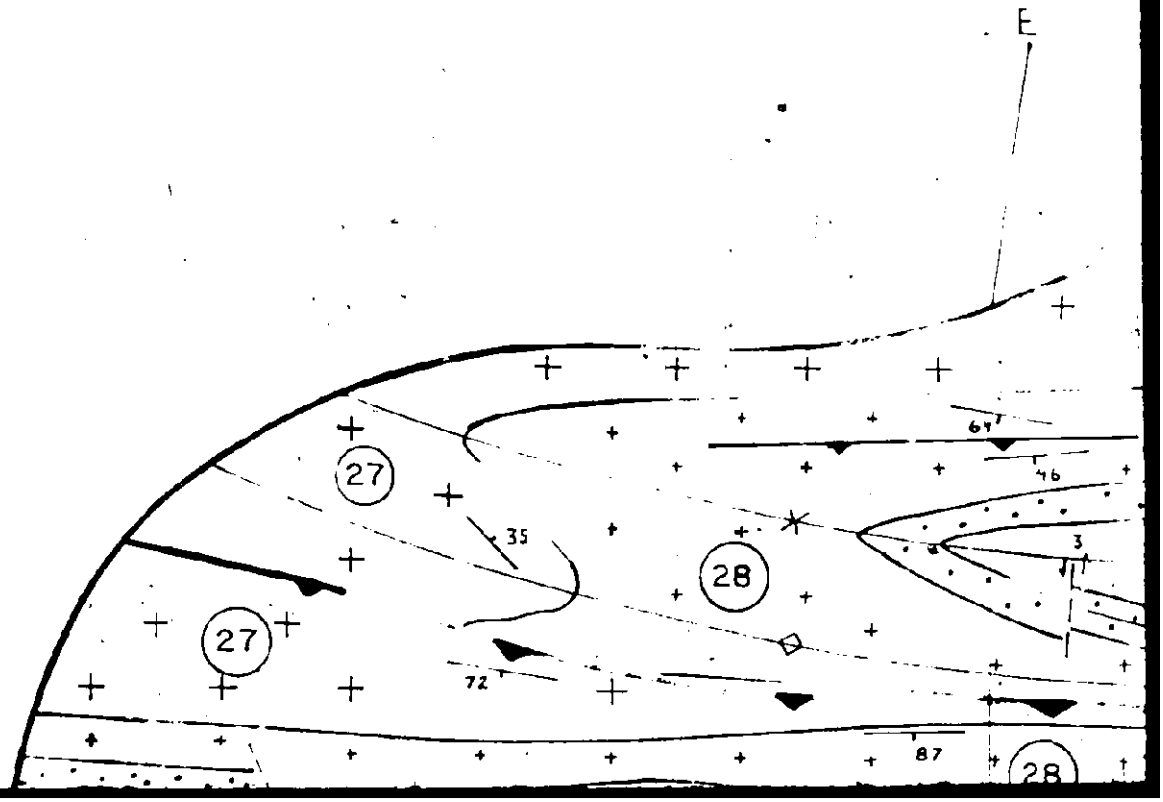

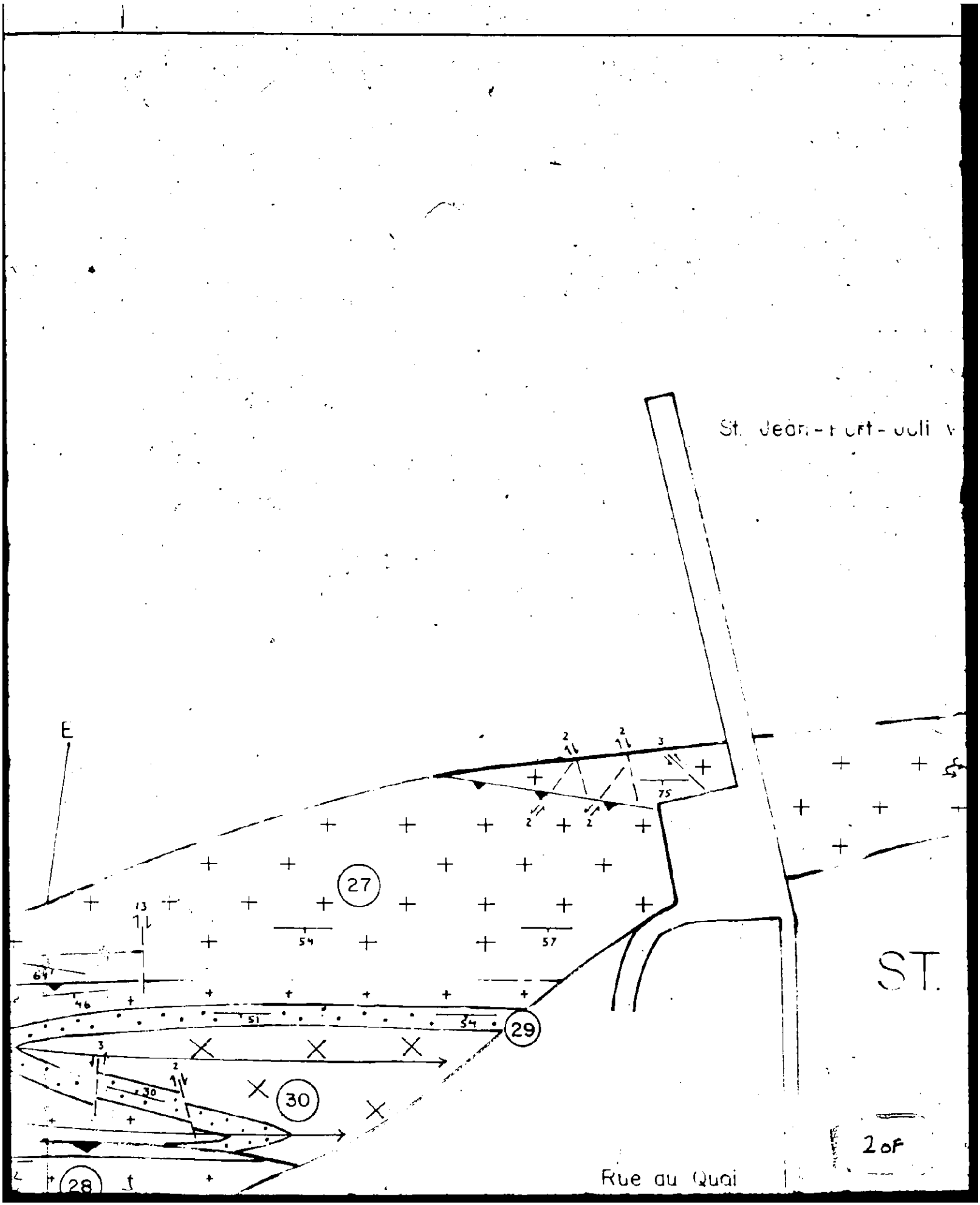
St. Jean-Port-Joli
E
27
29
30
28
54
57
75
51
34
46
64
Rue du Quai
ST.
2 OF

WESTERN ZONE

rt-joli wharf

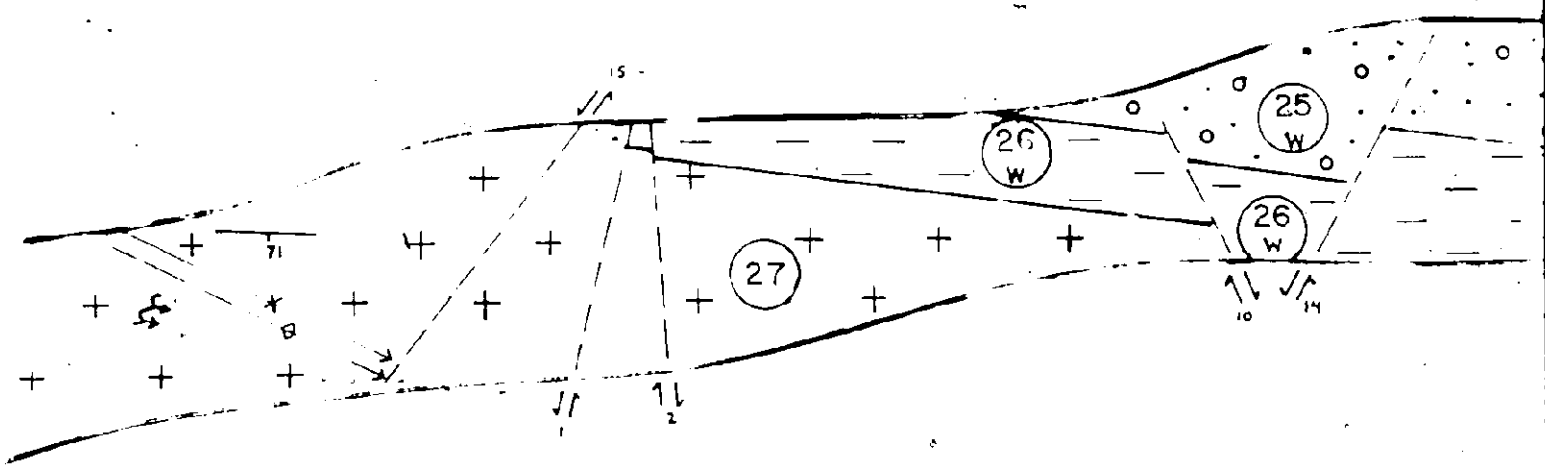

ST. JEAN-PORT-JOLI

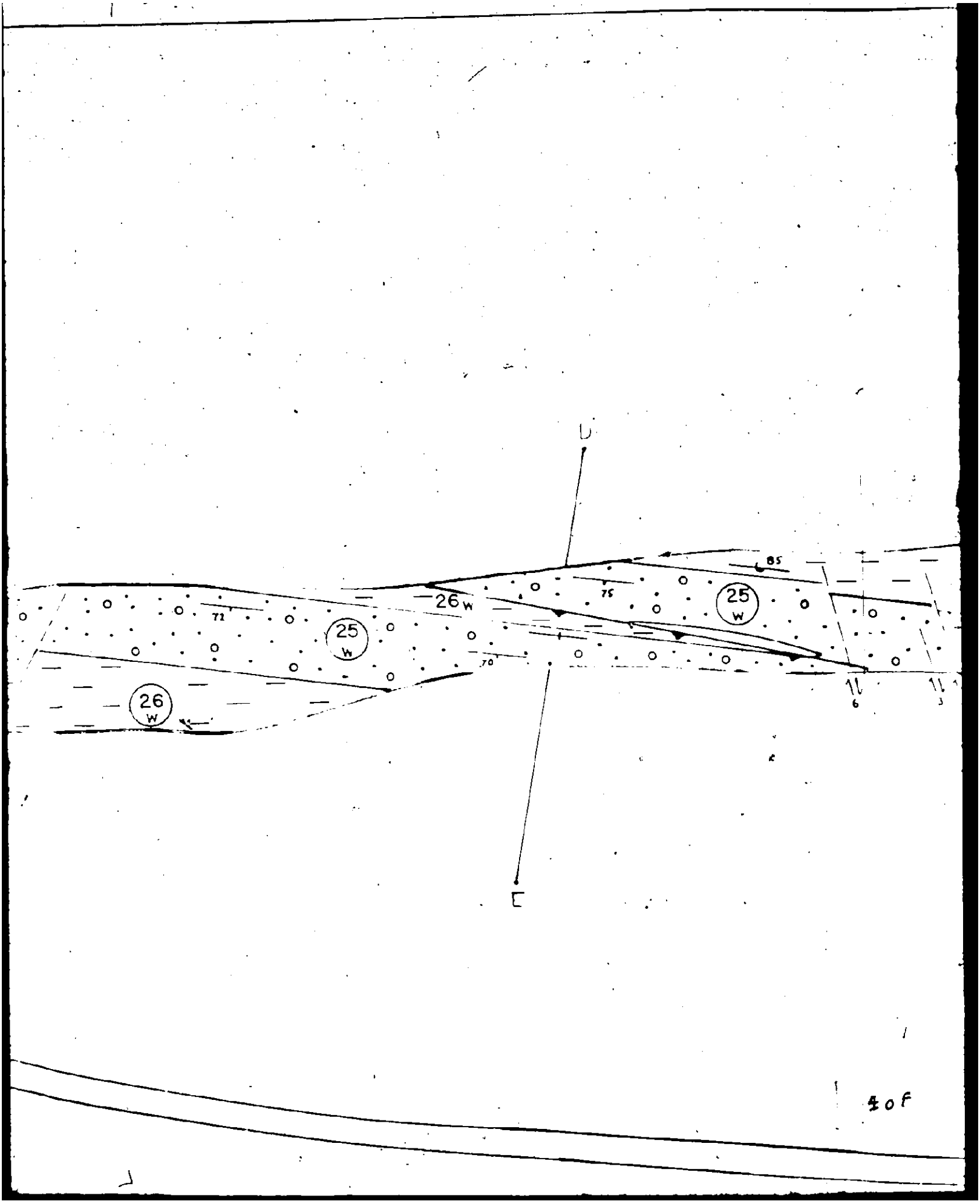
D
C
26 W
25 W
25 W
26 W
71
70
75
85
11
6
11
3

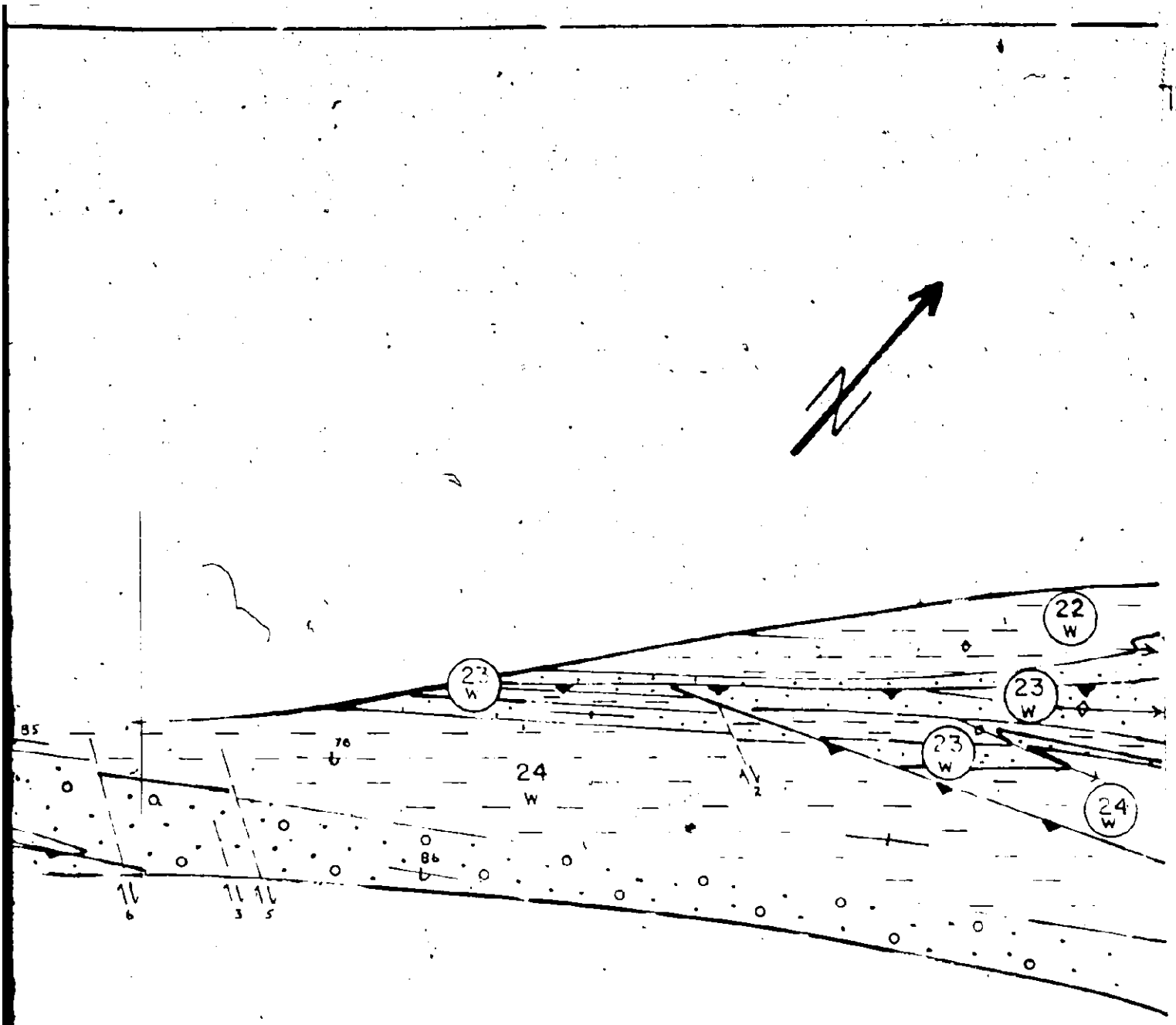
N
22 W
23 W
23 W
24 W
24 W
85
76
86
a
b
1
2
6
3
5

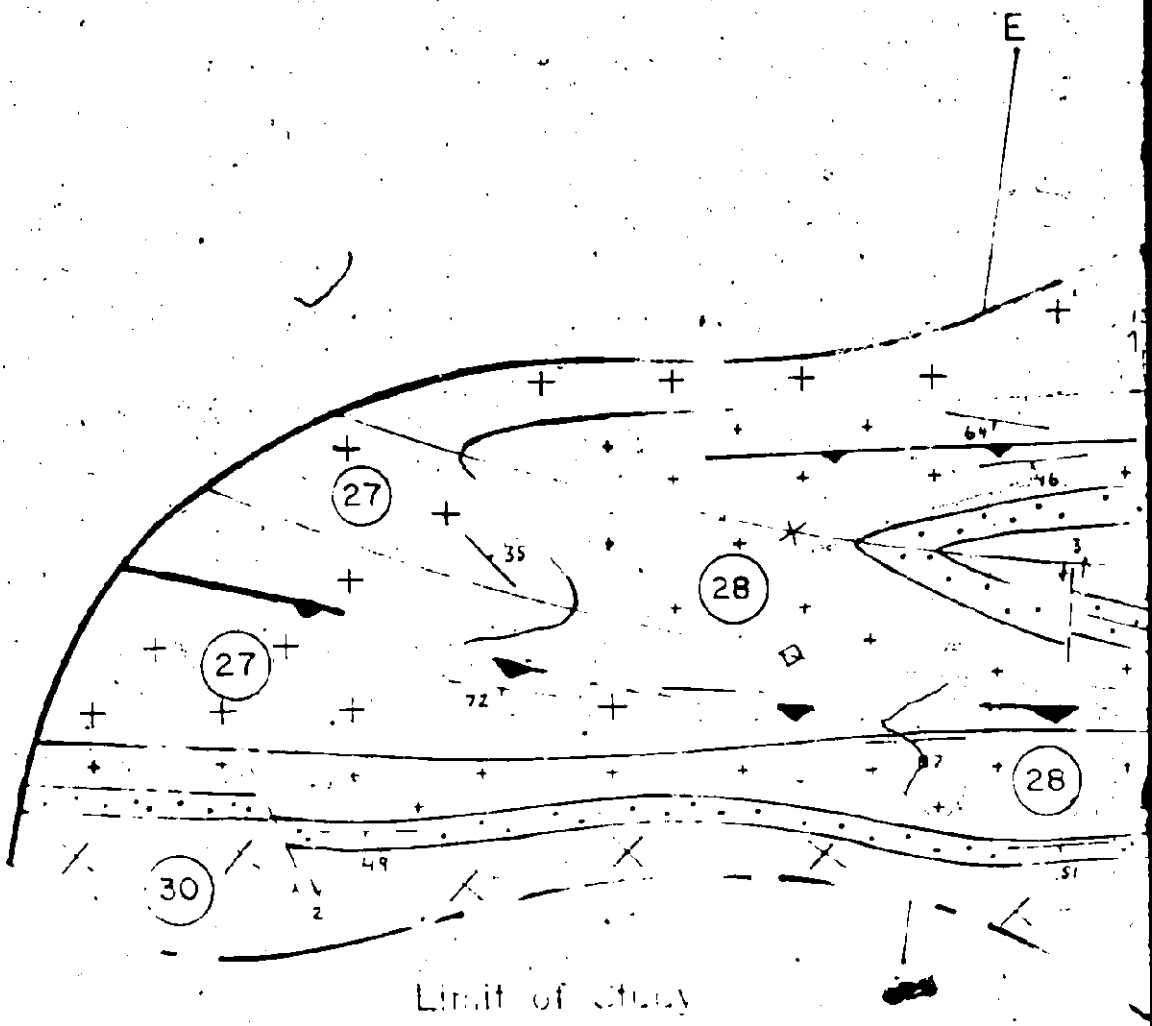

6 of F

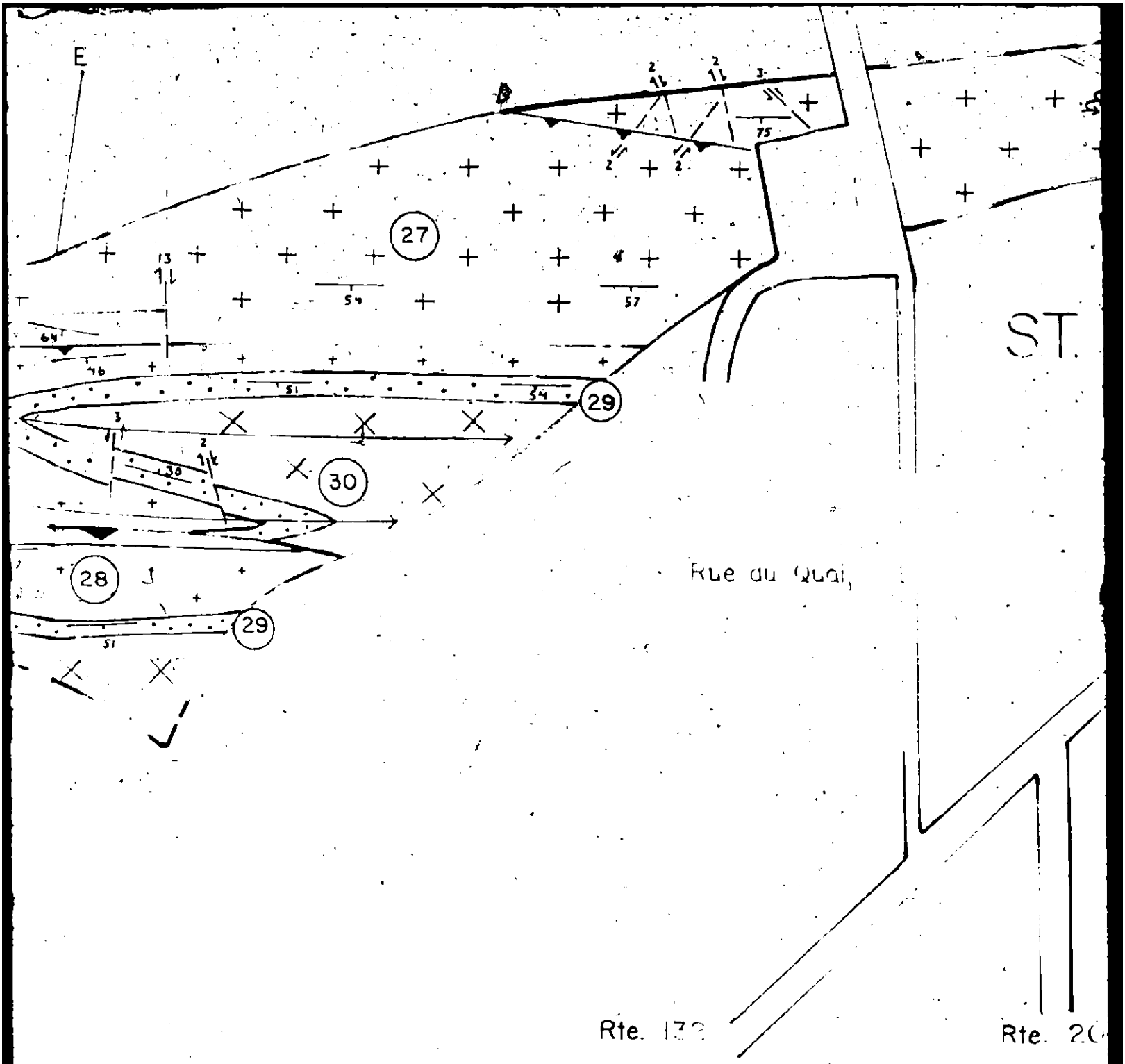
E
27
29
30
28
29
ST.
Rue du Quai
Rte. 132
Rte. 20

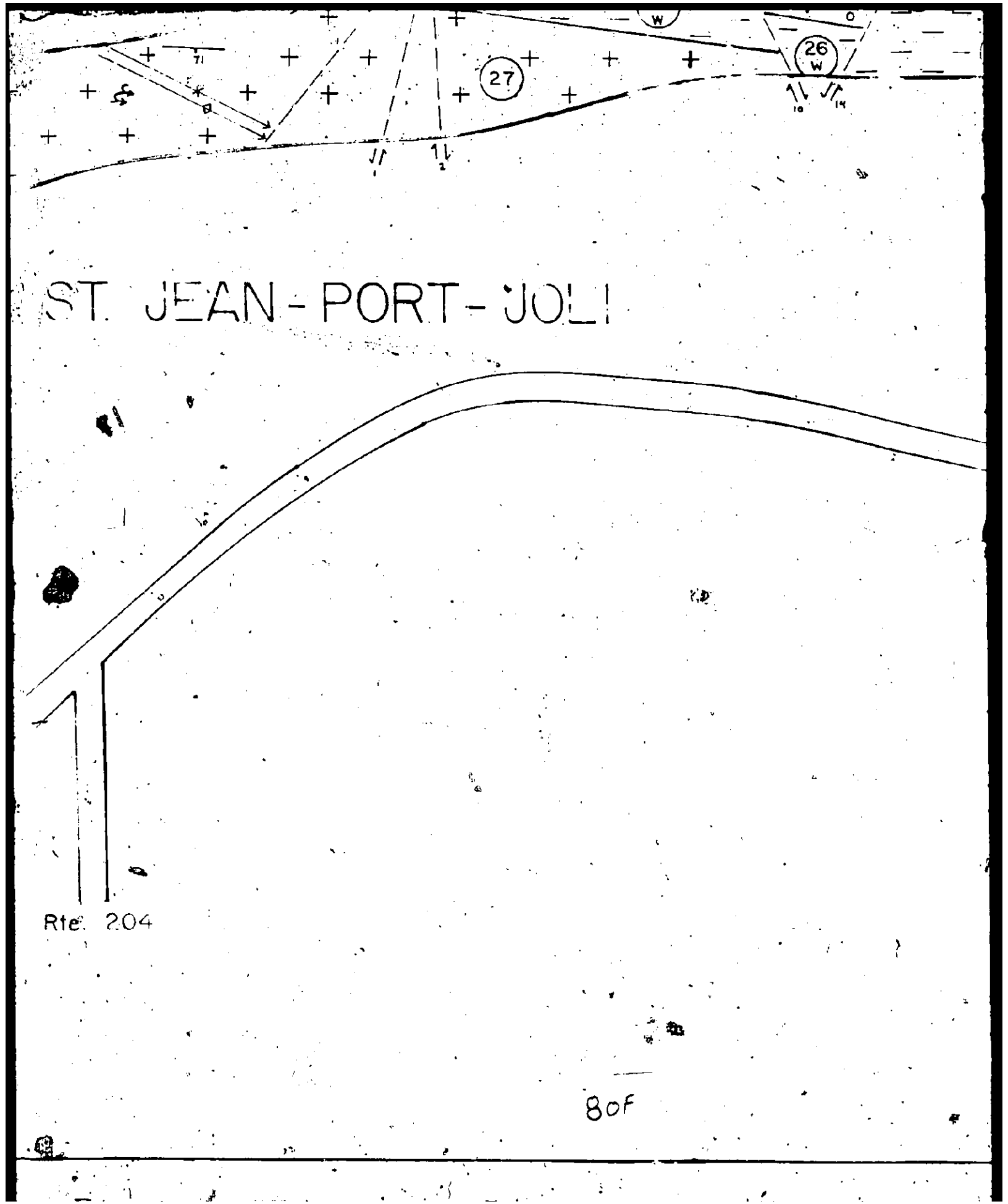

8 OF

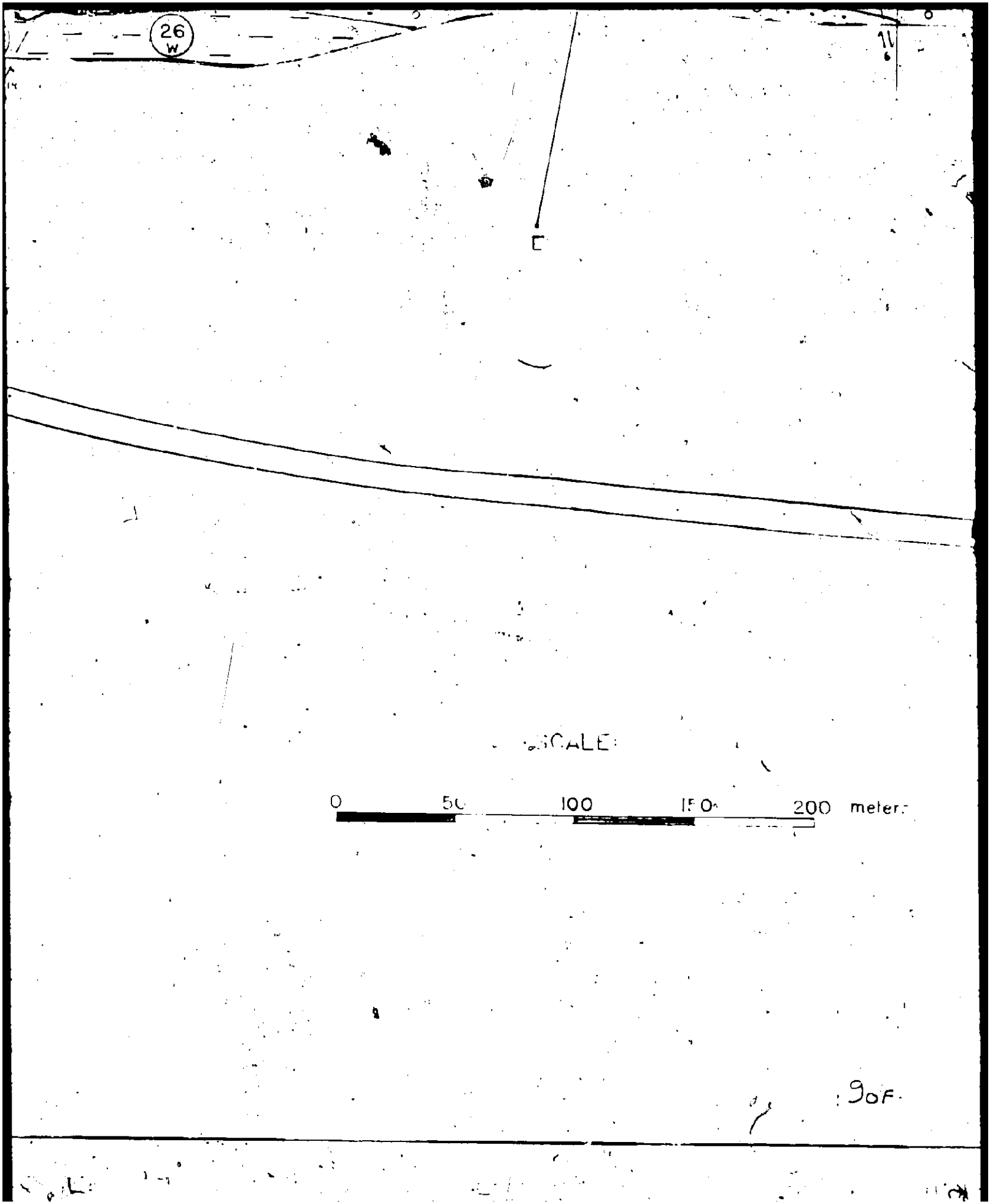
26
W
SCALE:
0
50
100
150
200 meters

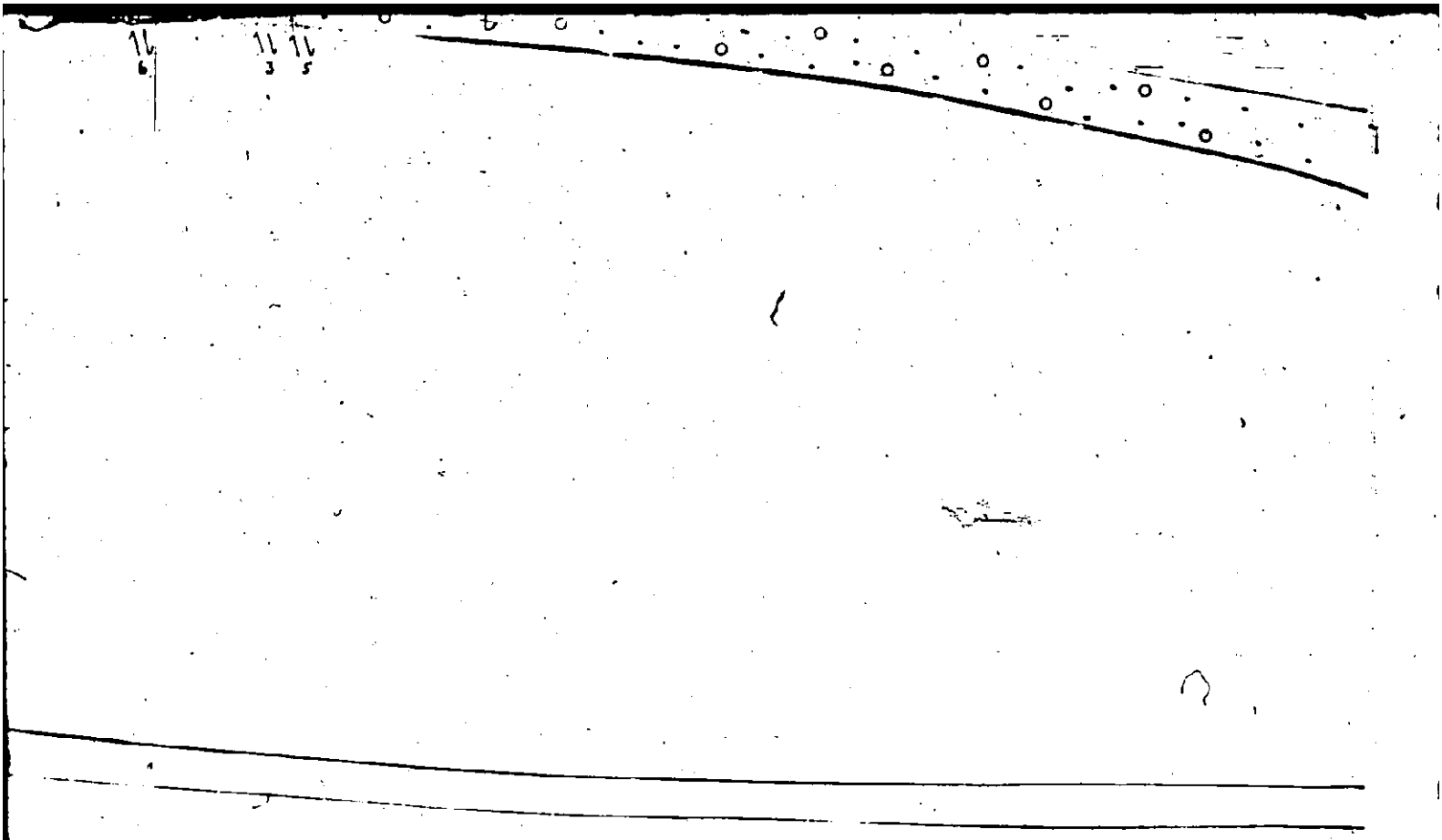

00 meters

(1 of 3)